THE OCULOMOTOR SYSTEM:

(1) VERTICAL-HORIZONTAL INTERACTION AND SIGNAL RECOGNITION

(2) TIME DELAYS AND POWER SPECTRA

Thesis by

Antony Wilfred Goodwin

In Partial Fulfillment of the Requirements

for the Degree of

Doctor of Philosophy

California Institute of Technology

Pasadena, California

1972

(Submitted February 1, 1972)

ACKNOWLEDGEMENT

I would like to express my appreciation to my advisor, Dr. Derek H. Fender for his guidance and advice.

I would also like to thank Cary Lu and Dr. Patrick W. Nye for their advice on optics, Rinus Decker for his technical assistance, Cameron J. Schlehuber for his patience and endurance as a subject, and Bob Kavanagh, Dr. Andrew E. Kertesz and Dr. Gaetan J. St-Cyr for their valuable discussions.

I am grateful to Virginia Conner, Vivian Dinwiddie and Jan Wader for typing the manuscript.

Finally, I thank my wife Valerie for her help and understanding.

ABSTRACT

In the first section of this thesis, two-dimensional properties of the human eye movement control system were studied. The vertical - horizontal interaction was investigated by using a two-dimensional target motion consisting of a sinusoid in one of the directions vertical or horizontal, and low-pass filtered Gaussian random motion of variable bandwidth (and hence information content) in the orthogonal direction. It was found that the random motion reduced the efficiency of the sinusoidal tracking. However, the sinusoidal tracking was only slightly dependent on the bandwidth of the random motion. Thus the system should be thought of as consisting of two independent channels with a small amount of mutual cross-talk.

These target motions were then rotated to discover whether or not the system is capable of recognizing the two-component nature of the target motion. That is, the sinusoid was presented along an oblique line (neither vertical nor horizontal) with the random motion orthogonal to it. The system did not simply track the vertical and horizontal components of motion, but rotated its frame of reference so that its two tracking channels coincided with the directions of the two target motion components. This recognition occurred even when the two orthogonal motions were both random, but with different bandwidths.

In the second section, time delays, prediction and power spectra were examined. Time delays were calculated in response to various periodic signals, various bandwidths of narrow-band Gaussian random motions and sinusoids. It was demonstrated that prediction occurred only when the target motion was periodic, and only if the harmonic content was such that the signal was sufficiently narrow-band. It appears as if general periodic motions are split into predictive and non-predictive components.

For unpredictable motions, the relationship between the time delay and the average speed of the retinal image was linear. Based on this I proposed a model explaining the time delays for both random and periodic motions. My experiments did not prove that the system is sampled data, or that it is continuous. However, the model can be interpreted as representative of a sample data system whose sample interval is a function of the target motion.

It was shown that increasing the bandwidth of the low-pass filtered Gaussian random motion resulted in an increase of the eye movement bandwidth. Some properties of the eyeball-muscle dynamics and the extraocular muscle "active state tension" were derived.

TABLE OF CONTENTS

1. INTRODUCTION

Studies of the eye movement control system have developed along two lines. For many years neurophysiologists and neuroanatomists have traced the central pathways involved in eye movements, both in man and in animals. Considerable effort has also been devoted to the study of the extraocular muscles. Reviews of this work, such as Cogan (1956), Whitteridge (1960) and Carpenter (1971) suggest that by the middle of the decade an impasse had been reached by these neurophysiologists and neuroanatomists. Although the volume of accumulated data was enormous, it did little to formalize the description of eye movements and did not reveal the functional relationships between eye movement and neural activity.

From about 1960, engineers approached the problem from a different point of view and began to apply the concepts of control theory to eye movements. The oculomotor system was essentially treated as a "black box" and its characteristics were inferred from input-output measurements. As a result, there now exists a considerable body of highly quantitative information about the external characteristics of the eye movement control system. Much of this information is illustrated in review papers by Robinson (1968), Fuchs (1970) and Westheimer (1970) and is increasing continuously.

Besides quantifying the nature of eye movements, the engineering approach has had a profound effect on the neurophysiological research. The challenge of explaining the central mechanisms involved in specific quantitative phenomena has attracted a relatively large and growing body of researchers who are combining the techniques of the classical neurophysiologist and the classical engineer. People such as Bizzi (1968), Cohen and Feldman (1968), Robinson and Fuchs (1969) and Schiller (1970), to name but a few, are now linking eye movement characteristics and central neural activity in a quantitative manner.

A beneficial side-effect of this interdisciplinary approach has been to disclose many gaps both in our knowledge of the eye movement characteristics and in our knowledge of the anatomy of the central pathways involved. There is still a great need for information on these two aspects.

This thesis is basically an engineering type of approach to the oculomotor system, although much of the evidence and logic used is of neurophysiological origin. At all times I have attempted to interpret my results within the framework of the known physiology of the oculomotor system.

The work consists of two basic sections. The first section deals with two-dimensional properties of the system. The nature of the interaction between the vertical and horizontal tracking mechanisms is elucidated, and it is shown that vertical and horizontal are not preset tracking directions. Rather, the system selects tracking directions according to the target motion so as to optimize its performance. The second section deals with the nature of the time delays between the target motion and eye movements and the eye movement power spectra. A theory is developed explaining time delays and prediction in the system as a function of target motion characteristics.

II. EXPERIMENTAL APPARATUS AND METHODS

The apparatus consists of two basic components, the eye movement measuring equipment and the target projector.

1. Measurement of Eye Movements.

There are several well established methods of measuring eye movements (Fender, 1964; Young, 1963). The differences of the various methods fall into three basic categories, namely resolution, range and convenience. In the experiments that follow, the target amplitudes were chosen so that the resulting eye movements were limited to less than two degrees. There are three main reasons for this choice. I wish to compare the data with those of other researchers who have used target magnitudes in this range (for example St - Cyr and Fender, 1969b), and by using these small amplitudes it is hoped to reduce the effect of some of the non-linearities of the oculomotor system to facilitate interpretation of the data. In addition, the design of the target projection system is considerably simplified if only small amplitudes are required. Therefore the eye movement measuring system need only operate over a small range (2 degrees from the primary position) but requires a correspondingly high resolution (of the order of minutes of arc). The high resolution is also necessary for the fixation experiments, where the movements are very small (Ditchburn and Foley-Fisher, 1967). An additional requirement was that eye movements could be compensated (open loop tracking) with

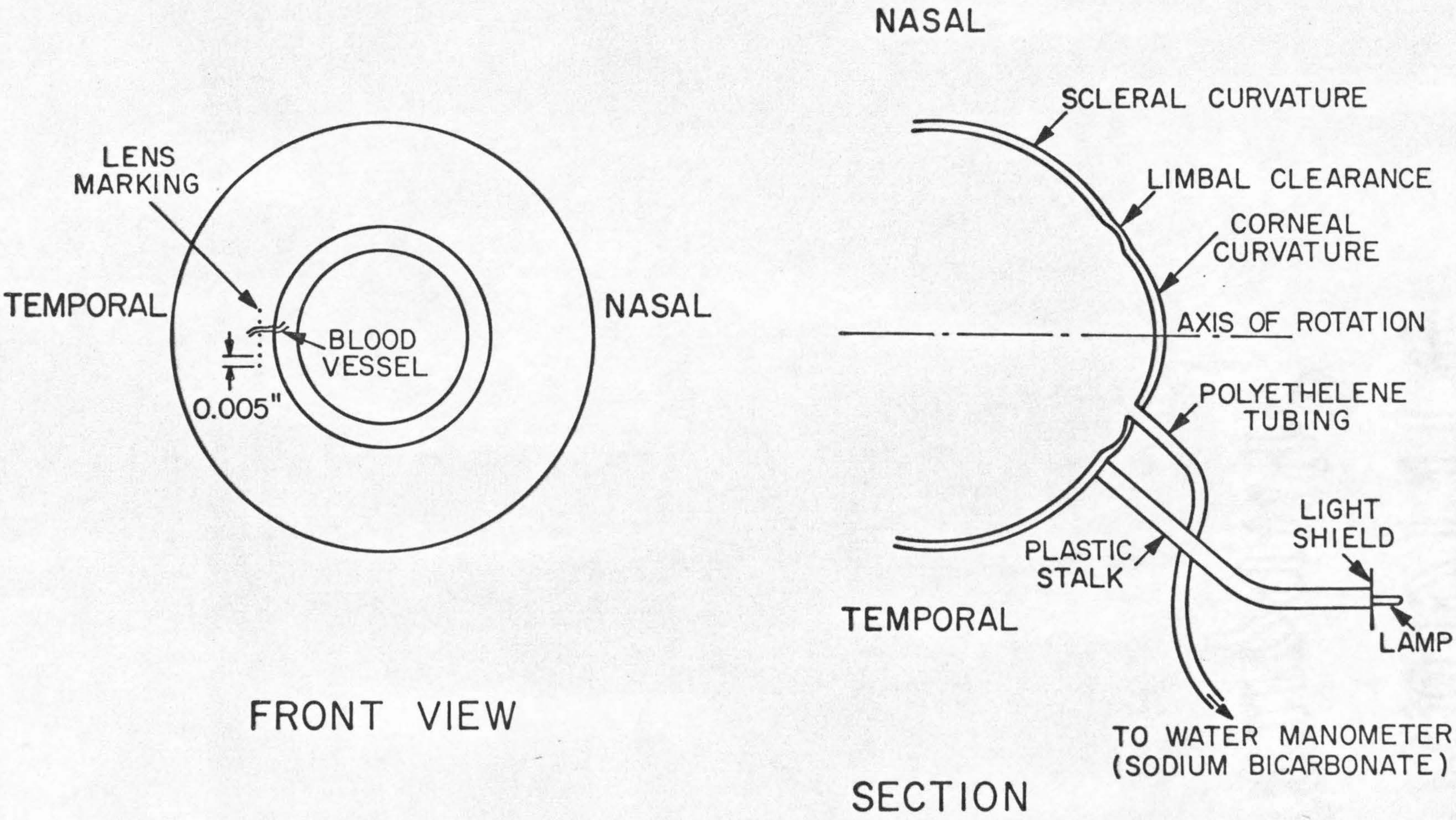

Fig. 2.1 Right contact lens. For clarity the lens engraving and blood vessels are exaggerated in the front view

reasonable accuracy. Thus, despite its inconveniences, a contact lens method was chosen.

1.1 The Contact Lens. A pair of three-curvature scleral contact lenses (Duke-Elder, Volume 5) was individually molded for each subject. Besides being expensive, this process limits the number of subjects and is probably the main objection to the contact lens method.

For optical reasons the central interior surface of the corneal portion has to be polished, slightly reducing the effectiveness of the molded fit. Because of the abundance of pain receptors, the limbal region is cleared, and the peripheral regions of the scleral portion, although close fitting, are reduced in effectiveness by the looseness of the conjunctiva to which they hold (Duke-Elder, Volume 2). Thus it is clear that the regions surrounding the limbus are the most critical for a close fit.

A light plastic stalk was glued to each lens as shown in Fig. 2.1, and a miniature incandescent lamp (Rimmer Bros. C11) could be pressed onto the end of the stalk. A circular shield prevented the lamp from shining in the subject's eyes. The lamp position was displaced from the line of sight by 15 mm in a temporal direction and 5 mm in a caudal direction, and was situated 16 mm in front of the anterior corneal surface. From Fig. 2.2 we see that the effective moment arm of the lamp is 32 mm for horizontal and vertical movements.

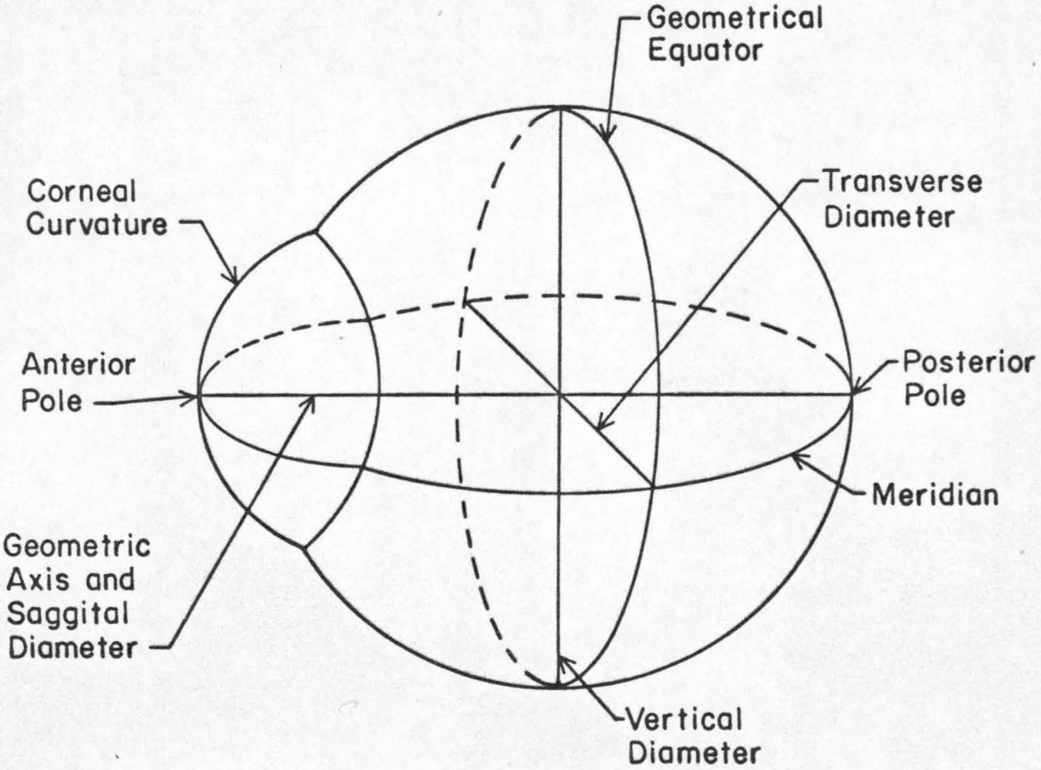

Saggital Diameter = 24.15 mm outer and 22.12 mm inner
Transverse Diameter = 24.13 mm
Vertical Diameter = 23.48 mm
Vertical Corneal Diameter = 10.6mm outer and 11.6mm inner
Horizontal Corneal Diameter = 11.6mm outer and 11.6mm inner

Fig. 2.2 Basic geometry of the eye. Redrawn from Duke-Elder

As will be discussed, it was deemed necessary to reduce slippage of the lens by suction. A small hole was drilled on the edge of the limbal clearance and a thin polyethelene tube (Intramedic PE 50, .023" inside diameter, .038" outside diameter) was press-fitted. The other end of the tube was attached to a simple water manometer which could be raised and lowered to vary the pressure between the lens and the eyeball. The manometer, tubing and lens-cornea space were filled with a sodium bicarbonate buffer solution (16.4 grams/litre).

1.2 The Photomultiplier Tube Assembly. Fig. 2.3 shows the photomultipliers for one eye with the lamp in position. It is clear that vertical displacement of the lamp changes the length of the shadow cast on the face of the vertical photomultiplier tube and hence the current output of the tube. The same is of course true for horizontal movements. I shall refer to movement of the left visual axis in a vertical direction as the left vertical component of eye movement, and similarly define the components left horizontal, right vertical and right horizontal. If the photomultiplier tubes are linear, four voltages proportional to these four eye movement components result.

With the eye fixating in the primary position, the assembly is adjusted so that the shadow covers half the exposed tube area, allowing equal movement on either side of the primary position. Non-linearities at the edges of the photocathodes are eliminated by the masks. Changing the optical leverage by repositioning the knife edges increases (or decreases) the measurement resolution, but at the same time decreases (or increases) the measurable range of movements. For the following experiments the knife edge was set to allow a measuring range of about 3 degrees on each side of the primary position. Each calibrating vane (Fig. 2. 3) is attached to a solenoid with a spring loaded return allowing it to be moved rapidly between two fixed mechanical stops. With the eye near the primary position, a pulse applied to the solenoid moves the vane to occlude a fixed portion of the photomultiplier face, causing a pulse in the output. As will be seen, this occlusion can be related to the eye movement necessary to produce an equivalent shadow lengthening, thus providing a means of calibration. The calibration rise time was about 50 milliseconds, making the effect of eye movements negligible.

1. 3 Objections to the Contact Lens. The fact that each subject requires a custom made set of lenses is a definite inconvenience.

A more serious disadvantage is the relatively short time for which a contact lens of this type may be worn. The cornea itself is avascular, receiving much of its nutrition from surrounding episcleral vessels (see Fig. 2. 4). A tightly fitting scleral contact lens tends to occlude these vessels, and of course also seals off the cornea from the surrounding air. The resulting anoxia leads

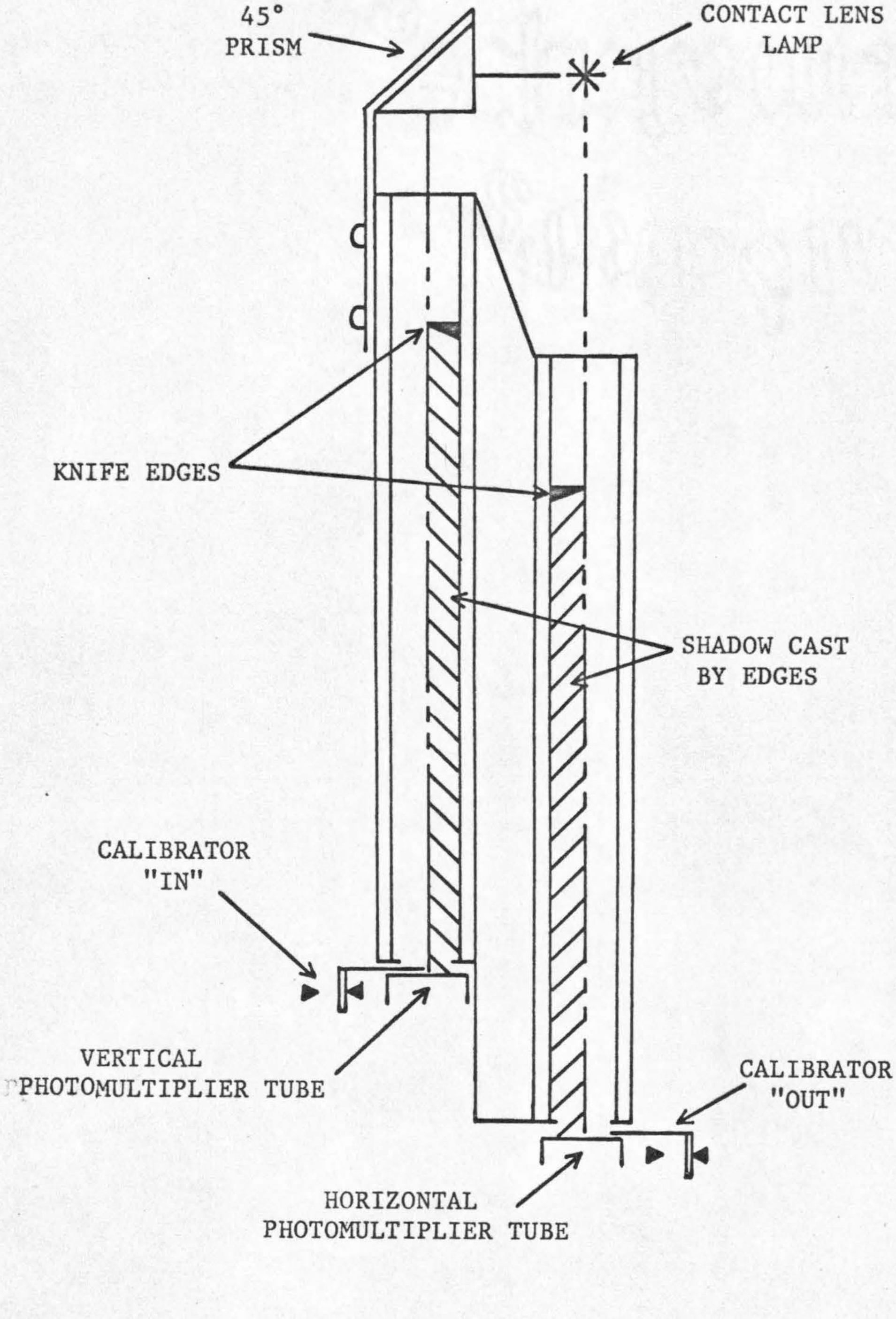

Fig. 2.3 Photomultiplier tube assembly

to the occurrence of corneal oedema which is first noticed as a blurring of vision known as veiling. Duke-Elder (Volume 5) states that the threshold for oedema is dependent on the particular cornea and lens, but that veiling usually commences within 40 minutes to 14 hours for scleral lenses. Since oedema can lead to considerable damage of the cornea, no subject wore lenses for more than 30 minutes per session. Not more than one session was held in a day.

Another criticism that may be levelled at the contact lens is that its very presence may effect the eye movements. A few authors such as Beeler (1965) and Riggs, Armington and Ratliff (1954) have given theoretical arguments against this criticism. There are a multitude of occurrences in the literature where identical or similar eye movement responses have been measured both by a contact lens method and by other methods. These comparisons have never (to the author's knowledge) revealed any differences. Robinson (1964) compared saccades measured by him using a contact lens technique with those measured by Westheimer (1954), Yarbus (1956) and Mackensen (1958) who used respectively corneal reflexions, another contact lens method and the electro-oculogram. He found no discrepancies. Nachmias (1959) compared his contact lens measurements of fixational movements with those measured by Cornsweet (1958), who scanned the subjects' optic disk with a spot of light, and found close agreement. These two examples are merely representative of a host of such vindicators of contact lens methods.

1.4 Lens Stability. Perhaps the most serious danger of a contact lens method is the possibility of slippage. In this thesis, the open loop condition was achieved by adding the measured eye movements to the desired target motion. The maleffects of slippage on the eye movements themselves are serious enough, but the multiplied effect in the open loop mode could be ruinous. Although a recurrent theme in the literature for many years, the question of slippage has not been adequately settled.

The most common approach to the problem has been what might be called theoretical justification. Typically, slippage is rejected on the grounds that the moment of inertia of the lens assembly is small compared to that of the eyeball (Fender, 1964; Riggs et al.,1954); and that the maximum frictional force required to accelerate the lens is well within what is guessed to be the capability of a scleral contact lens (Fender, 1964). Another popular argument is that the measurements do not appear to reflect slippage (Ditchburn and Ginsborg, 1953), although most authors concede that they may well be looking for the wrong signs. Many stabilized retinal image experiments rely on the absence of slippage, and their apparent success has been cited as proof of lens stability (Ditchburn and Ginsborg, 1953). However, at best this argument applies only to the relatively small movements of fixation. All these arguments are merely indicative of the situation, and do not prove anything about lens slippage.

I claim that the only reasonable approach to the problem is to objectively measure lens slippage during the execution of eye movements typical of those which are being studied. Moreover, since the amount of slippage depends on the shape of the subject's eyeball, the shape of the lens, the skill of the lens maker and many other factors, each measurement is accurate for only one subject-lens combination. It does not really make sense to say that because Byford's lenses were satisfactory (1962), we will assume ours are too. Byford (1962) measured slippage by comparing the contact lens measurements with concurrent high speed cinematographic records of the eye, during fixation and nystagmus. He found lens slippage of less than 6 min. arc for movements as large as 9 degrees, and negligible slippage for movements less than 1 degree. St.- Cyr and Fender (1969a) measured the motion of an ocular blood vessel relative to an engraved grid on the contact lens during saccades, and concluded that the amount of slippage was unacceptable. By introducing a suction of 23 cm water, they reduced the slippage to 9 min. arc for a 4 degree saccade. I believe that this method is the most reliable used to date, but may have been marred by their choice of a blood vessel. The same basic method is used here, and in order to make it effective, an appreciation of the vasculature of the anterior of the eye is essential.

As shown in Fig. 2.4, there is abundant anastomosis between the anterior and posterior conjunctival arteries. These anastomoses (the pericorneal plexus) lie in a broad belt round the region of the limbus, situated in the connective tissue between the conjunctival and episcleral tissues. Hence there are effectively two planes of blood vessels, the superficial conjunctival vessels forming a freely moveable branching network, and the cilliary arteries which lie more deeply in the episcleral tissue and run radially into the corneal margin (Davson, Volume 1; Duke-Elder, Volume 2). Fig. 2.5 shows the appearance of these blood vessels to the observer. It is clear then, that a blood vessel which emerges from the limbus in a radial direction should be chosen as the reference mark on the eyeball. Such vessels are short and not too well pronounced. While a truly deep seated scleral blood vessel would probably suffice, an experimenter observing the eye through a microscope (even of relatively low power) focused on the back surface of the contact lens is bound to pick up a conjunctival or shallow episcleral vessel instead. It seems quite probable that this occurred in St-Cyr and Fender's study.

A straight line of 7 dots, about .001 inches in diameter and separated by .005 inches between centers, was engraved on the inside surface of the lens. Black wax rubbed over the dots enhanced their visibility. The dots were positioned so as to intersect a suitably chosen blood vessel at approximately right angles, and

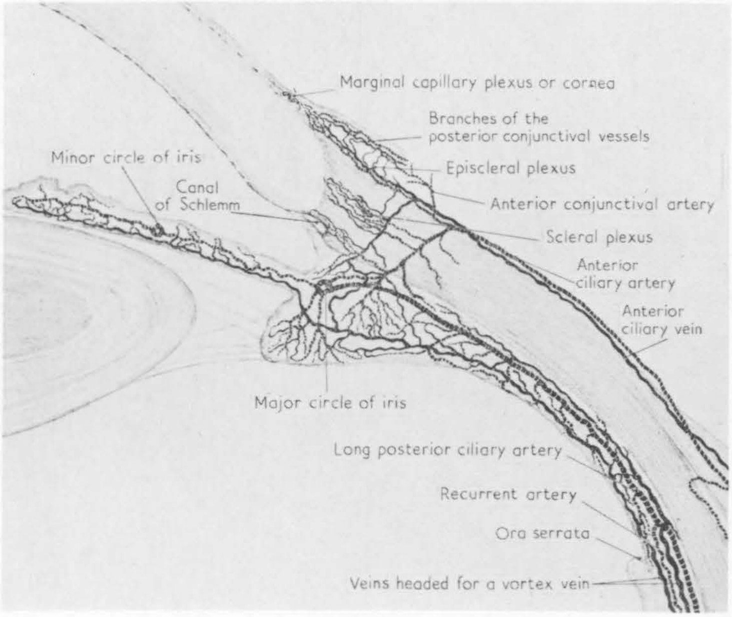

Fig. 2.4 Blood vessels of the anterior portion of the eye. Arteries are shown as dotted lines and veins as solid lines. Redrawn from Davson.

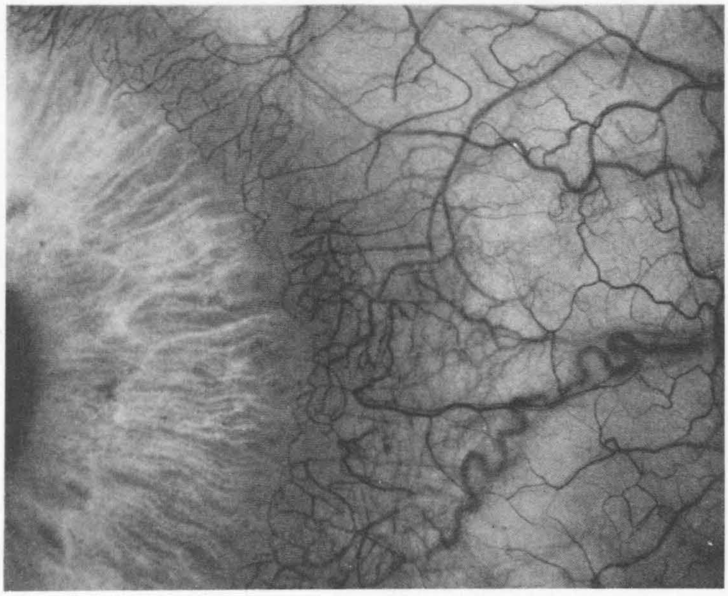

Fig. 2.5 Capillaries at the limbus (X9). Redrawn from Duke-Elder.

were thus situated slightly peripheral to the limbus and tangential to it. The blood vessel was chosen to lie approximately along the line joining the centers of the two eyes, so that the dots were optimally placed for the measurement of vertical and torsional slippage. Since there is some cross-talk from torsional movements to vertical measurements in our systems, it was considered necessary, especially for the open loop experiments, to prevent torsional slippage of the lens as well as vertical and horizontal. Horizontal slippage should be at worst of the same order as vertical slippage, so for convenience, only vertical and torsional slippage were monitored.

With the subject immobilized on a dental impression bite board, the blood vessel and lens grid were observed through a binocular microscope (Zeiss 34468) of magnification 40. Using fiber optics, the area of interest was illuminated with a green light to improve the blood vessel's visibility. For vertical measurements, the subject performed voluntary saccades between the primary position and marks 5 degrees up and down. Slow and nystagmus-type torsional movements of about 2 degrees were induced by an appropriate rotating sectored disk (Kertesz, 1969). The resolution of the method is determined by the fact that the smallest movement of the blood vessel relative to the lens grid that can be distinguished is at best .0005 inches. From Fig. 2.2 we see that this resolution is at best 4 min. arc for vertical slippage and 7 min. arc for torsional slippage. With no suction, slippage (particularly torsional) was found to be unacceptably high. A suction of 25 cm of water was found to reduce slippage to the limit of resolution for both subjects.

Fender (1964) claims that a negative pressure of about 26 cm water is developed between the eye and a close fitting lens anyway. However, this takes about 10 minutes to develop, and it is not known how individual lenses and eyeballs affect this pressure nor how stable it is. Thus external suction is not redundant.

2. Target Presentation Requirements.

The target to be tracked by the subject had to have several independently variable parameters. The shape, size, intensity and color characteristics of the target had to be easily and independently varied, and the target had to be able to move in two dimensions with any desired characteristics. It is apparent that the easiest and most common method of presentation, an oscilloscope, could not satisfy these requirements. A more versatile projector was built.

2.1 Projector Description. The heart of the system is a pair of precision mirror galvanometers housed in a single magnet (Honeywell L-330-120). Their frequency response is flat from DC to better than 200 hertz.

The optical system (Fig. 2.6) is telecentric and operates as follows. Lenses L1 and L2 and the pin hole form a collimator so that the target (a 35 mm transparency) is illuminated by parallel light. Lens L3 forms an image of the pin hole on the surface of the first mirror galvanometer MV, and an image of the target is formed at the rear focal plane of lens L4. Rotation of the mirror MV causes a lateral (horizontal) displacement of this image. Mirrors M2 and M4 lie in oblique planes forming 45 degree angles with the three principal planes, and mirror M3 lies in a horizontal plane above M2 and M4. This retro-reflector serves the same function as an achromatic dove prism, translating the horizontal displacements of the target image into vertical displacements. Lens L5 forms an image of the pin hole on the surface of the second mirror galvanometer MH, and a second image of the target is formed at the rear focal plane of lens L6. In summary, an image of the target is formed in plane A-A'. Rotation of the mirror MV causes a vertical displacement of this image while rotation of mirror MH causes a horizontal displacement.

A projection lens casts this image onto a rear projection screen (Polacoat Lenscreen) which is viewed by the subject. The optical axis of the system was located along the line of sight of the left eye, when held in the primary position. A lens eyepiece for the left eye and a lens and prism eyepiece for the right eye

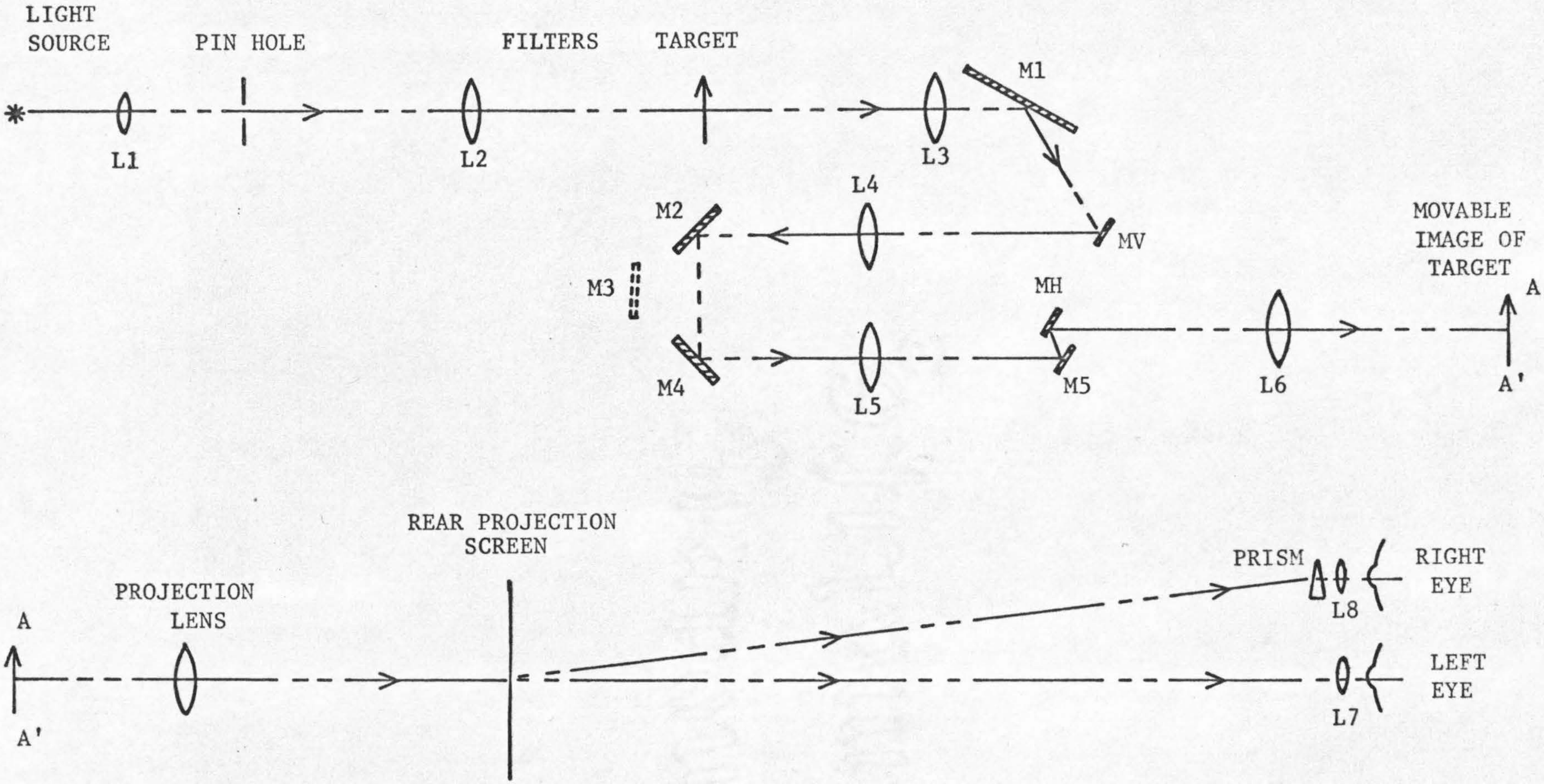

L=LENS M=MIRROR
MH=HORIZONTAL MIRROR GALVANOMETER
MV=VERTICAL MIRROR GALVANOMETER

Fig. 2.6 The optical system for projecting the target

(Fig. 2.6) placed the target optically at infinity. For a bright stimulus, the telecentric nature of the system demands a light source element with very small physical dimensions and with a large proportion of the output in the visible region of the spectrum. Besides satisfying these requirements better than standard incandescent or quartz-iodine lamps, a xenon arc with its color temperature of about 5000° K gives an illumination very similar in spectral content to sunlight. A 900 watt xenon arc (Hanovia 538C-9) driven by a well regulated constant current power supply (Oriel C-72-50) was used as the light source.

Any desired target shape and size can be obtained simply by using the appropriate transparency. Intensity is varied by inserting neutral density filters in the collimated beam before the transparency (Fig. 2.6), and color can be accurately controlled by inserting the required filters in the same place. If the system is linear, any desired two dimensional target motion is easily obtained simply by driving the two galvanometers with the appropriate waveforms. The size of the projection field is of course a function of the position of the projection lens. However, increasing the field simultaneously increases the magnification of the system (ratio of screen image size to transparency target size) and hence makes small targets more difficult to achieve with reasonable brightness and resolution. For all experiments except those performed in the open loop mode, the field size was set to 1 1/2 degrees from the primary position.

3. Calibration, Linearity and Resolution.

From the above descriptions it is clear that the success of the eye movement measurements depends upon the linearity of the photomultiplier tubes and the associated electronics. A device to check their linearity and objectively calibrate the system was constructed as follows. A steel sphere was mounted in a closely fitting nylon socket so that it could be rotated about either a vertical or horizontal axis by means of two micrometers. A miniature incandescent lamp (as used on the contact lenses) was mounted on a short shaft attached to the sphere radially and at right angles to both micrometers. Since the dimensions of the device are known precisely, and since the dimensions of the eye (Fig. 2.2) and contact lens attachments are known, the equivalence between micrometer movement and eye rotation is readily established.

With the device in place of the eye, the linearity of each photomultiplier tube was checked. Fig. 2.7 shows the curve of the left vertical photomultiplier. All four channels had a linear range of at least 3 degrees on either side of the primary, which is more than sufficient for my measurement requirements. To measure the calibration steps, the device was set in the equivalent of the primary position with the calibrating vane "out" (Fig. 2.3). The vane was then moved to the "in" position and the resulting step in the channel output voltage noted. With the vane back in

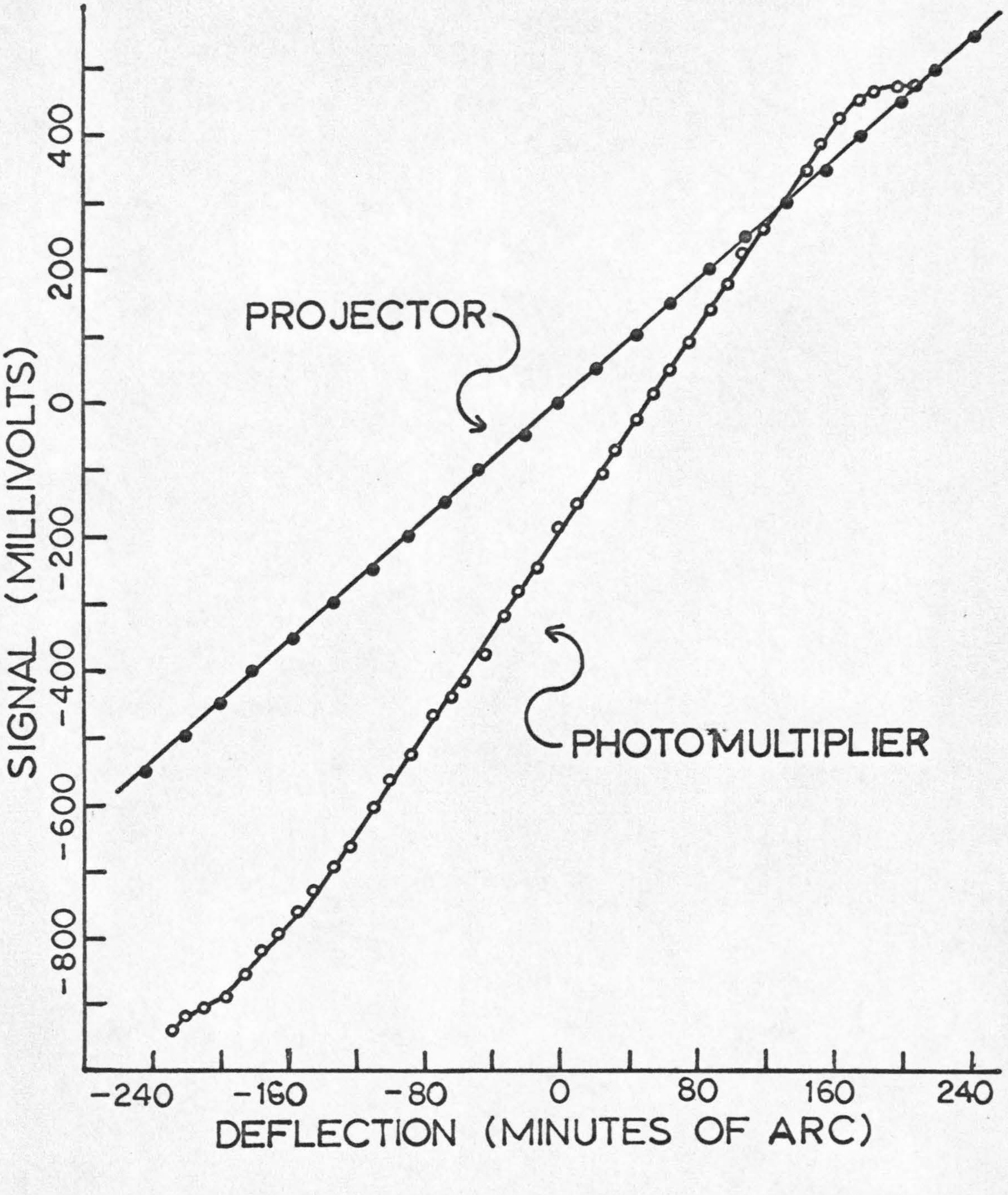

Fig. 2.7 Linearity check of left vertical photomultiplier tube and vertical channel of the target projector

the "out" position, the sphere was rotated until an identical voltage change was produced. The calibration step is of course equal to this equivalent eye movement.

The linearity of the target projector is trivially checked by measuring the deflection on the screen as a function of mirror galvanometer voltage. Fig. 2.7 shows the vertical channel characteristics. The horizontal channel was just as linear.

It is rather difficult to estimate the resolution of the eye movement measurements as so many factors are involved. In this system, slippage, instability of lamp intensity, photomultiplier tube noise, amplifier noise and digital quantization error are the basic limiters of resolution. Discounting slippage and quantization error, the resolution is estimated to be of the order of 30 sec. arc. Slippage was assessed at less than 4 min. arc for 5 degree saccades, and since eye movements in the work that follows are predominantly smooth pursuit movements of the order of 1 degree and even smaller saccades, it is probably safe to assume a resolution of about 1 min. arc in the analog eye movement output, particularly in the fixation experiments. For all moving target experiments the quantization error (and hence resolution) was 2 min. arc which is deemed quite sufficient. Resolution for fixation and stabilized retinal images is discussed in that section.

4. The Open Loop Condition.

The oculomotor system may be represented as a feedback control system with a unity feedback factor. If eye movements are compensated, so that there is no feedback from eye position to target displacement, then this condition is commonly known as open loop (Fender and Nye, 1961). In this mode of tracking, the angular displacement of the target image on the retina from the fovea is precisely the angular displacement of the target from its primary position, and is absolutely (in theory) independent of eye movements. If the target is held stationary in its primary position on the retina, the more common stabilized retinal image condition results.

The open loop condition is achieved by taking the analog output of the eye movement signal, amplifying it, and adding it to the target displacement signal. The amplifier gain must of course be set so that eye movements are compensated for exactly, and this was accomplished as follows. While the subject made voluntary saccades between marks accurately located at the primary position and on one degree horizontally on either side, the gain of the horizontal amplifier was adjusted so that the target (with no external signal) moved precisely between the markers. The same procedure was used to adjust the vertical amplifier gain. Since only one vertical and one horizontal eye movement can be compensated, the apparatus is limited to monocular use for the open loop condition. For convenience it was decided to use the left eye in such experiments.

One of the potential problems with open loop tracking is that of drift. Under normal conditions, if the eye started drifting in some direction, the retinal image would suffer an identical drift making it immediately noticeable and rectifiable. However, in the open loop mode, no retinal image drift results from a drifting eye and the subject, and apparently his oculomotor control system, are unaware of such drifting. As a result open loop experiments exhibit considerably more drift than their closed loop counterparts, particularly when the target is stationary (stabilized retinal image) and the required range of the apparatus is increased. In addition, the overall gain of the system is increased (Fender and Nye, 1961) so that the tracking excursions are greater for the same targets. As is apparent from Fig. 2. 7, the linear range of the system is 3 degrees on either side of the primary which proved sufficient for our needs. The projector was adjusted to give this field for open loop experiments.

How open is the open loop, or equivalently how stable is the stabilized retinal image? Despite its overwhelming importance, this fundamental question has been brushed aside in the literature to an astounding degree. The phenomenon of fading of stabilized retinal images is somewhat controversial and not fully understood (Barlow, 1963; Beeler, Fender and Nobel, 1964; Riggs *et al.*, 1953).

In particular it is impossible to say what degree of stability is required to cause fading (if it will occur); and if the image is of sufficiently low intensity and contrast it will probably fade even with relatively poor stability. Thus the most common argument for achievement of stabilization, namely image fading, is rather meaningless. Barlow (1963) had his subjects compare a stabilized retinal image with an after image, which may be considered as ideally stabilized, and found that the two images deviated by as much as 3 1/2 min. arc. His technique of stabilizing the image was to mount it on a 25 mm long aluminum stalk attached to a contact lens. The instability is naturally attributed to lens slippage. In a similar experiment, Riggs and Schick (1968) concluded that in a one minute interval the image shift had a maximum of about 1 min. arc and a standard deviation of .4 min. arc. They used an external optical system, with a small plane mirror embedded directly in the lens being the only attachment to the lens. Whether this difference is due to the added inertia of Barlow's attachments or Riggs and Schick's superior fitting lenses cannot be said. What can be stated once again is that the stability of the retinal image depends on many elements in the experimental setup, and free extrapolation from other workers' results is not very fruitful.

In my system two factors limit the effectiveness of the loop opening; namely, lens slippage and the precision with which the amplifier gains can be set. The gains can probably be set to an accuracy resulting in an error of about 4 min. arc for a 1 degree movement and of course a proportionally smaller error for smaller movements. From this and the previously measured lens slippage we estimate that for open loop tracking (moving target) the retinal image will differ from the desired image by at most 4 min. arc. For stabilized retinal images (stationary target) the deviation is probably less than 2 min. arc. Some special techniques pertaining to stabilized retinal images are discussed in the appropriate section. The finite bandwidth of the mirror galvanometers (200 Hz) should also be taken into consideration. This may be thought of as introducing a delay of about 5 milliseconds in the feedback loop. For my requirements this figure is quite acceptable.

5. Data Collection.

Data from four channels of eye movements and two channels of target motion were recorded. The analog data were fed into an analog to digital converter and multiplexor, and the result written on digital tape (Cipher 85H tape deck driven by our own logic). This tape was then analysed off line on the Caltech batch processor (IBM 360/75 and IBM 370/155). Target waveforms were generated on the batch processor and written on tape. This tape was read on the Cipher and passed to a demultiplexor and digital to analog converters. The two resultant analog channels were recorded on an FM tape recorder (CEC PR-3300) which was used to drive the target projector during an experiment.

Plug-board programmable timing circuits automatically controlled the time sequence of the experiments. At the beginning of a run the system was started and took care of the run duration, calibration procedure, data collection etc. For reasons discussed later, a sampling rate of 625/6 samples per second per channel was used. Each run was 63 seconds long and consisted of about 60 seconds of continuous tracking with the exception of stabilized retinal images which is discussed later.

6. Subjects.

Two subjects AWG (the author) and CJS were used. With contact lenses on, both had 20/20 vision or better in both eyes. Both subjects successfully completed the Ishihara (1960) color blindness tests (16 plate edition).

III. COMPUTATION OF POWER SPECTRA AND CORRELATION FUNCTIONS AND TARGET GENERATION.

1. Computation of Power Spectra and Correlation Functions.

Power spectra and correlation functions form the foundation of the analysis techniques used in this thesis. While the mathematical principles involved are old and well understood (Davenport and Root, 1958), the problems encountered in numerical computations from experimental data are numerous and far from completely solved (Richards, 1967). For the discussion that follows, consider computing the autocorrelation function and auto power spectrum of a real signal x(t), and the cross-correlation function and cross power spectrum of real signals x(t) and y(t).

The classical approach is to compute the correlation functions

$$R_{xx}(\tau) = \lim_{T\to\infty} \frac{1}{2T} \int_{-T}^{T} x(t+\tau)x(t)\,dt$$

$$R_{xy}(\tau) = \lim_{T\to\infty} \frac{1}{2T} \int_{-T}^{T} x(t+\tau)y(t)\,dt$$

and the power spectra are then obtained from their Fourier transforms.

$$S_{xx}(f) = \int_{-\infty}^{\infty} R_{xx}(\tau)\ \exp\,(j2\pi f\tau)\,d\tau$$

$$S_{xy}(f) = \int_{-\infty}^{\infty} R_{xy}(\tau)\ \exp\,(j2\pi f\tau)\,d\tau$$

But is this the best approach for digital computation? The two main objections are that the Fourier transform calculations require a lot of computer time, and for time sequences that are not impractically short, the same is true of the correlation calculations. The former stumbling block was removed by the discovery of the so-called fast Fourier transform (FFT) (Cooley and Tukey, 1965), but the latter one remains.

Fortunately it is a simple matter to obtain the following equivalent forms from the above expressions. Let X(f) and Y(f) be the Fourier transforms of x(t) and y(t) respectively; then if T is the time length of the two signals we obtain (Blackman, 1965; Richards, 1967):

$$S_{xx}(f) = \frac{1}{T} \mid X(f) \mid^2 \qquad (1)$$

$$S_{xy}(f) = \frac{1}{T} X(f) Y^*(f) \qquad (2)$$

The asterisk indicates the complex conjugate. From this formulation the power spectra can be computed very efficiently (in the compute-time sense) thanks to the FFT. However, if results are to be meaningful, an estimate of the stability and resolution of the spectra is needed. The following derivations are based on the assumption of Gaussian signals, which is indeed true in this work as will be shown in the next section. Actually, in practice the derivations are generally used even for non-Gaussian signals (Richards, 1967).

In order to prevent aliasing, the signals must be sampled at a rate at least twice that of the highest frequency present. Subsequent results will show that signal levels are always down at least 30 db by 8 hz, so that a sampling rate of 20 hz would be adequate. For reasons to be discussed, the sampling rate was in fact 625/6 hz. The length of the runs was limited to one minute since I found that the subjects could not track continuously for longer intervals without fatigue marring the records. A fundamental limitation of the FFT is that the number of data points in the sequence has to be a power of 2. I would therefore have to reduce the data sequences to 4096 samples, or 39.4 seconds. Blackman and Tukey (1958) show that the frequency resolution would have been .0254 hz, an admirable figure. Unfortunately the statistical error (see below) would be of the order of 1.23, a far less admirable figure.

The problem then is to find a way to surrender some frequency resolution in return for a greater statistical reliability. This is accomplished by windowing. In the time domain windowing is achieved by multiplying the correlation function by a window function $g(\tau)$, which is chosen to be unity for $\tau=0$ and zero for $|\tau|>T_m$, the width of the window. The decay of the function from $\tau=0$ to $|\tau|=T_m$ should be a compromise between a rather flat curve and a gently sloping curve. The particular choice of a window function is a rather arbitrary procedure governed mainly by experience. The difference in effect between the more common window functions is small, assuming the signals have no special structures that can be emphasized by a particular window. For my purposes any of the better window functions would suffice, and one devised by Julius von Hann and known as hanning, is used here:

$$g(\tau) = 1/2\left(1+\cos\frac{\pi\tau}{Tm}\right) \qquad \text{for } |\tau| \le T_m$$

$$= 0 \qquad \text{for } |\tau| > T_m$$

Since the power spectrum is the Fourier transform of the correlation function, the windowing may equally well be performed by a convolution in the frequency domain. Moreover, since the data is discreet, the convolution reduces to a weighted average which is a trivial matter. It can be shown that the resolution of the windowed spectrum is given by:

$$\Delta f = \frac{1}{T_m}$$

Consider a sequence of computed power spectra which approximate the same ideal spectrum. Then at any point there is an average value and an RMS deviation, and their ratio is defined as the statistical error which can be shown to be:

$$E = \frac{\text{RMS}\Delta S}{\text{Avg } S} = \sqrt{\frac{1}{T\Delta f}}$$

where T is the length of the original record.

A window width of 9.84 seconds (1024 samples) was chosen, allowing the sequences of length 49.2 seconds (5120 samples) to be split into 5 segments. It is felt that the resultant frequency resolution of .102 hz and statistical error of .447 (3.5 db) are the best compromise. The procedure was to break the signals into the 5 segments and to compute a raw spectrum for each segment from equation (1) for auto spectra and equation (2) for cross spectra. These spectra were averaged and smoothed by hanning, yielding the final smoothed or windowed spectra. The auto spectra are of course real, and the complex cross spectra are readily reduced to amplitude and phase components. Whenever spectra are plotted, the amplitude is plotted in decibels and the frequency on a logarithmic scale. The phase is taken to lie between $\pm 180^{\circ}$. It is important to bear in mind the resolution and error limitations of these spectra when interpreting results. Usually several spectra are plotted together and identification markers are used to distinguish them. These markers do not represent data points on the curves.

Having readily obtained the power spectra, it might seem logical to obtain the correlation functions by taking inverse Fourier transforms of the spectra. However, the result would be a windowed correlation function which is not suitable for my purposes. It is possible to multiply this by the inverse of the window function to retrieve the original correlation function.

This function would be the result of a Fourier transform, an inverse Fourier transform, a frequency domain windowing operation and a time domain inverse windowing operation together with the accumulated approximation errors and computation errors. What the extent of these errors may be, is difficult to say.

In the work that follows, the location of the peak of the cross-correlation function will be used to measure time delays in the oculomotor system. Since these delays are of the order of 200 milliseconds, only about 20 lag values of the correlation functions are needed (as opposed to more than 2000 to compute power spectra the conventional way), so that the standard computation can be used with low cost and good accuracy. All correlation functions were normalized to a maximum of unity. As in the case of power spectra, it is necessary to know how much faith can be placed in these functions. Strangely enough, in contrast to the spectra, there do not appear to be any simple theories which can handle this. As far as my results are concerned, this is not a severe restriction as all information extracted from these functions is subjected to standard statistical analysis. A data sampling rate of about 100 hz was dictated by the need for a resolution of about 10 milliseconds in the correlation functions. The actual frequency was 625/6 hz (this peculiar figure results from halving the frequency of a 10 khz oscillator 4 times and then multiplexing 6 channels) giving a resolution of 9.6 milliseconds.

2. Target Generation.

All target waveforms were generated digitally on the batch processor and then converted to analog form to drive the mirror galvanometers. The standard format was two multiplexed channels, with each sample point occupying one byte. The range was 150 min. arc giving a target resolution of the order of 1/2 min. arc. In all waveforms the signal was down at least 30 db by 8 hz demanding a sampling rate in excess of 16 hz. To facilitate digital filtering, a rate of 100 hz was in fact used. Three basic target types were used, namely: periodic signals, low-pass filtered Gaussian noise and band-pass filtered Gaussian noise.

2.1 White Gaussian Random Noise. In principle it is possible to generate a sequence of numbers with a Gaussian distribution and with a power spectrum (when treated as a time series) of any desired shape (Franklin, 1965). However, this approach is not practical and instead, the desired spectral characteristics were achieved by digitally filtering white noise. The problem is then reduced to generating a sequence of numbers, with a Gaussian distribution, that are random; so that when treated as a time series, their spectrum will be flat. This was done with a program "GAUSS" (IBM Scientific Subroutine Package) based on the method of Box and Muller (1958) of obtaining Gaussian random numbers from a uniform distribution of random numbers.

Examination of the autocorrelation functions and power spectra of these sequences verified that they were indeed random to at least the resolution of our computations.

2.2 Digital Filtering. A low pass digital filter was designed, by the frequency-transformation method (Blackman, 1965), to approximate the analog transfer function:

$$G(s) = \frac{1}{1+sT}$$

The approximation error is less than 1% for frequencies up to 5 hz and less than 3% for frequencies up to 10 hz. To generate the low pass filtered waveforms, the white Gaussian noise was passed through a cascade of five of the above filters. Six such waveforms were used in this work. Their future designations and cutoff frequencies in hz are respectively:

R0: 0.3, 0.5, 1.0, 2.0, 2.5 R1: 0.5, 0.8, 1.5, 2.0, 2.5
R2: 0.5, 2.0, 2.5, 3.0, 4.0 R3: 2.0, 2.0, 2.5, 2.5, 4.0
R4: 2.0, 2.5, 3.0, 4.0, 8.0 R5: 2.5, 3.5, 4.0, 8.0, 8.0

Fig. 3.1 shows the power spectra for these waveforms taken from actual experimental measurements of galvanometer voltages.

The same technique was used to design a digital approximation to the analog band pass filter:

$$\frac{(1+sT_1)}{(1+sT_2)(1+sT_3)} \qquad T_1 \geq T_2 \geq T_3$$

Six waveforms were generated by passing white Gaussian noise through a cascade of five such filters, all with a center frequency of 0.5 hz and a pass band approximately symmetric about 0.5 hz

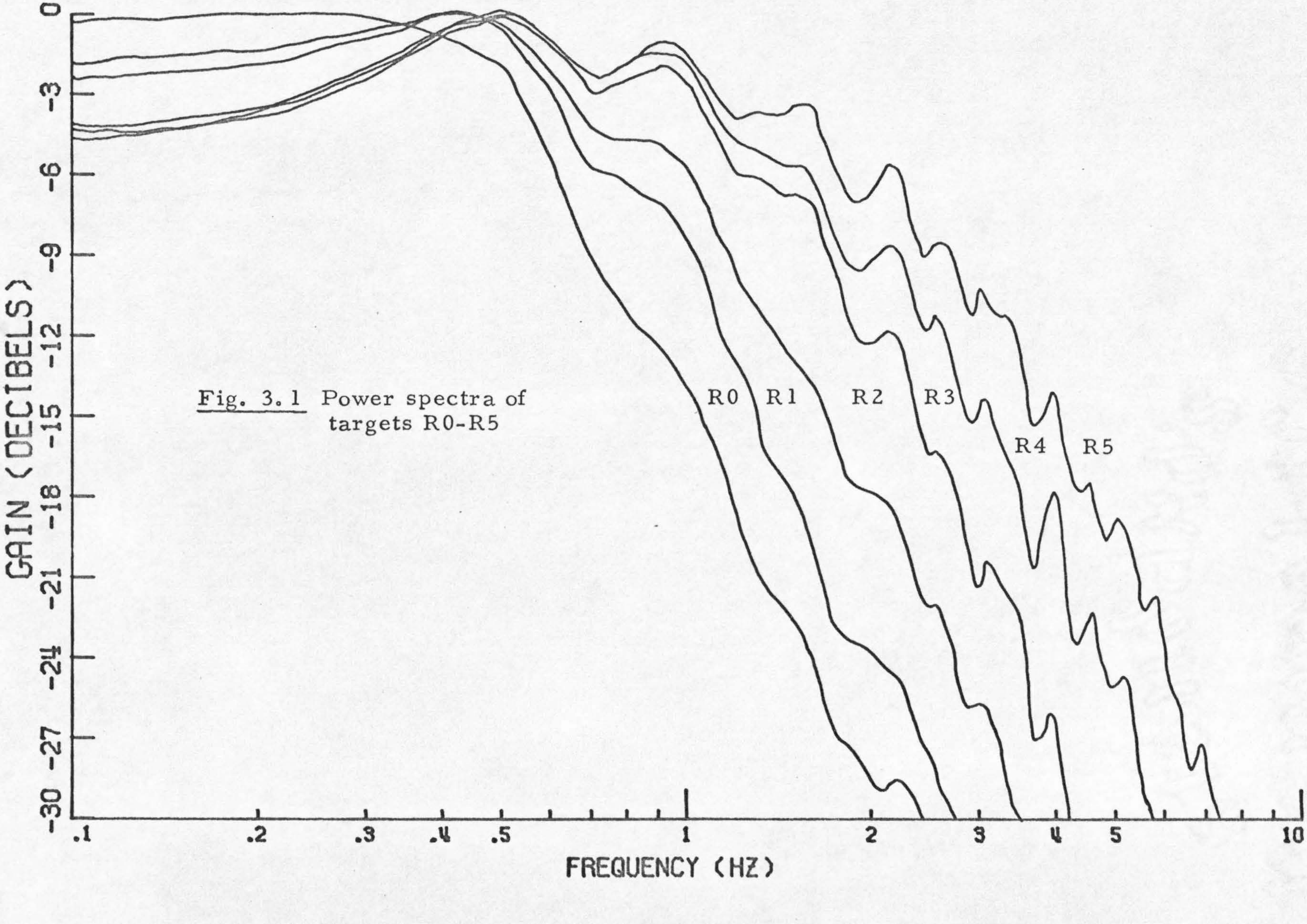

Fig. 3.1 Power spectra of targets R0-R5

on a logarithmic scale. The cutoff frequencies (in hz) for the six waveforms are:

B1: (0.001, 0.5, 0.5), (0.001, 0.5, 0.5), (0.001, 0.5, 0.5), (0.001, 0.5, 0.5), (0.001, 0.5, 0.5)

B2: (0.001, 0.45, 0.5), (0.001, 0.35, 0.7), (0.001, 0.25, 1.0), (0.001, 0.17, 1.5), (0.001, 0.17, 1.5)

B3: (0.001, 0.45, 0.5), (0.001, 0.31, 0.8), (0.001, 0.17, 1.5), (0.001, 0.13, 2.0), (0.001, 0.13, 2.0)

B4: (0.001, 0.35, 0.5), (0.001, 0.13, 2.0), (0.001, 0.1, 2.5), (0.001, 0.1, 3.0), (0.001, 0.06, 4.0)

B5: (0.001, 0.11, 2.0), (0.001, 0.11, 2.0), (0.001, 0.1, 2.5), (0.001, 0.1, 2.5), (0.001, 0.06, 4.0)

B6: (0.001, 0.11, 2.0), (0.001, 0.09, 2.5), (0.001, 0.08, 3.0), (0.001, 0.06, 4.0), (0.001, 0.03, 8.0)

The power spectra for these waveforms (also measured during an actual experiment) are shown in Fig. 3.2.

2.3 Periodic Waveforms. In addition to simple sine waves, 5 periodic waveforms were used. These were generated simply by adding together the desired harmonics of chosen amplitude. The fundamental frequency fo was chosen to be 0.5 hz. The relative amplitude[*] of the harmonics present in the five waveforms are:

---

[*] By relative amplitude I mean that, for example in P2, if the component at fo has a magnitude of 100 millivolts, then the component at 2fo has a magnitude of 50 millivolts.

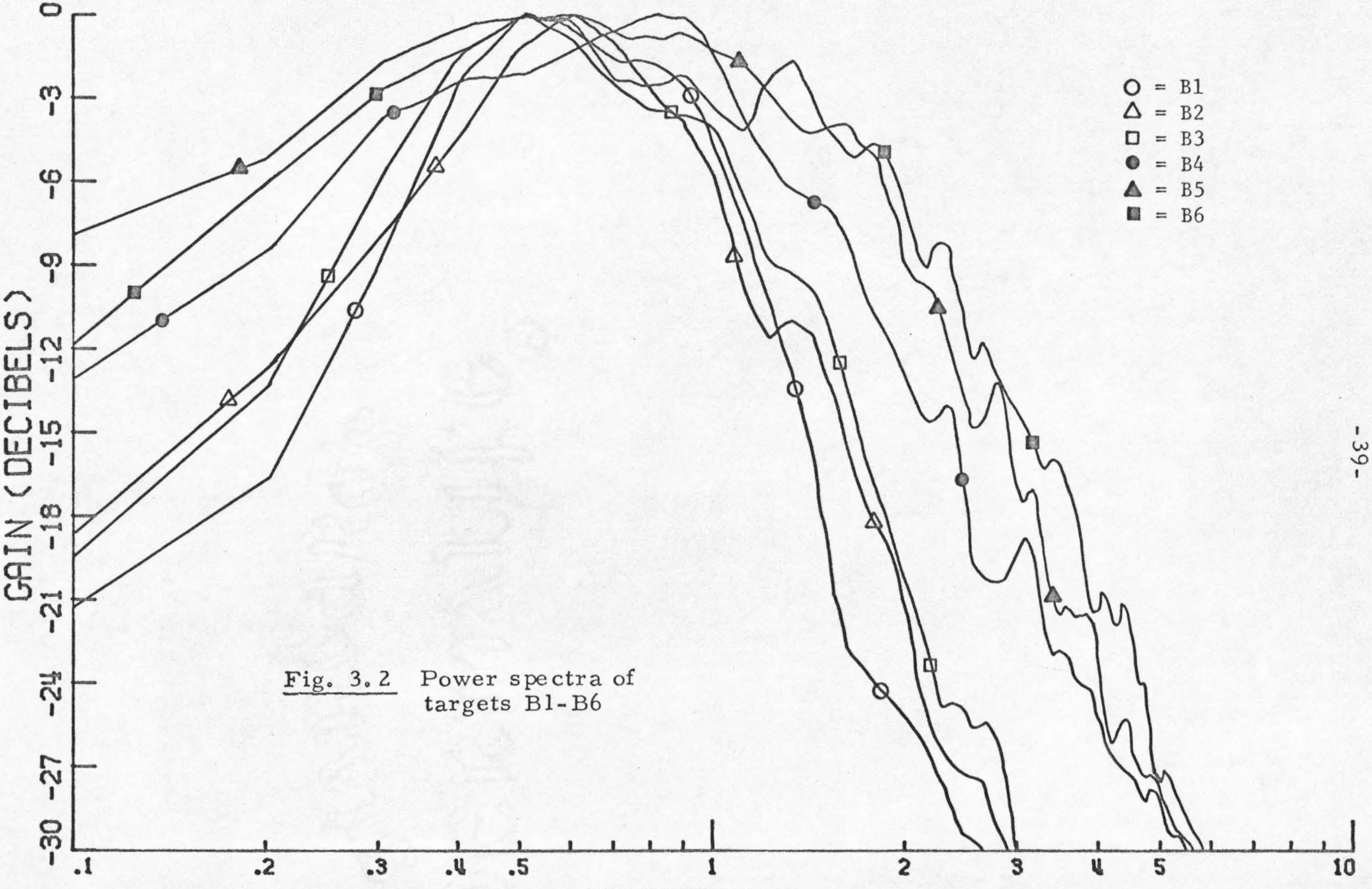

Fig. 3.2 Power spectra of targets B1-B6

P2: $f_0(100)$, $2f_0(50)$

P3: $f_0(100)$, $2f_0(25)$, $3f_0(25)$

P4: $f_0(100)$, $2f_0(35)$, $3f_0(25)$, $4f_0(25)$

P5: $f_0(100)$, $2f_0(35)$, $3f_0(25)$, $4f_0(20)$, $5f_0(15)$, $6f_0(15)$, $7f_0(10)$, $8f_0(20)$

P6: $f_0(100)$, $2f_0(50)$, $3f_0(70)$, $4f_0(20)$, $5f_0(10)$, $6f_0(10)$, $7f_0(10)$, $8f_0(10)$

In the section on periodic signals, P1 refers to a 0.5 hz sine wave.

2.4 Gaussian Verification

We have yet to show that the filtered waveforms have a Gaussian distribution. This is illustrated in Fig. 3.3 which compares the distribution of R1 with the ideal Gaussian curve. Fig. 3.3 also shows the distribution of one of the eye movements, in response to target R1, for both subjects. These too are Gaussian, justifying our assumption made in Section 1. In view of the central limit theorem, these results are not surprising.

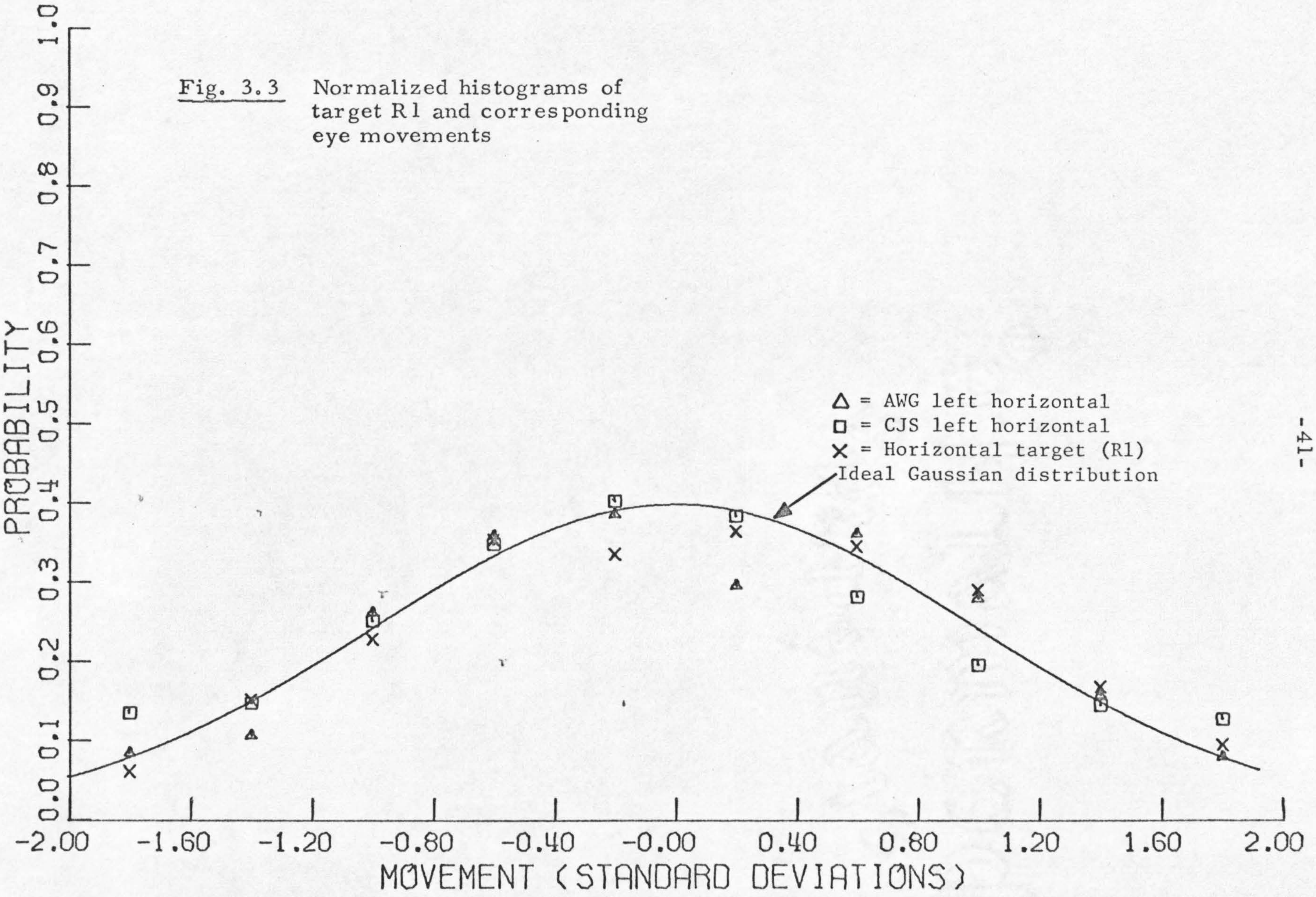

Fig. 3.3 Normalized histograms of target R1 and corresponding eye movements

IV. INTERACTION BETWEEN VERTICAL AND HORIZONTAL TRACKING

1. Introduction.

A complete description of eye movements has six degrees of freedom, that is vertical, horizontal and torsional movements for each of two eyes. If torsional movements are not a feature of the experiment, only four channels need be monitored. However, the bulk of eye movement information available has been gathered with one or more of the following restrictions: horizontal only, monocular only, vertical only. These data can only be used comparatively if the above restrictions are not important.

The binocular problem is twofold, since there is the option of viewing the target monocularly or binocularly, and the resulting movements may be recorded for either one or both eyes. The literature indicates that there are no consistent differences between movements of the left eye in response to a target viewed monocularly by the left eye, and movements of the right eye in response to the same target viewed monocularly by the right eye. There is always the possibility of a subject having some unsuspected abnormality in one eye, so that a comparison between eye movements has to be made separately for each set of experiments. The problem of binocular versus monocular viewing is more complex. In binocular tracking tasks, the eyes move mainly in synchrony (conjugate movements), but there are small asynchronies leading to retinal disparities. These disparities are partly corrected by vergence eye movements. Monocular viewing differs from binocular viewing in the absence of these disparities and their effect on tracking. Rashbass and Westheimer (1961a, 1961b) have shown that disjunctive eye movements are slow and independent of conjugate movements, and since disjunctive movements are small compared to conjugate movements in tracking, the difference between the two viewing conditions does not appear to be significant in general. The situation is similar for fixational movements, but of course here the relative size of disjunctive movements is greater (Krauskopf et al., 1960; Nachmias, 1959). In short then, although the motions of the left and right eyes may in general be treated as similar, there are differences between monocular and binocular viewing, and their relevance to a particular result can only be judged from the data.

The situation is somewhat parallel for vertical and horizontal movements. In the first place, are the vertical movements in response to some vertical target motion essentially the same as horizontal movements in response to the same target motion presented horizontally? Here too, a review of the literature shows that this is indeed true in general (see also section 4 of this chapter) although once again conclusions can only be drawn from particular data. The second, and more important question is, what effect do vertical stimuli have on horizontal movements and vice versa? It is interesting to speculate on this point using the known neurology of the oculomotor system. While small horizontal and vertical movements are mediated by essentially separate sets of extraocular muscles, there is only one of each of the relevant brain centers such as the lateral geniculate or visual cortex (Whitteridge, 1960). Thus, on the one hand, the neurology points to the oculomotor system as being a two channel system, and on the other hand as a single channel system.

Although this topic is barely mentioned in the literature, it seems to be generally accepted among workers in the field that the vertical and horizontal systems are independent. For instance, most modelers of the system model only a one dimensional system, and suggest an identical replication for the second dimension. It is true that if the raw eye movements are examined in response to a target consisting of say a 0.8 hz sine wave in the vertical direction and a 0.5 hz triangular wave in the horizontal direction, there appears to be no gross interaction between the two systems. However, St-Cyr and Fender (1969c) did find some interaction. Their stimuli consisted of the sum of 4, 7 or 13 sinusoids on the vertical channel and a similar sum on the horizontal channel, with all 8, 14 or 26 sinusoids having no low-integral relationship. From power spectra of the eye movements, they showed that one subject had vertical eye movements at frequencies present only in the horizontal stimulus, whereas the horizontal movements contained no frequencies present in the vertical stimulus. A second subject showed no cross-talk at all.

Feinstein (1970) considered the problem by isolating smooth pursuit and saccadic movements. He studied the saccadic interaction by presenting a vertical (or horizontal) target step followed after a random time interval by a horizontal (or vertical) target step. The fact that the reaction time to the second step was a function of the interval between steps, showed that there is some interaction between the vertical and horizontal saccadic systems. Next he moved the target vertically with a triangular waveform and added a horizontal step with random phase relative to the triangular wave. The saccade reaction time was dependent on the frequency of the triangular wave and the phase difference, leading to the conclusion that the vertical smooth pursuit and horizontal saccadic systems are interrelated. He also comes to the rather tenuous conclusion that the vertical and horizontal smooth pursuit systems are independent. In my opinion this conclusion is not supported by his data.

2. Assessing Interaction.

We have established the need for a better understanding of the interaction between the vertical and horizontal tracking systems. The crucial question is how is this cross-talk best measured? There are, of course, a multitude of experiments that could be designed to probe this cross-talk, and each has, to some degree, the same weakness of specificity. As an illustration of this specificity, it is impossible to conclude, from the above experiments, how the time delays (see below) of sine wave tracking would be effected by a random signal in the orthogonal direction.

At the one extreme we can look at specific properties of the oculomotor system such as saccades or smooth pursuit movements, and at the other extreme we can look at very broad properties such as information handling capacity or compute capability. While the latter approach is potentially more powerful and in theory covers the former properties as special cases, our present level of sophistication forces us to compromise between the two. A natural compromise is suggested by the close correspondence between information content and correlation coefficients and power spectra in Gaussian random functions (Bell, 1962; Gel'fand and Yaglom, 1957). The idea then is to use a high information content or complex waveform on one channel (i. e., tracking direction), and a low information content or simple waveform on the other channel.

Fig. 3. 1 shows that the waveforms R0-R5 have a progressively increasing high frequency content. Initially I shall rather loosely refer to this increase as an increase in bandwidth, and in section 5 I shall formally define bandwidth as a quantitative measure. In appendix 1 it is shown that increasing the bandwidth increases the information content of the waveform. Thus R0-R5 may be thought of as random waveforms of increasing information content or complexity. As discussed in appendix 1, it can also be shown that if two Gaussian random signals have a cross-correlation coefficient r, then the mutual information between the signals is given by:

$$H = 1/2 \log (1-r^2)$$

This definition will be used in later sections.

A 1 hz sine wave was used for the vertical component and low-pass filtered Gaussian random noise (targets R1-R5 as described previously) as the horizontal component. The amplitude of the sine wave was one degree peak, and the noise had a mean of zero and a standard deviation of 30 min. arc. Each session consisted of six runs, the horizontal component being successively zero (to provide a reference point for the sine wave tracking), R1, R2, R3, R4 and R5. The target image was a white (color temperature 5000° K) dot with a luminance of 52 footlamberts, and subtending an angle of 6.5 min. arc at the retina. Background luminance was .0005 fL. Occasionally one of the runs was fouled by equipment failure. These will be noticed by omission in the results.

The analysis is based on the normalized cross-correlation functions between vertical and horizontal target components and their respective eye movement responses, and on the auto power spectra of the eye movements. The peak value of the correlation function indicates the proficiency of tracking or the mutual information between target and eye movements (as shown in appendix I), and the location of the peak indicates the time delay of the system. In a subsequent chapter the meaning of this "time delay" is discussed in detail, but for the moment it may be considered as a definition. From the power spectra we can learn about the frequency domain charateristics of the system, and in particular how it is responding to different bandwidth signals.

3. Analysis of Interaction Between Vertical Sine and Horizontal Noise Tracking.

Figs. 4.1a and 4.1b show a section of the time course of the vertical sine component and horizontal noise component (R3 in this case) together with the responding eye movements for AWG and CJS respectively. The situation is the same for the other noise components, except that they differ in their "randomness". These figures seem to indicate that the vertical movements are indeed sinusoidal without noticeable interference from the noise, and that the horizontal movements mimick the noise without sinusoidal contamination. However, it is quite apparent that such an insensitive analysis technique is very vague, and could not hope to detect anything but the grossest of interference. It is worth mentioning that although the dot wanders all over the screen, the subject is definitely aware of periodic motion in the vertical direction and random motion in the horizontal direction. Since the eye movement system and the perceptual mechanism do have common elements, these subjective impressions are not irrelevant.

Tables 4.1a and 4.1b show the peak cross-correlation coefficients and time delays for AWG and CJS respectively, for two complete sets. It is felt that the coefficients are reliable (from the computational error point of view) to at least three significant figures, while the time delays, with their 9.6 millisecond interval, are adequately represented by integers.

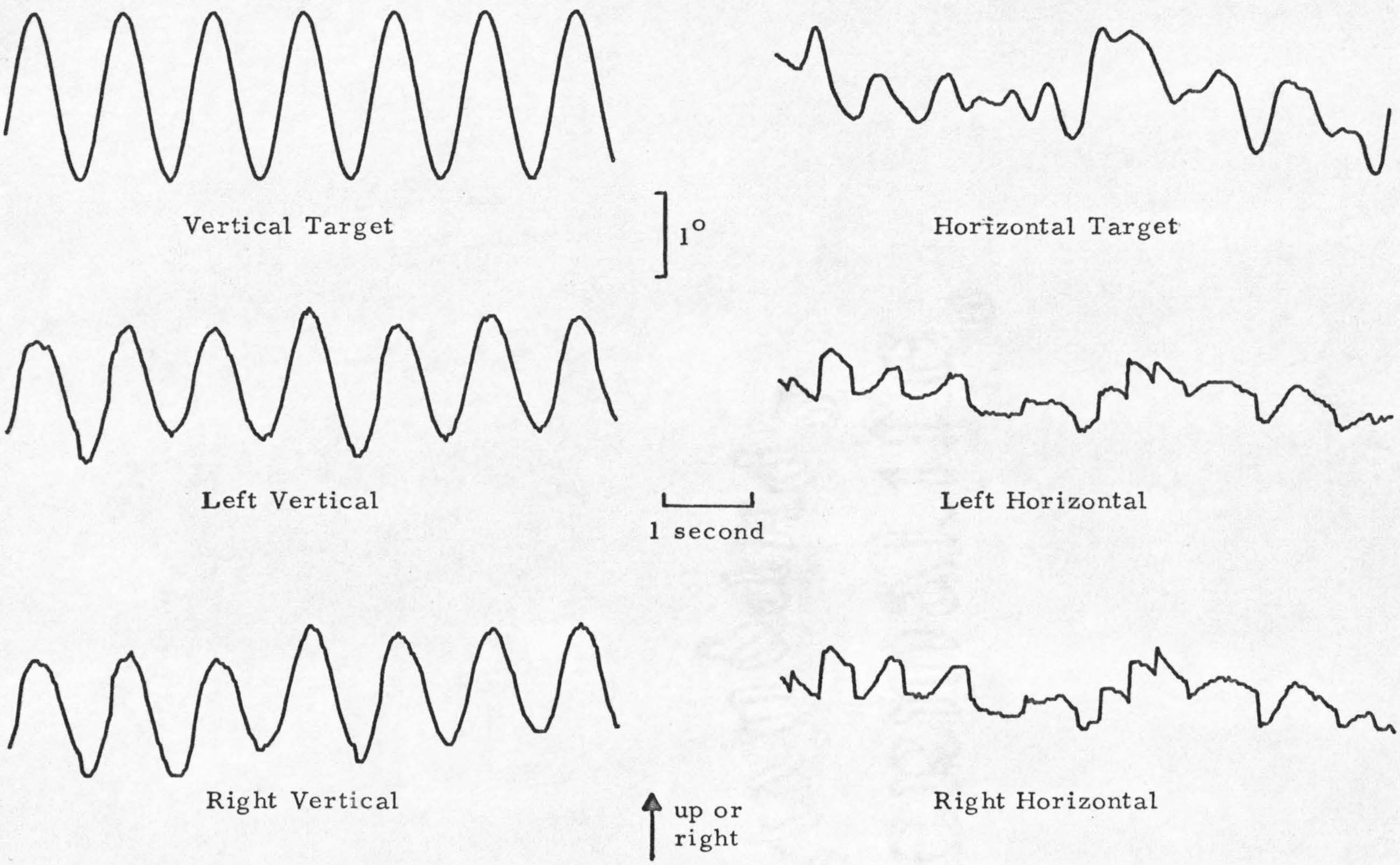

Fig. 4.1a Eye movements for AWG. Vertical target is a 1 hz sine; horizontal target is R3

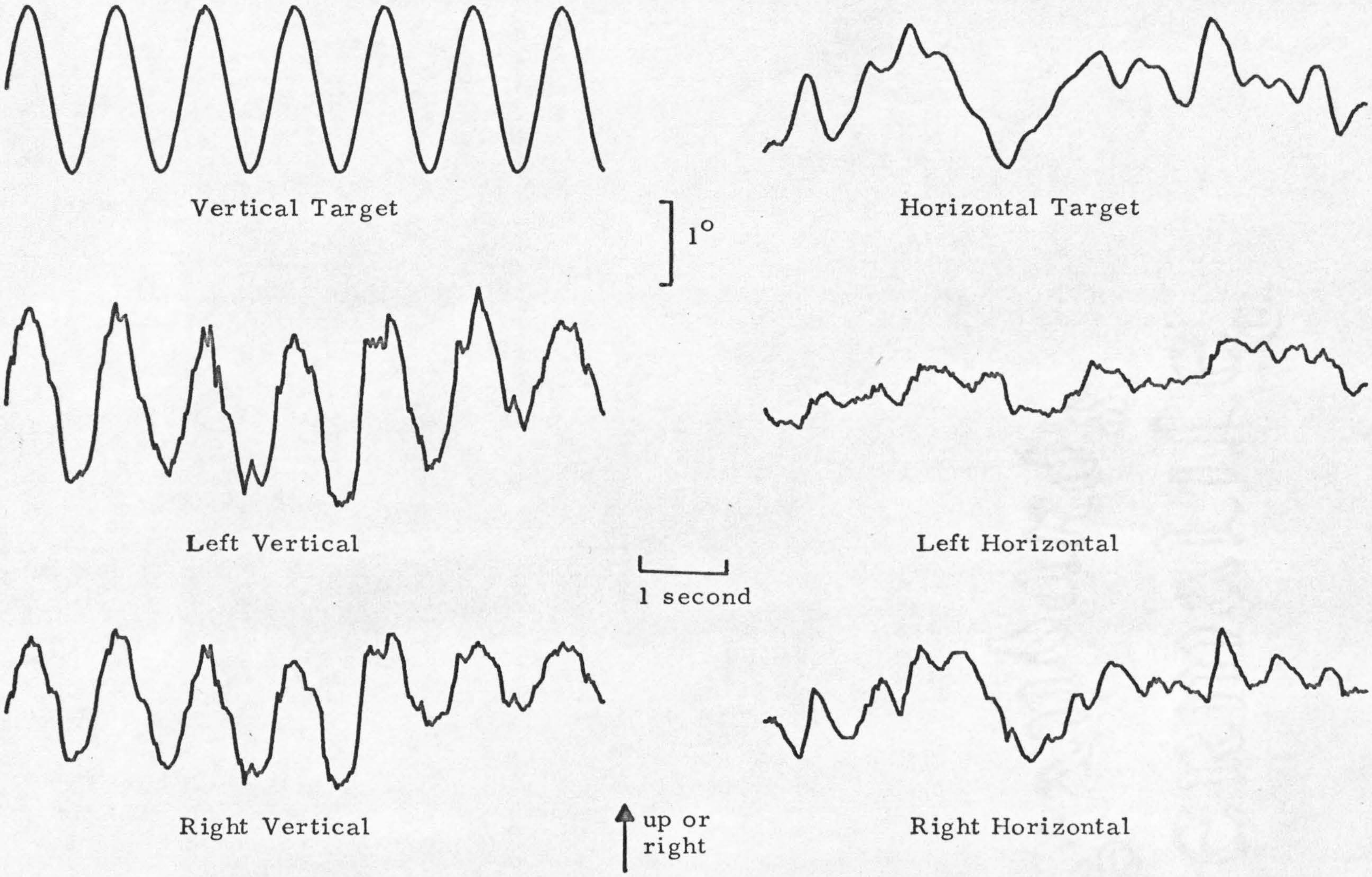

Fig. 4.1b Eye movements for CJS. Vertical target is a 1 hz sine; horizontal target is R3

Run	Horizontal	Left Vertical		Left Horizontal		Right Vertical		Right Horizontal	
No.	Target	Delay MS	Coef.	Delay MS	Coef.	Delay MS	Coef.	Delay MS	Coef.
61	0	10	.977			0	.972		
62	R1	19	.950	134	.949	10	.954	125	.944
63	R2	19	.953	154	.910	10	.964	154	.905
64	R3	29	.933	154	.772	19	.951	134	.761
65	R4	29	.914	154	.696	19	.941	144	.699
66	R5	48	.920	154	.631	38	.938	144	.626
73	0	10	.983			10	.978		
74	R1	19	.961	163	.918	19	.953	154	.922
75	R2	19	.953	154	.874	19	.958	134	.891
76	R3	29	.941	154	.800	19	.937	134	.794
77	R4	29	.952	154	.654	19	.933	144	.681
78	R5	29	.940	163	.512	29	.915	154	.521

Table 4.1a Interaction between vertical sine and horizontal noise tracking for AWG

Run No.	Horizontal Target	Left Vertical		Left Horizontal		Right Vertical		Right Horizontal	
		Delay MS	Coef.	Delay MS	Coef.	Delay MS	Coef.	Delay MS	Coef.
67	0	10	.927			10	.935		
68	R1	29	.910	125	.628	29	.797	154	.756
69	R2	19	.869	163	.536	19	.763	163	.580
70	R3	38	.874	154	.652	29	.761	154	.676
71	R4	38	.891	154	.255	29	.785	163	.620
72	R5	38	.874	144	.303	29	.809	154	.522
79	0	10	.901			10	.816		
81	R2	29	.874	163	.692	0	.768	182	.726
82	R3	38	.873	144	.620	29	.745	134	.420
83	R4	38	.861	182	.336	19	.790	163	.521
84	R5	48	.836	182	.154	38	.740	192	.444

Table 4.1b Interaction between vertical sine and horizontal noise tracking for CJS

Two complete runs are shown for each subject to indicate the variations between subjects and the day to day fluctuations of each subject. Throughout this thesis it was found that coefficient magnitudes would change from day to day or week to week, depending on many factors, not least of all the subject's disposition. However, it is the trends in these coefficients (for example their change with target bandwidth) that we examine rather than their absolute values, and these trends show remarkable consistency. Note that the fluctuations are much greater for CJS than for AWG.

It is not at all surprising to find that the variation of the cross-correlation coefficients of the horizontal eye movements with the horizontal target is heavily dependent on the target bandwidth. After all, the more random, or "faster moving", or "unpredictable" a target is, the more difficult it is to follow. The exact nature of this dependence is more interesting and complex and will be discussed later. It is a little surprising to find that the horizontal time delays are more or less constant. The details of this too are deferred to a later chapter.

Although the vertical target component is always the same 1 hz sine wave, the tables show that the correlation coefficients of the vertical eye movements decrease as the bandwidth of the horizontal target increases. This leaves no doubt that there is significant cross-talk from the horizontal target component to the vertical eye movements. The time delays for vertical tracking seem to be only slightly dependent on the horizontal target motion.

The peak cross-correlation coefficient does not explain everything. For example, in run 62 AWG tracks the sine wave with a coefficient of .950 (LV) and the noise R1 with a coefficient of .949 (LH). Although the coefficients are almost identical, the waveforms are very different, and different tracking mechanisms may be involved. It is also impossible from these coefficients to tell whether the vertical target sinusoid is affecting the horizontal tracking. To elucidate these aspects, the power spectra are studied. This is effectively the same as looking at the shape of the correlation functions, but power spectra are much easier to interpret.

Figs. 4.2a and 4.2b show the auto power spectra for the right horizontal eye movements for one sequence of runs for subjects AWG and CJS respectively. All the horizontal spectra for AWG were of this nature and about ninety percent of the horizontal spectra for CJS were of this nature. Fig. 4.2c is typical of the remaining ten percent for CJS. The spectra show a relatively smooth roll-off. There is no evidence of consistent peaking at 1 hz, so I conclude that there appears to be no significant cross-talk from the sinusoidal target to the horizontal tracking. However, this measurement is not as sensitive as the correlation measurements. If we wished to pursue this point, a comparison of the noise tracking correlation coefficients with and without the vertical sine wave present would yield much more information. Fig. 4.2a also shows that AWG responds to higher bandwidth targets by

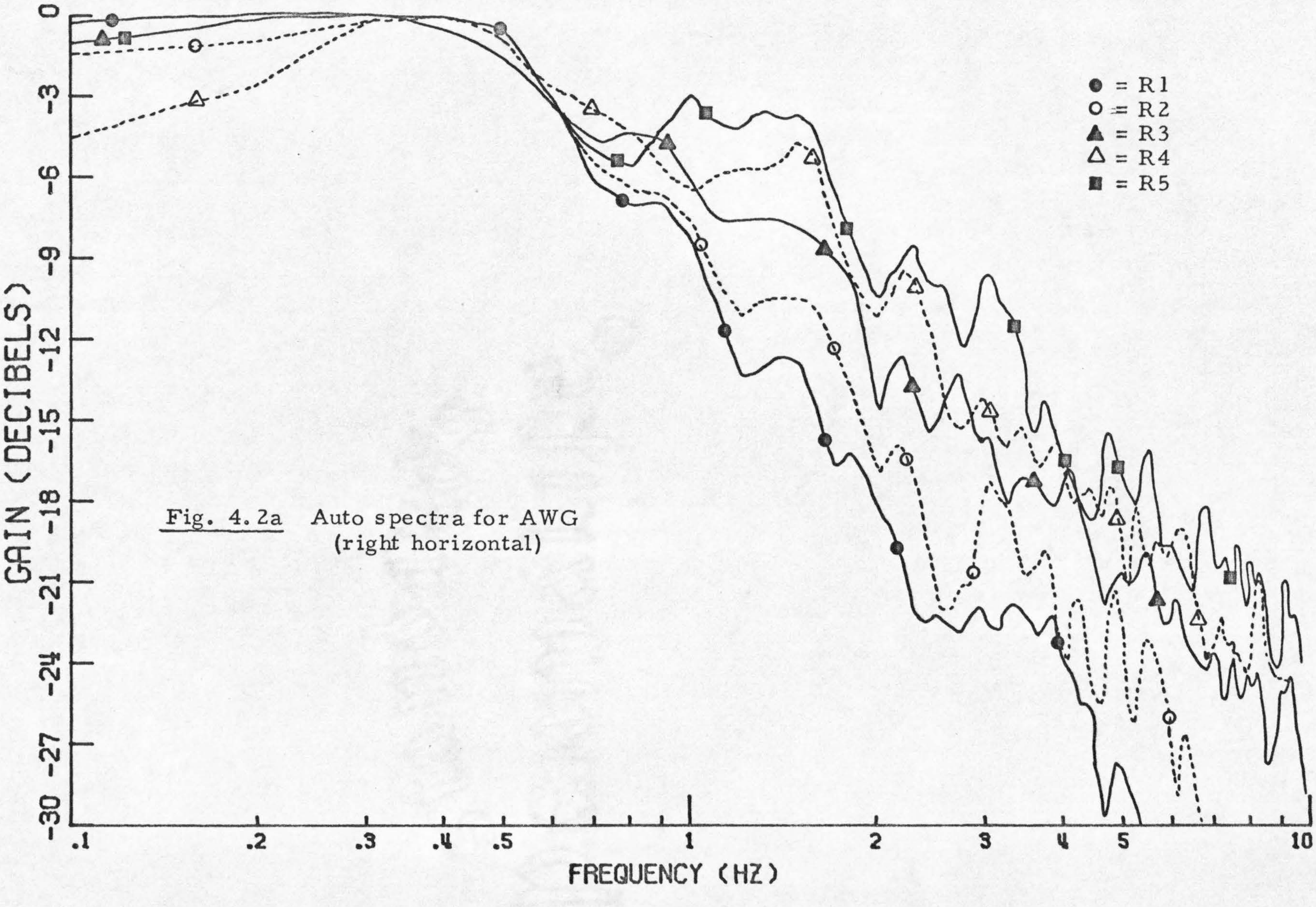

Fig. 4.2a Auto spectra for AWG (right horizontal)

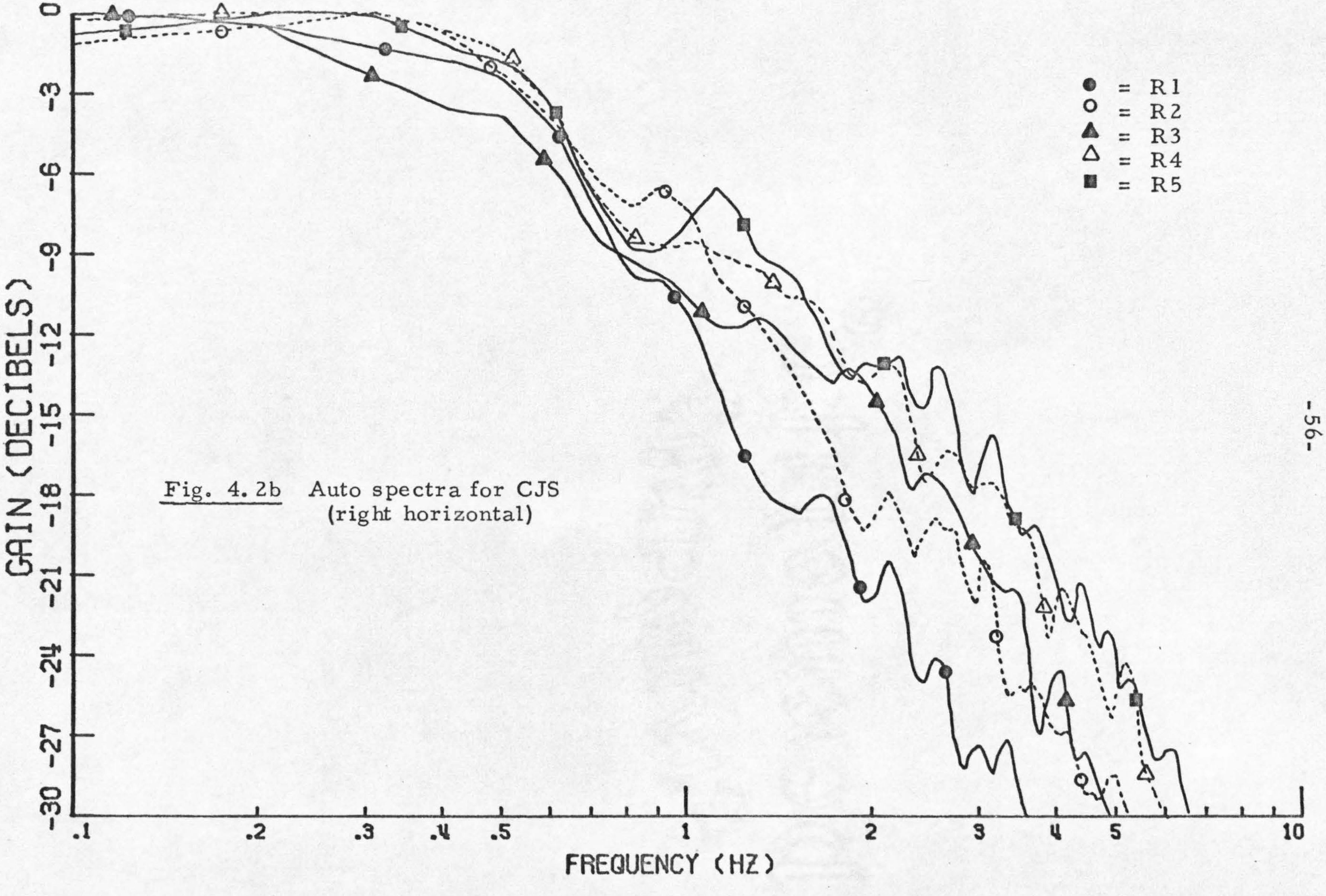

Fig. 4.2b Auto spectra for CJS (right horizontal)

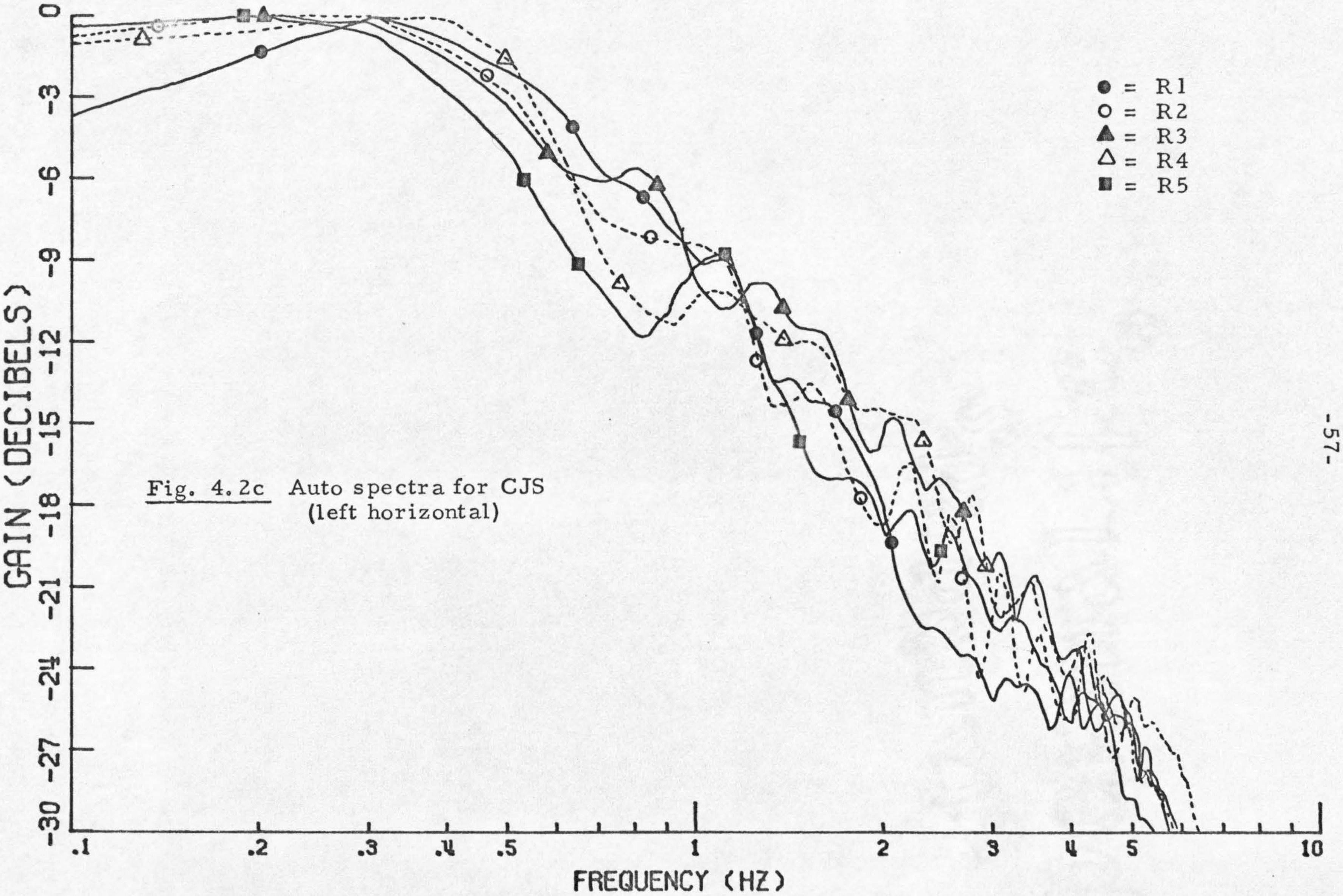

Fig. 4.2c Auto spectra for CJS (left horizontal)

increasing the bandwidth of his eye movements. The situation is not always as clear cut as Fig. 4.2a in that there is sometimes more mingling of the curves and sometimes for example, the bandwidth for tracking R2 may exceed that for R3. However, the general trend is always the same. The same applies to most of CJS's tracking as typified by Fig. 4.2b. This situation is logical enough. The situations such as Fig. 4.2c where CJS appears to have a constant output spectrum regardless of the input bandwidth are indeed unexpected. Note that in these situations (e.g., Fig. 4.2c corresponds to runs 68-72 LH), the effectiveness of tracking, as measured by the correlation coefficients, is far inferior to the more common situation. This is particularly true for the higher bandwidth targets as may be expected.

4. Analysis of Interaction Between Horizontal Sine and Vertical Noise Tracking.

Is the interference from horizontal target to vertical tracking the same as the interference from vertical target to horizontal tracking? This question is easily answered by simply reversing the above experiment and presenting the sinusoid as the horizontal component and the noise as the vertical component. The results of this experiment are illustrated in tables 4.2a and 4.2b. It is clear that these tell the same story as tables 4.1a and 4.1b. In general the correlation coefficients in tables 4.2a and 4.2b are slightly lower than their counterparts in tables 4.1a and 4.1b, but this is within the range of normal fluctuation. The power spectra

Run	Vertical	Left Vertical		Left Horizontal		Right Vertical		Right Horizontal	
No.	Target	Delay MS	Coef.	Delay MS	Coef.	Delay MS	Coef.	Delay MS	Coef.
85	0			19	.984			10	.985
86	R1	96	.921	48	.944	86	.888	29	.953
87	R2	154	.931	38	.950	144	.912	29	.960
88	R3	144	.724	48	.927	134	.700	38	.932
89	R4	144	.618	58	.878	144	.578	38	.890
90	R5	134	.351	38	.903	125	.263	19	.913
97	0			10	.970			0	.964
98	R1	115	.944	29	.952	106	.932	29	.957
99	R2	144	.899	29	.950	134	.908	19	.950
100	R3	144	.705	38	.929	134	.645	29	.937
101	R4	154	.574	29	.910	144	.634	29	.902
102	R5	154	.394	29	.888	144	.366	19	.897

Table 4.2a Interaction between horizontal sine and vertical noise tracking for AWG

Run No.	Vertical Target	Left Vertical		Left Horizontal		Right Vertical		Right Horizontal	
		Delay MS	Coef.	Delay MS	Coef.	Delay MS	Coef.	Delay MS	Coef.
91	0			10	.870			10	.883
92	R1	96	.829	38	.792	134	.679	0	.706
94	R3	154	.711	48	.631	173	.556	48	.700
95	R4	163	.708	48	.770	173	.513	38	.796
96	R5	154	.634	38	.776	144	.445	48	.829
104	R1	96	.849	19	.895	106	.776	19	.793
105	R2	144	.833	29	.904	154	.753	10	.808
106	R3	144	.744	29	.830	154	.699	19	.854
107	R4	163	.655	38	.794	154	.476	19	.792
108	R5	154	.720	29	.844	144	.519	29	.829

Table 4.2b Interaction between horizontal sine and vertical noise tracking for CJS

for the vertical eye movements show no difference from those for horizontal movements in the previous experiment. Since there are no differences, none of these spectra are reproduced here.

Apparently then, the nature of the cross-talk from the horizontal target component to vertical eye movements is the same as the cross-talk from the vertical target component to horizontal eye movements, at least for the experiments performed here. This result is not surprising as there is no a priori reason to suspect that the physiological mechanisms would be different for the two cases.

5. Conclusions about Horizontal - Vertical Interaction.

In order to formalize the conclusions about the horizontal vertical interaction; it is desirable to analyse the trends of the data in a reduced form. For these purposes, tables 4.1a, 4.1b, 4.2a and 4.2b show that there is no significant difference between left eye and right eye, or vertical tracking and horizontal tracking in response to the same target motion. Thus for statistical reduction, the results are lumped together and I consider the interaction between a "sine channel" and a "noise channel", bearing in mind that if the sine channel is vertical, then the noise channel is horizontal and vice versa.

The reduced data for AWG and CJS are shown in tables 4.3a and 4.3b respectively. To make full use of this data, a meaningful quantitative measure of the "randomness" of the noise targets is necessary. So far I have indicated this by loosely

Noise Channel Target	Sine Channel Coef Mean	Sine Channel Coef S.D.	Sine Channel Delay MS Mean	Sine Channel Delay MS S.D.	Noise Channel Coef Mean	Noise Channel Coef S.D.	Noise Channel Delay MS Mean	Noise Channel Delay MS S.D.
0	.977	.00748	8.6	6.2				
R1	.953	.00496	25.3	11.4	.927	.0198	122.4	27.1
R2	.955	.00531	22.8	8.7	.904	.0166	146.5	8.9
R3	.936	.00762	31.1	9.9	.738	.0535	141.5	8.9
R4	.915	.0255	31.3	12.4	.642	.0496	147.8	5.2
R5	.914	.0184	31.1	9.9	.458	.135	146.5	12.4

Table 4.3a Reduced data for vertical-horizontal interaction for AWG

Noise Channel Target	Sine Channel Coef Mean	Sine Channel Coef S.D.	Sine Channel Delay MS Mean	Sine Channel Delay MS S.D.	Noise Channel Coef Mean	Noise Channel Coef S.D.	Noise Channel Delay MS Mean	Noise Channel Delay MS S.D.
0	.889	.0434	10.0	0.0				
R1	.816	.0757	22.3	13.1	.753	.0856	118.5	23.3
R2	.831	.0596	17.7	11.2	.687	.111	161.5	12.6
R3	.784	.0891	34.8	10.1	.635	.104	151.4	11.4
R4	.810	.0424	33.4	10.2	.520	.158	164.4	9.3
R5	.817	.0419	37.1	7.9	.468	.179	158.5	18.4

Table 4.3b Reduced data for vertical-horizontal interaction for CJS

speaking of bandwidth. Fig. 3.1 shows that from about -12 db to -30 db all of the spectra R0 - R5 are approximately linear and fall off at approximately the same rate, 50 db per decade. It therefore makes a great deal of sense to extend the definition of bandwidth of a first order linear filter as follows. A straight line was least squares fitted to each of the spectra R0 - R5 from -12 db to -30 db, and the intercept of this line with the 0 db axis was taken as the bandwidth of that waveform. From this definition it is clear that increasing complexity or randomness is reflected in increasing bandwidth. This definition is only meaningful for spectra with very nearly the same slope. The bandwidths in hz are:
R0: 0.47, R1: 0.58, R2: 0.89, R3: 1.26, R4: 1.46, R5: 2.16

In Fig. 4.3a and 4.3b the peak correlation coefficients for both the noise and sine channels are plotted as a function of the bandwidth of the noise channel for AWG and CJS respectively. The sine channel reference point of no signal on the noise channel is not plotted, as our concept of bandwidth is not applicable here. Straight lines were fitted to the data points using a weighted least squares technique. These lines are meant only to indicate the linear trend of the data and are not meant to imply a linear relationship. In other words, the straight line fitted for the noise channel shows that the coefficients decrease with increasing target bandwidth, but it is not meant to suggest that it does so in a precisely linear fashion. However, it is clear from the data point distribution and the standard deviations calculated for the

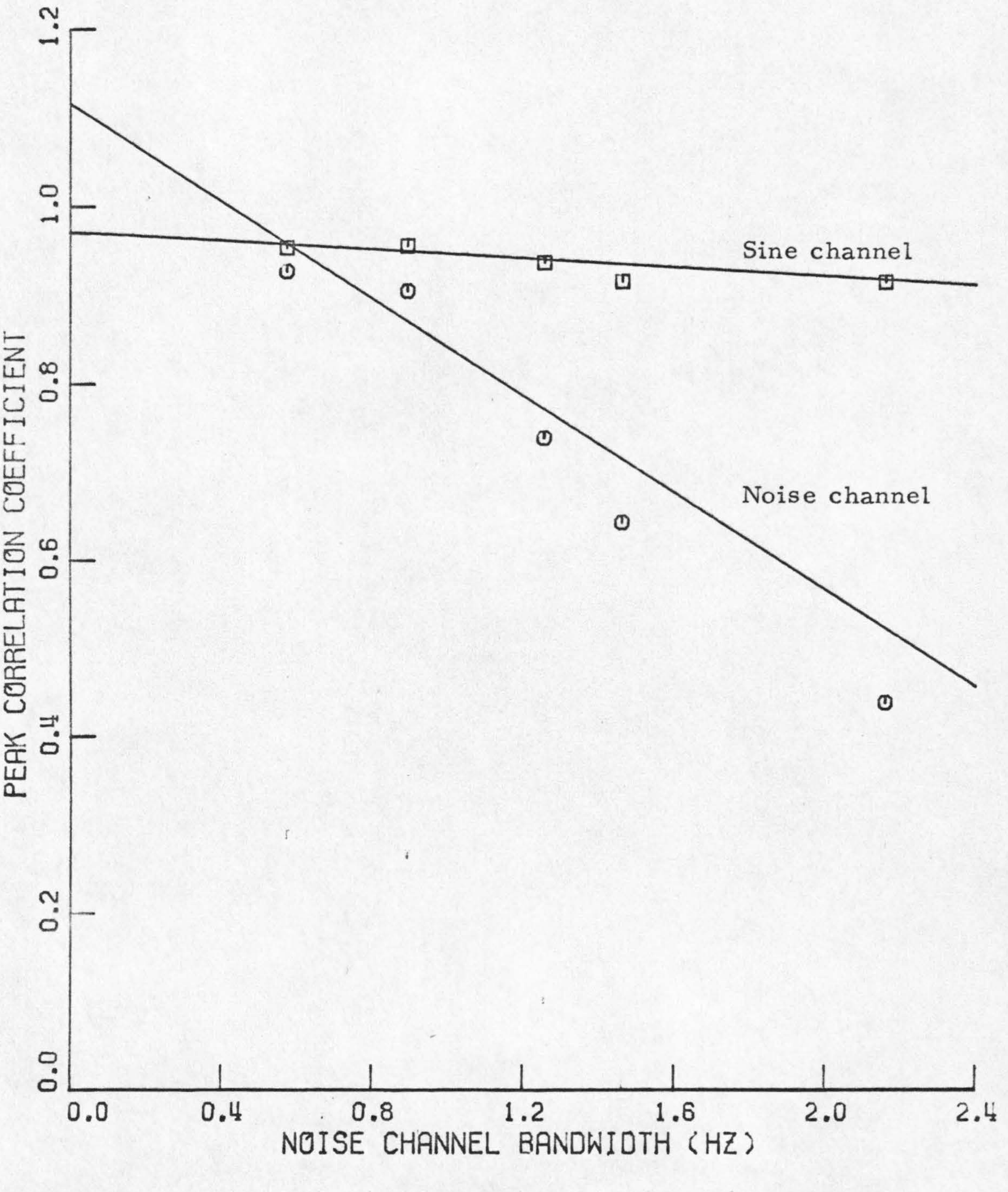

Fig. 4.3a Linear trend of peak correlation coefficients for AWG

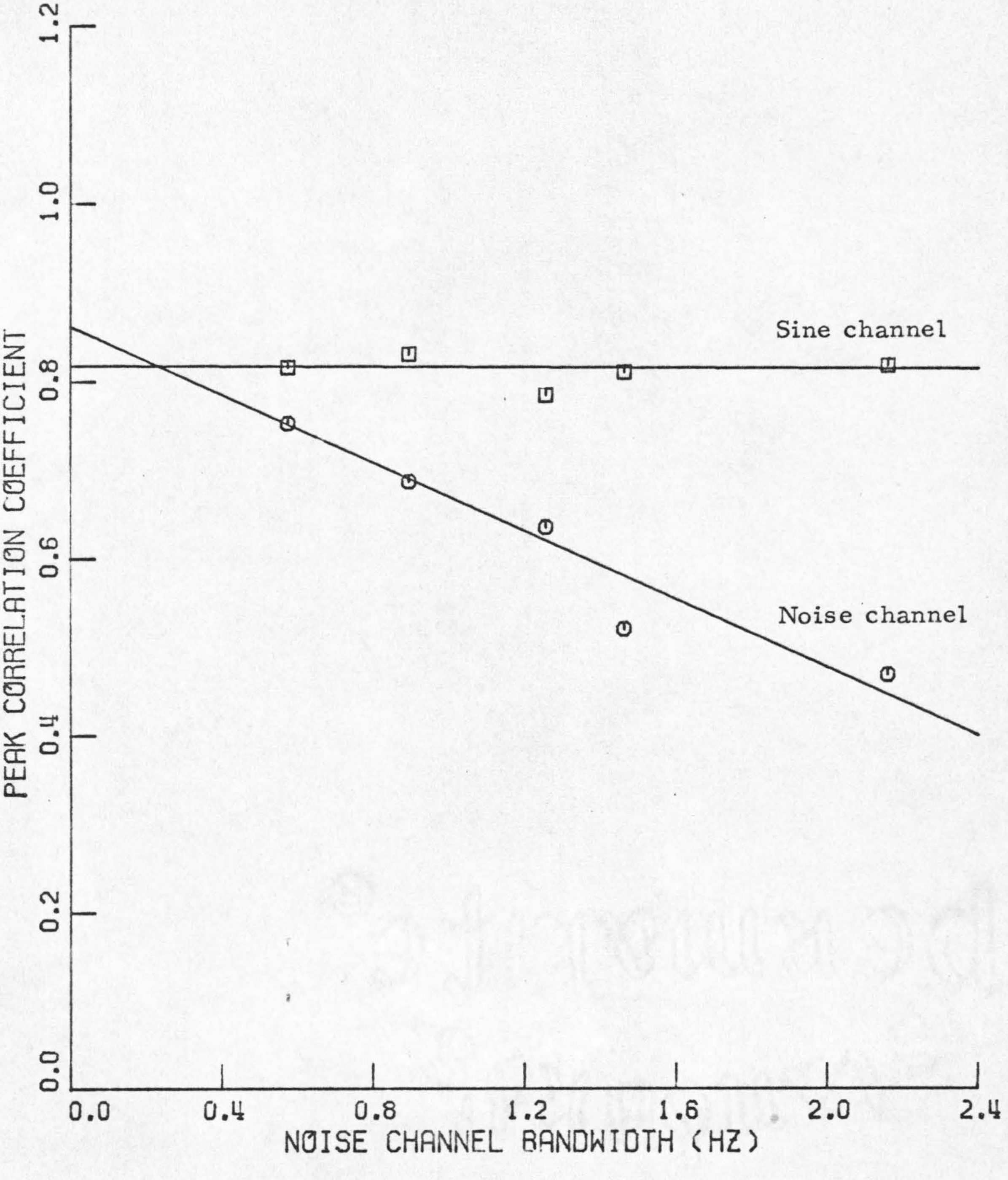

Fig. 4.3b Linear trend of peak correlation coefficients for CJS

straight lines, that the linear trend is close enough to the actual functional relationship to be meaningful and informative.

The intercepts and slopes for Figs. 4. 3a and 4. 3b together with their standard deviations are shown in the table below. No physical significance is ascribed to the intercepts, particularly for the sine channel. However, these values and their standard deviations indicate the accuracy of the linear fit.

SUBJECT	TARGET	SLOPE	INTERCEPT	SD OF INTERCEPT	SD OF SLOPE
AWG	sine	-.0253	.971	.00871	.00929
AWG	noise	-.275	1.116	.0392	.0446
CJS	sine	-.00214	.818	.0706	.0443
CJS	noise	-.1929	.862	.1249	.1105

Note also that the appearance of the curves is similar for both subjects but the coefficients are consistently greater for AWG, indicating superior tracking. For both subjects, the strong dependence of the noise channel coefficients on the noise bandwidth is obvious. For AWG the slope of the sine channel line is definitely negative, and the straight line is obviously a good approximation to the data. Hence it is clear that for AWG, the sine wave tracking deteriorates, albeit not a great deal, as the bandwidth of the noise channel increases. However for CJS, although the slope is negative, it is only just negative, and the size of the standard deviation of the slope makes its significance dubious. Therefore, for CJS I am forced to conclude that changing the bandwidth of the noise channel does not appear to affect the tracking for the sine channel. This of course does not mean that the noise channel is not affecting the sine channel, but merely that it is affecting it in a manner independent of bandwidth. In fact from tables 4.1a, b and 4.2a, b, it is evident that with no signal on the other channel, the sine tracking coefficient is always significantly greater than the coefficient when there is noise on the other channel. This is also seen in tables 4.3a, b where for CJS, the mean coefficient is 0.889 with no noise and is scattered between 0.784 and 0.831 with noise.*

---

* The standard deviations in table 4.3b are not relevant to this comparison. This is because although the coefficients vary quite a bit from sequence to sequence, giving large standard deviations, the difference between the coefficient without noise and those with noise does not vary very much. In other words the standard deviation of this difference, which is the relevant measure here, is much smaller than the standard deviation of the coefficients themselves.

The variation of the time delays with the bandwidth of the noise channel is shown in Figs. 4.4a and 4.4b. The slopes and intercepts and their standard deviations are shown below. Again no physical significance is attributed to the intercepts.

SUBJECT	TARGET	SLOPE	INTERCEPT	SD OF INTERCEPT	SD OF SLOPE
AWG	sine	5.186	21.3	11.7	8.4788
AWG	noise	4.568	139.6	15.5	11.002
CJS	sine	10.788	15.4	12.5	8.0662
CJS	noise	13.187	139.9	20.3	14.8888

Both subjects do show a slight trend of increasing time delays on both channels as the noise bandwidth increases, but the large standard deviations discourage vindictive conclusions. It is interesting to note the obvious gross differences in the time delays for the sine channel and the noise channel.

The conclusions can now be summarized. I have shown that when tracking a target with distinctly different vertical and horizontal components of motion, the currently postulated vertical and horizontal tracking systems are not independent. This finding is in agreement with the more restricted findings of Feinstein (1970). The cross-talk between the movements appears to be symmetric, that is,the same from horizontal target motion to vertical movement as from vertical target motion to horizontal movement. The cross-talk is sufficiently small that the oculomotor system is better

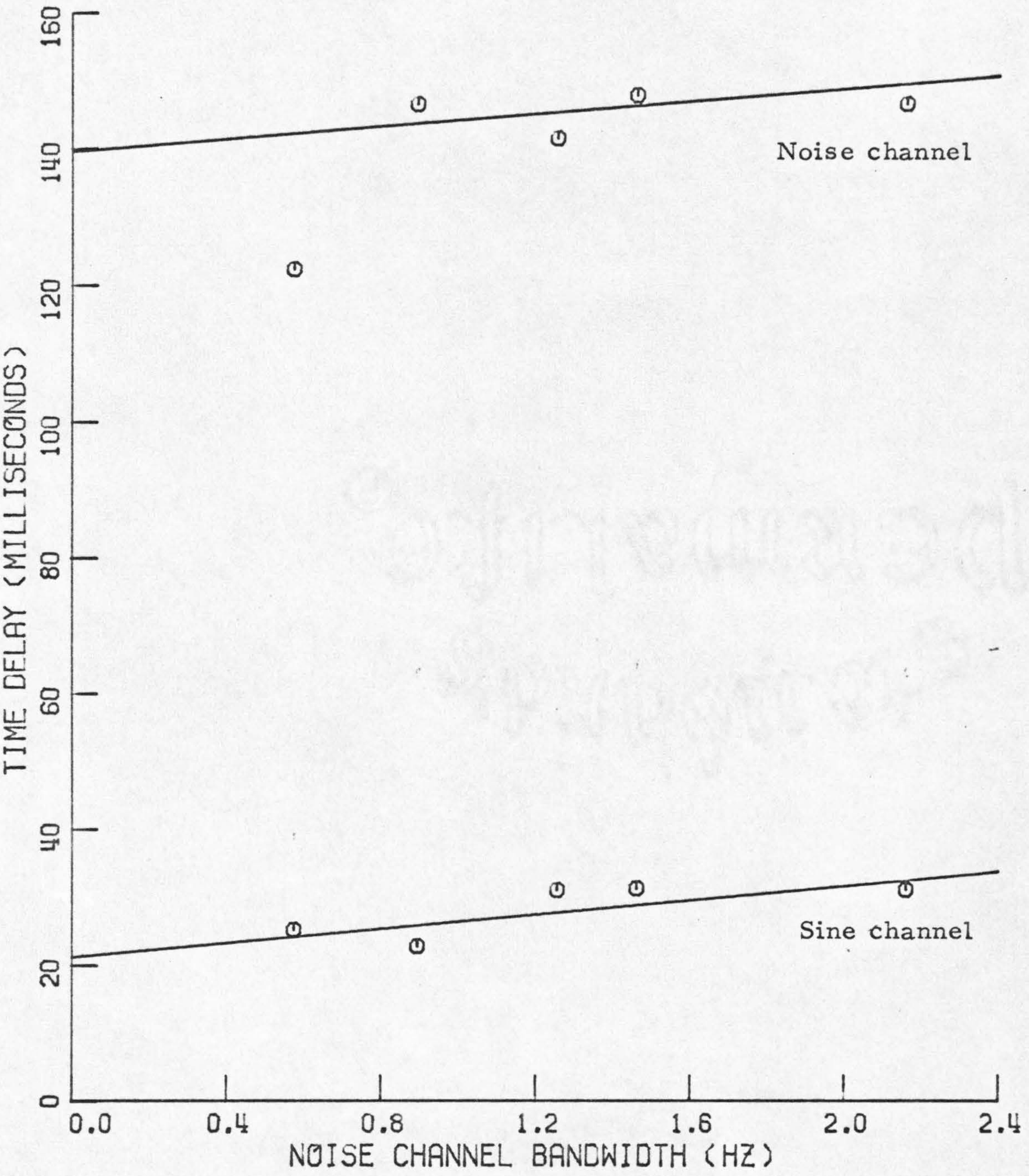

Fig. 4.4a Linear trend of time delays for AWG

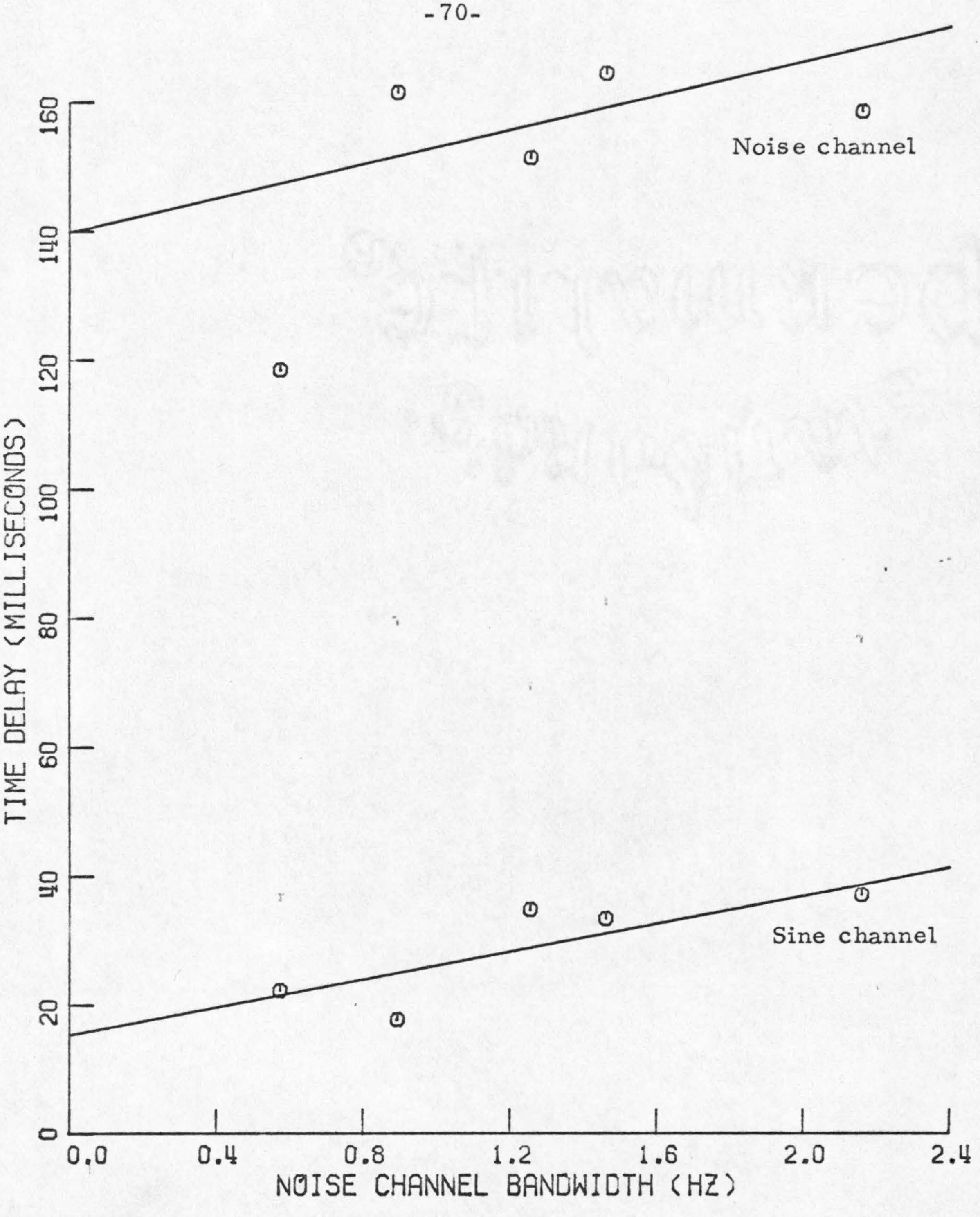

Fig. 4.4b Linear trend of time delays for CJS

described as having independent vertical and horizontal channels with relatively small mutual cross-talk, than as consisting of two mutually dependent channels. In view of this, all eye movement data obtained for tracking either only vertical or only horizontal movements, may be used comparatively without modification. On the other hand, in using data obtained for two dimensional tracking tasks, allowance must be made for this cross-talk. Whether or not it is significant, depends entirely on the nature of the tracking task and how the data are being used. Again I stress that my measurements were of a broad nature and did not attempt to single out specific properties such as saccades or smooth pursuit movements. In fact Figs. 4.1a and 4.1b show quite clearly that both types of movement are present.

V. SIGNAL RECOGNITION IN THE PLANE

In view of the results of the preceding chapter, it is tempting to fall back on the traditional approach of characterizing the oculomotor system as independent vertical and horizontal processors, modifying this concept only by the inclusion of a small amount of cross-talk between the channels. There are some factors that question the credence of such a simple minded approach. A target moving along a straight line at some arbitrary angle to the horizontal axis is only one-dimensional, yet the above system would handle it as a fully fledged two-dimensional motion. This roughly doubles the processing requirements of the relevant portions of the central nervous system, a hardly desirable state of affairs. On the other hand, one might argue that such arbitrary one-dimensional motions are not that common in nature, and that most one-dimensional motions are in fact vertical or horizontal (such as predators running or climbing). Moreover, in the world we evolved in, horizontal and vertical were more common and significant directions than any others, so from the evolutionary point of view, the horizontal-vertical tracking mechanism is quite reasonable.

The fact that the subjects were distinctly aware of the sinusoidal motion in the previous experiments, suggests that something other than simple component processing is occurring. Would the sine wave have been picked out if it were in some arbitrary direction? To answer this question, the targets used to study the vertical-horizontal interaction were rotated counter-clockwise by 35°. In other words the 1 hz sine wave moved along a line at 35° counter-clockwise to the

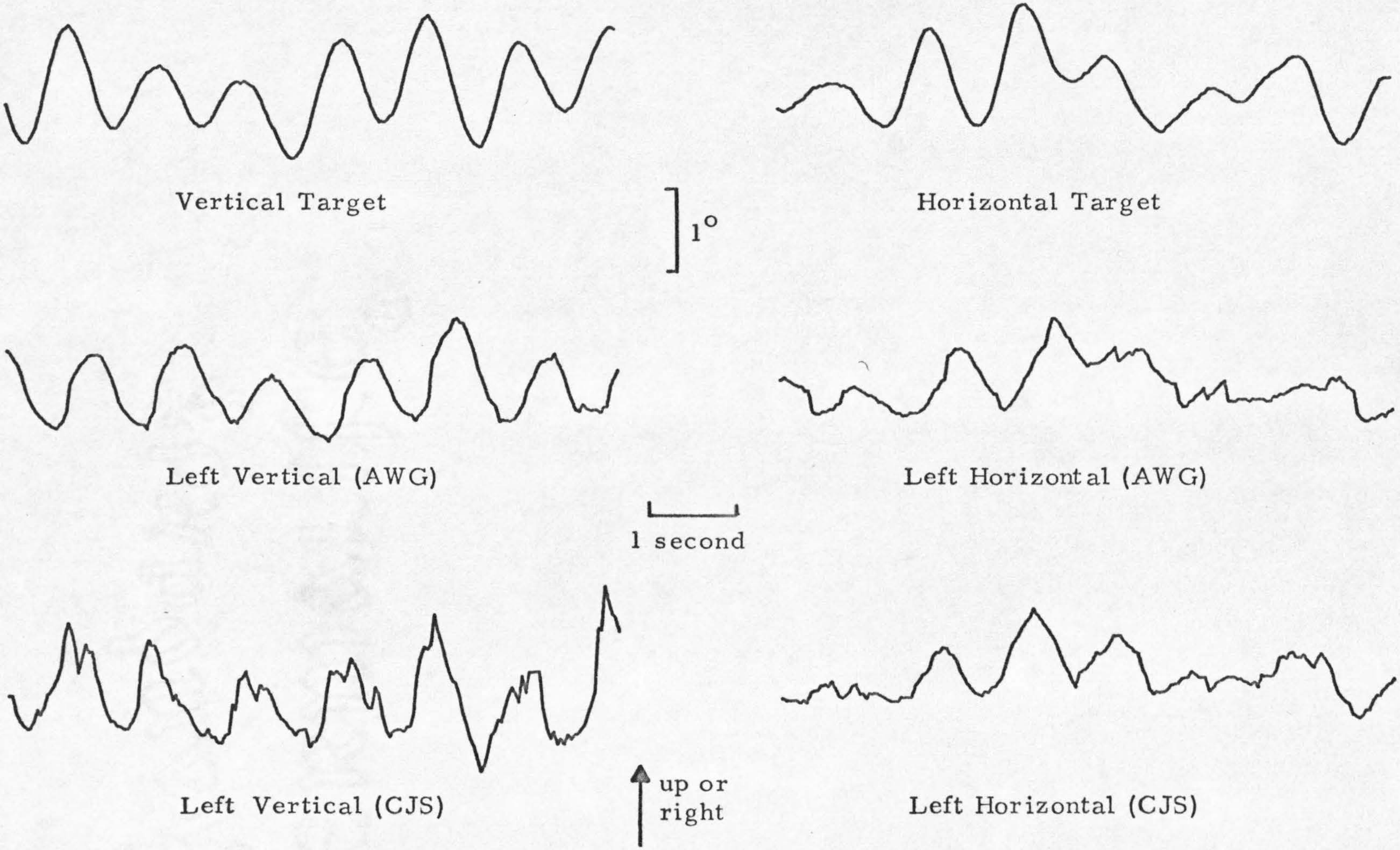

Fig. 5.1a Eye movements in response to a rotated target. (R2 and 1 hz sine)

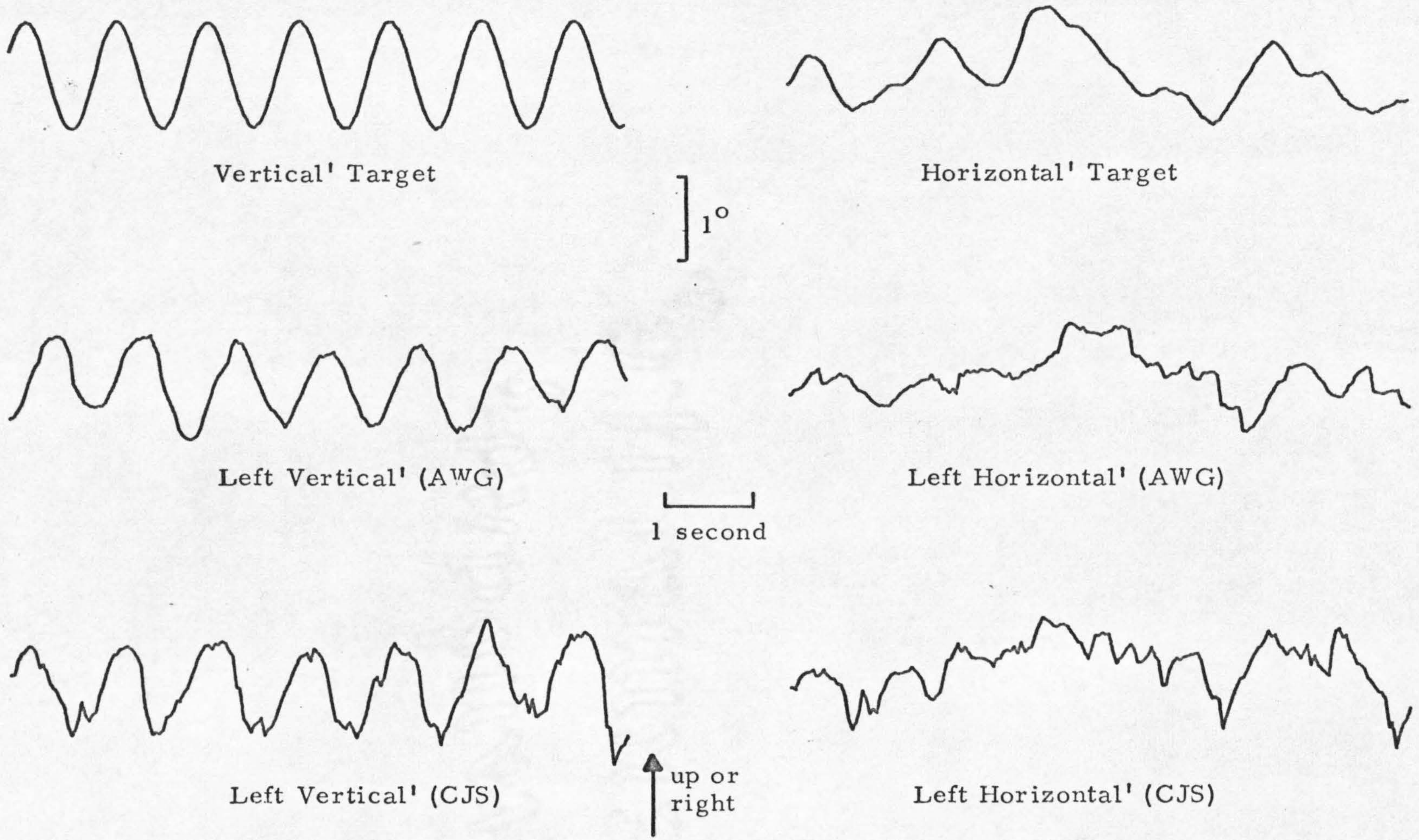

Fig. 5.1b Rotated eye movements in response to a rotated target. (R2 and 1 hz sine)

vertical axis, and the noise (whose standard deviation was reduced to 22 min. arc for these experiments) moved along a line at 35^o counter-clockwise to the horizontal axis. Henceforth these are referred to as rotated targets.

1. Analysis of Rotated Target Results

Both the vertical component and the horizontal component of the target motion are now a mixture between the sinusoid and the noise, and thus appear somewhat random. This is illustrated in Fig. 5.1a which also shows the responding eye movements for AWG and CJS. Table 5.1a shows the peak correlation coefficients and time delays for a single sequence for AWG. All the sequences for both subjects show the same behaviour as in this table, so that a single representative sequence is deemed sufficient for display. Comparison with Table 4.1a shows that both the coefficients and the time delays of all four eye movements, which are identical in nature, behave in a manner expected for a mixture of noise and a sinusoid. It is particularly interesting that the time delays vary between the two nearly invariant delays for sine waves and noise in Table 4.1a. The spectra of Fig. 5.2a, which are representative of all the spectra in this series of experiments, show quite clearly that the eye movements are a mixture of the two responses. Since the power spectrum of a sine wave is an impulse, the height of the 1 hz peak if Fig. 5.2a should not be interpreted as a measure of the sinusoidal content of the eye movements. As before, the measurements for the left and right eyes are lumped together to obtain the table of statistics for AWG shown in Table 5.2a.

Run No.	Horizontal Target	Left Vertical		Left Horizontal		Right Vertical		Right Horizontal	
		Delay MS	Coef.	Delay MS	Coef.	Delay MS	Coef.	Delay MS	Coef.
122	R0	19	.956	38	.934	0	.954	19	.932
123	R1	19	.955	48	.917	10	.949	29	.916
124	R2	38	.913	67	.854	19	.916	38	.874
125	R3	48	.896	77	.782	38	.862	58	.786
126	R4	77	.870	96	.718	58	.852	86	.741

<u>Table 5.1a</u> Response to a rotated target for AWG

Run No.	Horizontal Target	Left Vertical' (Left Sine)		Left Horizontal' (Left Noise)		Right Vertical' (Right Sine)		Right Horizontal' (Right Noise)	
		Delay MS	Coef.	Delay MS	Coef.	Delay MS	Coef.	Delay MS	Coef.
122	R0	19	.958	173	.936	0	.968	182	.931
123	R1	19	.957	192	.901	0	.959	173	.917
124	R2	29	.941	134	.844	10	.937	144	.885
125	R3	38	.931	134	.745	19	.905	144	.766
126	R4	58	.906	154	.519	38	.912	154	.680

<u>Table 5.1b</u> Rotated response to a rotated target for AWG

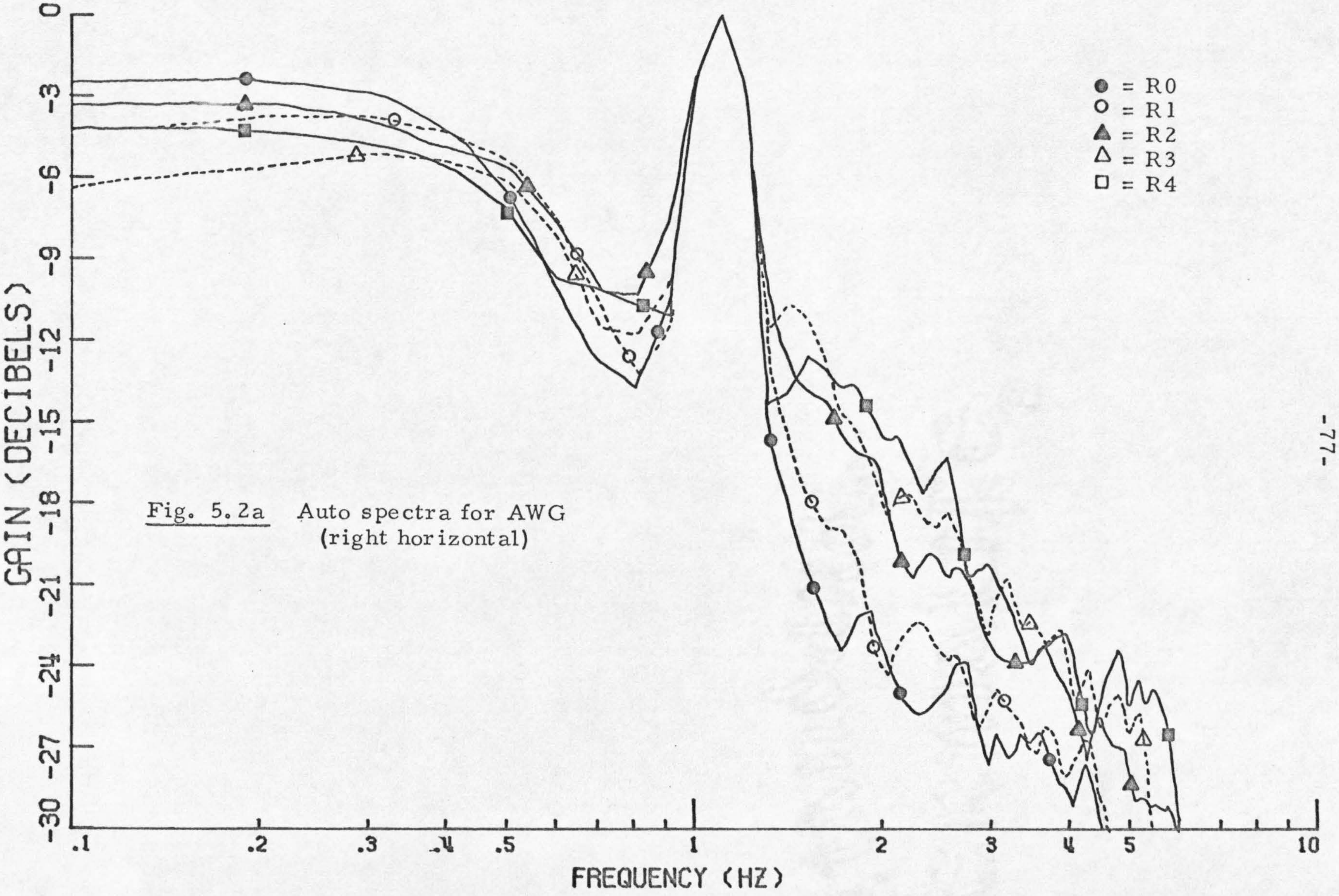

Fig. 5.2a Auto spectra for AWG (right horizontal)

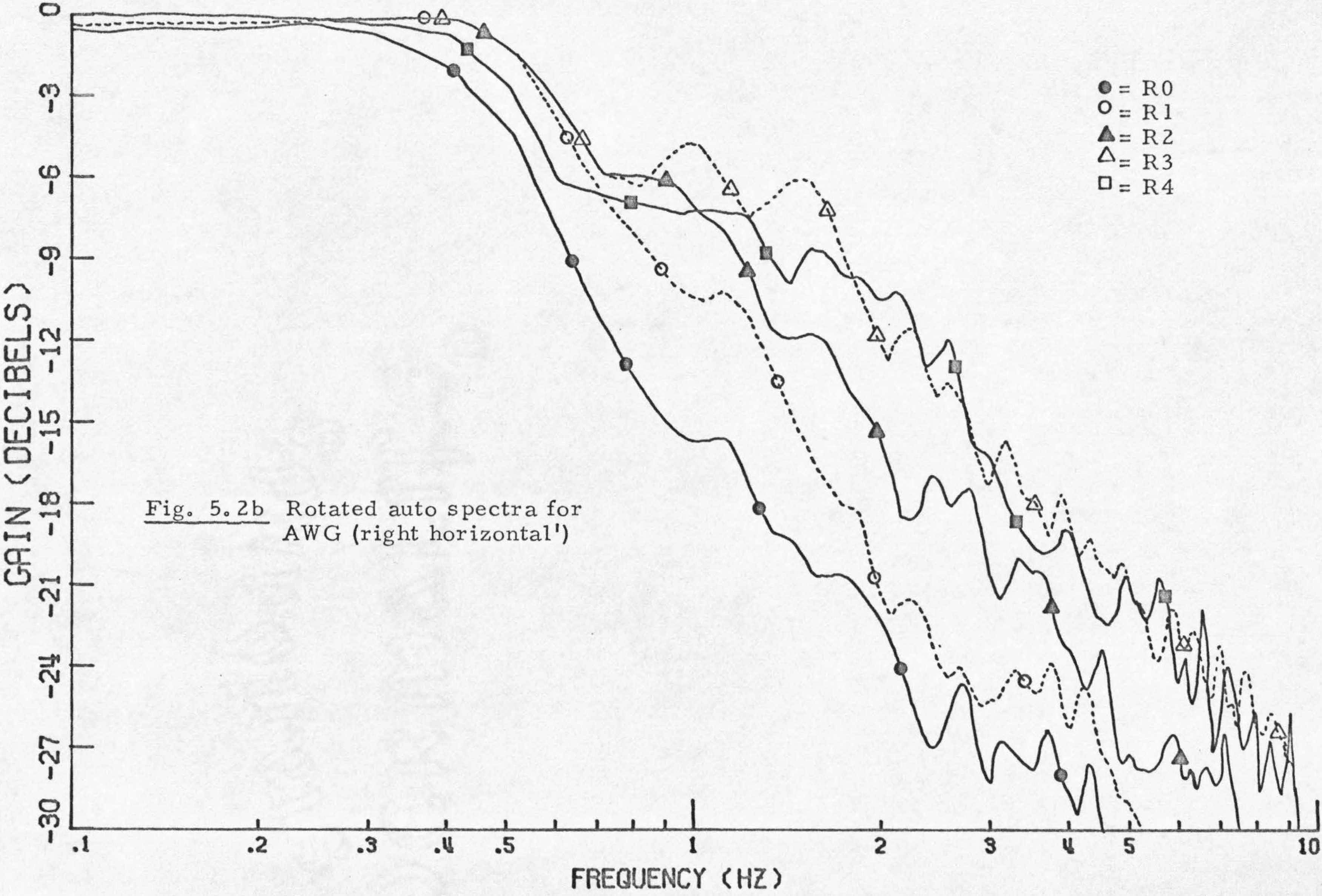

Fig. 5.2b Rotated auto spectra for AWG (right horizontal')

Unfortunately, due to equipment failures, many of the runs for CJS were useless, so that a statistical reduction was not feasible. The results for CJS, however, were very similar to those for AWG so that Table 5.2a can be considered representative.

Why have I gone to the trouble of a detailed exposure of these totally expected results? I will now do the same analysis, except that I will replace the vertical and horizontal movements, both eye and target, with the components taken along the directions of the sine wave and noise. In other words, I will have sine components and noise components defined by the vertical-horizontal axes rotated 35° counter-clockwise. These rotated components are henceforth referred to as vertical' and horizontal', or sine channel and noise channel respectively. By comparing the two sets of results, I hope to answer the original question.

Is it possible that the eye movements in Fig. 5.1a do have a sinusoidal component in the appropriate direction that is as sinusoidal as the sinusoidal responses to a vertical or horizontal sine wave? At this point the non-ideal tracking characteristics of the eye must be stressed. If the eye were to track the vertical and horizontal channels with a peak correlation coefficient of one, and with the same time delay for both, then of course the eye movements would have a sinusoidal component and a noise component, both with peak correlation coefficients of one and with the same time delays. However, as seen in Table 5.2a, the eye is tracking with considerable inaccuracies and with time delays that are different for both channels.

Noise Channel Target	Vertical Channel				Horizontal Channel			
	Coef Mean	Coef S.D.	Delay MS Mean	Delay MS S.D.	Coef Mean	Coef S.D.	Delay MS Mean	Delay MS S.D.
R0	.960	.00622	14.3	10.7	.942	.00827	25.5	7.2
R1	.949	.00363	26.3	7.9	.918	.00377	33.8	8.2
R2	.923	.00844	38.3	11.8	.855	.0187	50.3	12.7
R3	.888	.0145	48.0	8.2	.781	.0268	64.2	10.6
R4	.838	.0382	62.7	7.2	.746	.0187	76.8	14.4

Table 5.2a Reduced data in response to rotated targets for AWG

Noise Channel Target	Sine Channel				Noise Channel			
	Coef Mean	Coef S.D.	Delay MS Mean	Delay MS S.D.	Coef Mean	Coef S.D.	Delay MS Mean	Delay MS S.D.
R0	.966	.00541	11.2	8.5	.927	.0252	166.3	21.0
R1	.957	.00245	12.0	7.8	.908	.0121	161.0	32.7
R2	.942	.00356	24.3	8.2	.854	.0176	129.5	10.7
R3	.927	.0118	31.8	7.0	.742	.0178	129.5	9.1
R4	.904	.00811	41.7	10.7	.659	.0635	137.7	14.5

Table 5.2b Reduced rotated data in response to rotated targets for AWG

The rotated targets and corresponding eye movements are illustrated in Fig. 5.1b. A casual inspection of Fig. 5.1b, showing sinusoidal eye movements comparable to those in response to vertical or horizontal sine wave targets, would tempt the conclusion that the eye has recognized the oblique sine wave and is tracking along the rotated coordinates. Further evidence is provided by the eye movement auto power spectra in the direction of the noise target component, illustrated in Fig. 5.2b. This shows no contamination from the sine wave, and is indistinguishable from spectra in response to vertical or horizontal noise. A few spectra did show a very small amount of sine wave contamination. An illustration of the correlation coefficients and time delays along the rotated axes is given by Table 5.1b, and the statistical reduction for AWG is shown in Table 5.2b.

Comparison of Tables 5.1a and 5.1b and especially 5.2a and 5.2b shows the following. Despite the similarities of the coefficients for the vertical and horizontal channels, which are lower than those for sine wave tracking and higher than those for noise tracking, the coefficients for the sine channel and noise channel are similar to those for non-rotated targets. The sine wave coefficients are much higher than the noise coefficients, and decrease only slightly with increasing noise bandwidth, while the noise coefficients decrease rapidly with increasing noise bandwidth. Although the time delays for the vertical and horizontal channels are similar and spread between 14 and 77 milliseconds, the time delays for the sine channels are all low (11 to 42 milliseconds), and the delays for the noise channel are all high (130 to 166 milliseconds) just as for the non-rotated targets.

Is it possible that the eye is merely following horizontal and vertical target components as best as it can, and that the considerable inaccuracies involved (low correlation coefficients and varying time delays) are of such a fortuitous nature that the appropriately rotated movements are indistinguishable from those in response to vertical sine waves and horizontal noise? This is hardly credible. I propose rather, that the oculomotor system has detected the oblique sinusoidal motion (or perhaps the noise component), and has decided to perform the majority of its tracking computation in the corresponding rotated coordinate system. As a result it is once again faced with tracking a pure sine component and an orthogonal noise component. This reduces the amount of computation required and ensures better tracking. Moreover, although this rotation may sound complex and messy in the context of our mathematical calculations here, the neural nets in the central nervous system have no reason to prefer any particular axis orientation, and could function as easily this way as in a horizontal-vertical mode.

2. Conclusive Proof of Signal Recognition

While the evidence presented above is compelling and lends good support to my theory, the purist may quite correctly argue that nothing has been proved conclusively. After all, no matter how unlikely, it has not really been proved that the tracking errors in the vertical and horizontal channels are not of such a nature as to cancel out and produce sine wave tracking of smaller error in an oblique direction. The following set of experiments were run to test this possibility.

The oculomotor system is forced to track the rotated targets by utilizing horizontal and vertical components only, and a comparison is made with its normal performance. A two-dimensional target motion, consisting of a one hz sine wave at 35° counter-clockwise to the vertical axis and noise R2 at 35° counter-clockwise to the horizontal axis (i. e., one of the rotated targets) was used. For the first 62 second run, both vertical and horizontal components of the target were presented as usual. For the second run, only the vertical component was presented, and for the third run only the horizontal component. This sequence was repeated to make up one session. The first run is, of course, the normal two-dimensional representation of the target motion and eye movements. By utilizing the vertical components of the second run and the horizontal components of the third run, a second two-dimensional representation is possible. However, in this representation it is assured that the two-dimensional eye movements are formed by tracking in the vertical and horizontal directions. In the discussion that follows, the former results are referred to as "plane" and the latter as "merged".

It is now a simple matter to compare the merged data with the plane data. If the oculomotor system operates by tracking vertical and horizontal target components, then the merged data should be indistinguishable from the plane data. If, on the other hand, the data differ, then the oculomotor system is taking advantage of the structure of the target motion. Table 5.3 shows peak correlation

Run No.	Plane or Merged	Left Vertical' (Left Sine)		Left Horizontal' (Left Noise)		Right Vertical' (Right Sine)		Right Horizontal' (Right Noise)	
		Delay MS	Coef.	Delay MS	Coef.	Delay MS	Coef.	Delay MS	Coef.
389	P	38	.968	125	.878	29	.962	115	.871
391	M	67	.964	106	.844	58	.957	96	.831
392	P	38	.967	125	.875	29	.970	106	.859
394	M	58	.951	106	.784	48	.942	96	.789

Table 5.3 Rotated response to a rotated target (1 hz sine and R2) for normal and forced component tracking (AWG)

coefficients and time delays for subject AWG. This is representative of all the data.

There are obvious differences in the data. The correlation coefficients in all four channels are significantly higher for the plane results than for the merged results. For the merged data, the sine wave time delays are much higher than those for the plane data, which are in the range expected for sine wave tracking. The merged time delays for R2 are lower than the plane values, which again are closer to the numbers obtained in direct noise tracking. These results leave no doubt that the oculomotor system is utilizing the distinctive structure of the target motion to facilitate tracking.

The point is further confirmed in the following set of experiments, whose purpose is to find out whether something as distinctively different as sine waves and noise is necessary for this recognition to occur. In particular, if the sine wave component of the above experiment is replaced by a second random waveform of a band-width different from that of the existing noise component, how will the system behave? The experiments were performed with R0 on the line 35^o to the vertical and R3 on the line 35^o to the horizontal, each with a mean of zero and standard deviation of 22 min. arc.

Tables 5.4a and 5.4b show correlation coefficients for AWG and CJS, and once again these are typical of all the results obtained. Tables 5.5a and 5.5b show the corresponding mutual information calculated as described in Chapter IV and Appendix 1. Analogous to the sine wave case above, it is seen that the coefficients for the low band-width channels are much greater for the plane runs than for

Run No.	Plane or Merged	Left Vertical' (Left R0)		Left Horizontal' (Left R3)		Right Vertical' (Right R0)		Right Horizontal' (Right R3)	
		Delay MS	Coef.	Delay MS	Coef.	Delay MS	Coef.	Delay MS	Coef.
377	P	192	.966	144	.853	192	.960	144	.867
379	M	173	.922	144	.859	163	.898	144	.864
380	P	202	.956	154	.848	202	.926	154	.842
382	M	173	.904	154	.878	221	.912	154	.867

Table 5.4a Rotated response to a rotated target (R0, R3) for normal and forced component tracking (AWG)

Run No.	Plane or Merged	Left Vertical' (Left R0)		Left Horizontal' (Left R3)		Right Vertical' (Right R0)		Right Horizontal' (Right R3)	
		Delay MS	Coef.	Delay MS	Coef.	Delay MS	Coef.	Delay MS	Coef.
383	P	173	.918	154	.798	115	.790	173	.852
385	M	259	.793	163	.645	134	.662	163	.635
386	P	221	.825	163	.591	115	.632	192	.746
388	M	230	.743	154	.688	221	.615	163	.724

Table 5.4b Rotated response to a rotated target (R0, R3) for normal and forced component tracking (CJS)

the merged runs. In fact this difference is even more dramatic than for the sine wave data. Tables 5.5a and 5.5b show that the total mutual information between the input to the system and the output of the system is greater for plane tracking than for merged tracking, showing the improvement caused by definite structure in the target motion. It is also interesting to note that while the difference between mutual information for the low band-width channel and that of the high band-width channel is considerably greater than zero for plane tracking, it approaches zero for the merged data. This shows that in the plane case, the system is making good use of its ability to track lower band-width targets more precisely, while in the merged case it is displaying what might be termed nearly equal confusion in all directions because of the forced absence of target motion structure.

It is apparent, then, that the oculomotor system is capable not only of distinguishing orthogonal sinusoidal and noise components in the plane, but even of distinguishing orthogonal noise components of different bandwidth at some arbitrary angle of rotation. This is no mean feat, especially since the bandwidth difference between R0 and R3 is not immense (0.79 hz from my definition).

3. Conclusions about Recognition of Structure of Target Motion, and their Implications

The representation of the oculomotor system by two fixed component mechanisms may be very attractive to the control engineer, but it is not a true representation. I have shown this by using a target motion consisting of a sine wave and band-limited Gaussian random noise in two orthogonal directions, at some arbitrary orientation in the

Run No.	P or M	LV' (R0)	LH' (R3)	LV'-LH'	RV' (R0)	RH' (R3)	RV'-RH'	TOTAL
377	P	1.958	0.938	1.02	1.833	1.003	0.83	5.732
379	M	1.371	0.968	0.403	1.182	0.991	0.191	4.512
380	P	1.768	0.914	0.854	1.406	0.892	0.514	4.98
382	M	1.227	1.063	0.164	1.283	1.005	0.278	4.741

Average total information: P = 5.356 M = 4.626

Table 5.5a Mutual information for tracking target R0, R3 rotated (AWG)

Run No.	P or M	LV' (R0)	LH' (R3)	LV'-LH'	RV' (R0)	RH' (R3)	RV'-RH'	TOTAL
383	P	1.332	0.732	0.6	0.705	0.933	0.229	3.701
385	M	0.713	0.387	0.326	0.416	0.373	0.044	1.89
386	P	0.823	0.309	0.514	0.368	0.587	0.218	2.087
388	M	0.58	0.462	0.118	0.343	0.535	0.193	1.92

Average total information: P = 2.894 M = 1.905

Table 5.5b Mutual information for tracking target R0, R3 rotated (CJS) plane. The system was able to pick out the target orientation and reorient its tracking components to match, improving the tracking efficiency. When the sine wave was replaced by noise of a bandwidth lower than that of the already existing noise component, the same reorientation occurred. It is not clear what criteria the eye is using for establishing the preferential orientation. From my experiments, it seems feasible that it is choosing its prime direction to coincide with a line in the plane along which the target motion bandwidth is a minimum (or maximum). Or more likely, which amounts to the same thing in my case, it is choosing its axes so that the difference in bandwidth between the two target motion components is a maximum.

What advantage could there be in this approach to justify the additional burden of this pattern recognition? Consider a target where the movement in one particular direction is much "simpler" than the movement in the orthogonal direction. It is well known that the eye tracks simpler motions more precisely than complex motions (chapter 6 of this thesis; Michael and Jones, 1966; Dallos and Jones, 1963; St-Cyr and Fender, 1969b; Stark et al., 1962), so that with the appropriate orientation we may think of the oculomotor system as readily dispensing with the simple motion, leaving it free to concentrate on the complex motion. Along any other axes, the simple motion is always obscured to some extent by the complex motion, increasing the demands on the system and hindering tracking. This somewhat loosely stated theory is supported by the finding that when the system is prevented from isolating the simple motion, the total mutual information in the plane between target motion and eye movements is reduced. This total mutual information is a good measure of tracking effectiveness. The disadvantages of target motion pattern analysis are apparently more than compensated for by the improvement in tracking performance.

This recognition ability is important in its own right, and provides an additional small insight into the workings of the oculomotor system and information processing in the central nervous system in general. Further speculation along these lines is beyond the scope of this thesis, but I do consider the immediate implications of this finding on current research in eye movements. Any conclusions based on two-dimensional tracking that do not allow for this effect are in danger of being erroneous. Moreover, it is important that any models proposed can be made to fit into this framework. It is still possible to accept current models, based on independent horizontal and vertical tracking, provided these are interpreted as independent orthogonal components with cross-talk, and these models are preceded by an additional section. This additional section would then handle the target motion structure analysis, and select the optimum orthogonal coordinates for the tracking section as illustrated in Fig. 5.3.

I do not favor this approach for several reasons. It is quite clear that in order to select the optimum tracking directions, a large amount of processing must occur in the first section, and it seems illogical that these results would not be passed on to the tracking sections. On the other hand, it may be argued that this information is about the target motion only, and may not be that significant for a

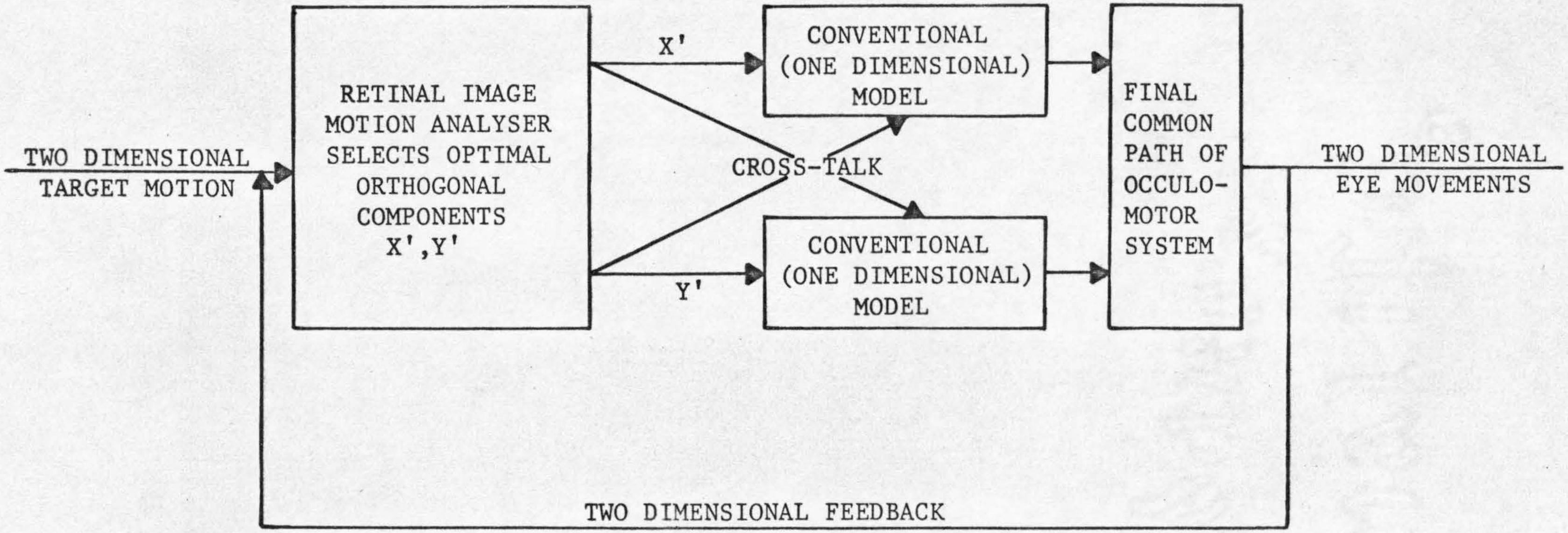

Fig. 5.3 A simplified model of two dimensional tracking

feedback control system. The parallel processing concept is also called for by the physiology of the situation. Undoubtedly both the recognition and the tracking computations are occurring simultaneously in several levels of the system from the retina up, and clearly such basic information as photoreceptor stimulation patterns must be shared by both sections. To entirely divorce these two segments in the model would be artificial to an extent that may be misleading. Before the ideal model can be constructed, a lot more has to be learned about the system, and until that time, judicious use of the simplified scheme proposed above may prove helpful.

VI. TIME DELAYS

In previous chapters I have used time delays and power spectra as analysis tools, but I have not yet dwelt on their significance *per se*. In order to do this, a brief review of current models of the oculomotor control system is necessary.

1. Review of Models of the Oculomotor Control System

As may be expected, the first attempts to model the eye movement control system relied entirely on the techniques of linear control theory. Even though they used only sinusoidal inputs, Fender and Nye (1961) (who were probably the first to produce a model) found that the phase lag was much less than the lag calculated on the basis of a minimum phase system. This suggested that the system may be "predicting" the input. Pursuing this possibility, Stark, Vossius and Young (1962) presented subjects with "unpredictable" target motions consisting of the sum of non-integrally related sinusoids, while Dallos and Jones (1963) achieved the same effect with band-limited Gaussian random motions. In both cases the phase lags computed for these unpredictable stimuli were much greater than the lags at corresponding frequencies for simple sine waves. Both sets of authors concluded that a predictor did exist and Dallos and Jones derived its transfer function. Their predictor consisted essentially of a high gain element and a negative time delay. Although they demonstrated that a physically realizable network could be constructed to approximate their predictor, it became clear (and is even clearer now) that the exercise was obviously contrived and not very fruitful. Along similar lines, Michael and Jones (1966) showed that there is a direct relationship between the phase lag and the predictability of the target motion (they equated predictability and band-width).

These earlier models treated eye movements as a single control system, although Dallos (1962) did mention the problems involved in trying to obtain the correct step response (saccades) from a model derived from the so-called unpredictable signals. Rashbass (1961) demonstrated that while saccadic eye movements are triggered by displacement of the target image on the retina, smooth pursuit movements are made in response to velocity of the retinal image. Furthermore, by using a step-ramp target motion, he showed that the saccadic and smooth pursuit systems appeared to be totally independent. This conclusion is reinforced by his finding that barbiturate drugs can eliminate the smooth pursuit movements without affecting saccades. Starr (1967) found that certain patients who had Huntington's Chorea could not perform saccades, but had normal smooth tracking responses, lending further support to the independence of the two systems.

Based on this evidence, Young and Stark (1963) proposed a model with two branches, one for saccadic movements triggered by displacement of the retinal image from the fovea, and one for smooth pursuit movements responding to retinal image velocity. Westheimer (1954) reported that a target motion consisting of a pulse of duration less than 200 milliseconds produced a response consisting of two opposing saccades separated by a 200 millisecond interval, even though such action would seem irrational. Young (1962) also found that the open loop response to a target step was a staircase of steps occurring at 200 millisecond intervals. These facts lead Young and Stark to cast their model as a sample data system, with the retinal image position being impulse sampled every 200 milliseconds. Their model was remarkably successful in mimicking saccadic responses of the eye, but had several shortcomings.

Wheeless, Boynton and Cohen (1967) elaborated on Westheimer's basic experiment by using pulse-step target motions with various pulse durations, and demonstrated that the saccadic system is not impulse sampled. For example, when the pulse width was 50 milliseconds, only 8.5% of the saccades followed the pulse. Rashbass (1961) showed that the step size and ramp velocity of a step-ramp target motion could be chosen so that the response was devoid of saccades. Robinson (1966) used a target motion consisting of a ramp of one velocity for a period of 150, 100 or 75 milliseconds, followed by a ramp of a different velocity. He found that the response consisted of two corresponding ramps, with the duration of the first ramp being 150, 100 or 75 milliseconds respectively, and concluded that the smooth pursuit system is continuous in nature, or else has a sample interval of less than 75 milliseconds.

In view of this subsequent evidence, Young, Forster and Van Houtte (1968) revised the original model of Young and Stark. They replaced the fixed 200 millisecond sample interval by a target-synchronized, stochastically distributed sample interval, and represented the smooth pursuit branch as an open loop continuous system. The model is claimed to be valid only for non-predictable signals and is not suitable for sine waves, square waves or any other predictable wave form. While this modification appears to improve the step-ramp response, the model still cannot respond correctly to the pulse-step targets. The authors suggest a finite width sample to remedy this situation, but this would require revision of the whole model which already is losing physiological realism. No model of the oculomotor system proposed to date can predict all or even most of the responses found so far. However, this does not detract from the usefulness of these models, especially as stepping stones to improved versions. In this light, the revised model of Young et al. does provide insight into the saccadic system. On the other hand, I feel that the smooth pursuit system is handled far from adequately in this model (see section 2.2).

St.-Cyr and Fender (1969b) approached the question of predictability from a different point of view. The oculomotor system is obviously highly non-linear, so that the concept of "phase lag" has no real meaning. They reasoned that it is more sensible to measure the time delay between the target motion and the eye movements. These time delays were interpreted as consisting of a constant delay, due to such factors as neural propagation time and muscle system time constants, plus a "compute time" dependent upon the structure of the target motion. It was reasoned that the simpler a target waveform was, the smaller would be the compute time. They went on to suggest a simple and physiologically feasible mechanism for this computation procedure namely:

$$(\delta s-\delta s_o)(\overline{\delta t}-\delta t_o) = C$$

δs = average distance swept by the retinal image in a "compute time."

$\overline{\delta t}$ = average time spent by the retinal image on one receptor.

δs_o, δt_o and C are constants.

This explanation automatically takes care of the predictability of the signal, and St-Cyr and Fender rejected the idea of an overriding predictor in the Dallos and Jones sense. Rather, the signal is processed in the above fashion regardless of what it is, and the oculomotor system does not handle different classes of signals by different mechanisms. Note that they did not distinguish between saccadic and smooth pursuit systems, and the signal was analyzed as above in toto. As will be shown, there are many problems with this model, but there is much to be said for this approach.

The final common path, consisting of the oculomotor nuclei, cranial nerves, extraocular muscles and globe suspension, has also been modeled in a variety of ways, but since this is common to all of the above models, the point is not pursued any further for the moment.

All the models proposed to date may be grouped into two categories. The first category consists of quasi-linear models made of standard control theory transfer functions. These are modeled for "unpredictable" signals, and some mechanism (inevitably not treated in detail) has to be postulated to recognize "predictable" targets and predict them. The model of Young, Forster and Van Houtte is probably the best representative of this category. The second category consists of non-linear or quasi-linear models that do not distinguish between target structures and are self sufficient in themselves. St-Cyr and Fender's model is, to my knowledge, the sole representative of this category.

1.1 Does the System Operate in an Open or Closed Loop Manner? Is it Continuous or Sample Data in Nature? Are the Smooth Pursuit and Saccadic Systems Independent?

Even though most authors treat eye movements as a closed loop control process, the most complete model to date, that of Young et al. (1968) has a closed loop saccadic branch, but an open loop smooth pursuit branch. Their main motivation for an open loop smooth pursuit system seems to be to avoid the limit cycles resulting from modelling it as a continuous closed loop system. This suggests a deficiency in the model rather than good reason for an open loop system.

Information about motion of the target is conveyed to the oculomotor system by the displacement of the retinal image from the fovea. Since this displacement is simply the difference between target motion and eye movement, the system is of necessity closed loop with unity feedback. The only way that eye movements can be mediated in an open loop fashion is for the brain to effectively open the loop by adding the eye movements to the target motion. To achieve this, the position of the eyes could be monitored either by feedback from eye muscle proprioceptors or by efference copy, both still areas of controversy. In the absence of visual cues, even if a person is aware of where he is looking, this is undoubtedly not to the precision of a few minutes of arc as would be required for tracking. If a subject fixates on a light source ten degrees from the primary position and is asked to maintain his direction of gaze when the light is extinguished, Skavenski and Steinman (1970) have shown that the fixation error is of the order of two degrees. In an open loop mode, even a small change in one of the system parameters would effect tracking precision. In fact even the change of inertia due to a contact lens would effect smooth pursuit tracking, a fact not supported by the literature. It has also been shown (Fender and Nye, 1961), by imposing varied external feedback on the system, that sine wave tracking is compatible with a system operating with a feedback factor of unity. Thus, I believe that the system is closed loop for both saccadic and smooth pursuit movements.

As outlined in the previous section, there is considerable evidence that the oculomotor system is handling target motions made up of pure position displacements in a sampled data manner. However, there is really no evidence to suggest that the sample interval is constant, or even nearly constant with small stochastic variation. Robinson's two-ramp experiments are the only real evidence suggesting that the oculomotor system handles target motions consisting of pure velocities in a continuous fashion. The fact that a target motion consisting of a 75 millisecond ramp of one velocity followed by a ramp of a different velocity, elicited eye movements consisting of two ramps with the first ramp duration being 75 milliseconds, does not necessarily mean that the "smooth pursuit" system is continuous. Strictly speaking, it merely shows that the oculomotor system handles that particular (and very specific) target motion continuously or with a sample interval of less than 75 milliseconds. Initially I shall make no exclusive assumptions about the continuous or sample data nature of the system.

While the evidence presented in section 1 showing that the smooth pursuit and saccadic systems are functionally distinct seems considerable, much of it is becoming less credible and is subject to reinterpretation. Although there are undoubtedly some neurological differences, it is not clear at what stage the two systems separate, nor at what stage they rejoin. Rashbass' (1961) step-ramp experiments indicate that the saccadic system is sensitive not only to position, but also to velocity, a parameter traditionally reserved for the smooth pursuit system. In addition St-Cyr (1969) has shown that there are sometimes smooth pursuit movements mixed in with the saccadic responses to a target step, a parameter traditionally acted upon only by the saccadic system. Thus the classical concept of a position sensitive saccadic branch and a velocity sensitive smooth pursuit branch is not accurate.* All in all, the functional distinction between the two systems is not clear cut, and initially I shall make no arbitrary decision. It should be noted that attempts to separate the two systems have been based on target motions consisting of pure position displacements, constant velocities, or at best a step-ramp

---

[*] Young _et al_, were able to reproduce some of the responses to step-ramp targets where no saccades occurred using a saccadic branch sensitive to position only. However, they concede that the nature of the stochastic sampling required for this is not very feasible.

type combination. How the two systems would interact in the case of a motion as complex as Gaussian noise is impossible to say.

2. Time Delays

From the preceding discussion it is evident that time delays offer a powerful tool for analyzing the oculomotor control system. It is important that the meaning and ambiguities of these time delays are fully understood. So far St-Cyr and Fender (1969b) are the only authors to have published time delay data. They computed gain and phase curves from the cross power spectra of the eye movements and target motion. Restricting themselves to frequencies below that at which the gain curve reached an attenuation of 30 db, they least squares fitted a pure delay time to the phase curve. In view of the fact that the system is non-linear, so that phase curves are not of necessity meaningful (as they themselves stated), this method of calculating time delays requires careful appraisal.

For a non-linear system, the phase curves may be of any shape, and may not at all resemble those of a pure time delay. In such a case, least squares fitting a time delay to the phase curves would be frivolous, and the result of such a calculation would be difficult to interpret. On the other hand, if fortuitously the phase curves do closely approximate a pure delay, then the method is reasonable, and the results can be interpreted meaningfully. Thus, although the method is not valid in general, it may be used sensibly in certain cases. The phase curves published by St-Cyr and Fender are close enough to pure delays to use this method. In my experiments, the majority of phase curves were not suitable for such a treatment.

Discarding the linear systems oriented concept of phase lag, consider rather the cross-correlation function between target motion and eye movement. The peak value of this function indicates the proficiency of tracking (see chapter 4), and the location of the peak is a measure of the time delay of the system. In the case of a pure time delay the suitability of this definition is obvious. In the case of a general non-linear system, the output correlates with the input best when the input is delayed by this amount. Although not as clear cut as a pure time delay, here, too, the significance is apparent. This method can therefore be applied to any system, without the need to worry about the shape of the phase curve.

For a pure delay, both methods give the same result, but in the general case the results will be different. The frequency domain method of St-Cyr and Fender is based on the postulate that the system delay is equivalent to a pure delay. In this context it is interesting to note the difference between the phase curves of a simple time constant (the Laplacian $1/S+a$) and a pure delay (the Laplacian e^{-as}). The output can then be thought of as the sum of its frequency components, with the phase lag at each frequency being proportional to the product of that frequency and the delay time. Since the least squares fit is performed in the frequency domain, the relative amplitudes of the frequency components (that are within 30 db below the maximum component amplitude) do not affect the result. Thus, for example, the phase of a component of magnitude 1 min. arc at some frequency would have as much influence on the result as the phase of a component of magnitude 30 min. arc at another frequency.

In contrast, my method treats the signal as a single time series, based on the postulate that the oculomotor system is attempting to minimize the retinal image displacement from the fovea regardless of its temporal course. I do not believe that the system responds to each frequency component separately, and therefore do not wish to ascribe equal weight to all frequency components regardless of amplitude. In my method, the characteristics of a component of magnitude 1 min. of arc at some frequency would have a small effect on the time delay compared to a component of magnitude 30 min. arc at some other frequency.

When comparing my data with those of St-Cyr and Fender, cognizance must be taken of the above differences. In section 2.4 further comparison is made to explain the differences in time delays obtained for low-pass filtered Gaussian random noise from those obtained by St-Cyr and Fender.

2.1 Time Delay as a Function of the Target Waveform

In chapter 4 time delays were computed for sinusoidal target motions and for the low-pass filtered Gaussian random motions R0-R5. The results were summarized in Tables 4.3a and 4.3b and Figs. 4.4a and 4.4b. The delays for the sine waves were of the order of 10-20 milliseconds, while those for the random motions were of the order of 140-150 milliseconds. Perhaps the most striking facet of these time delays is the distinction between the sine waves and the random motions.

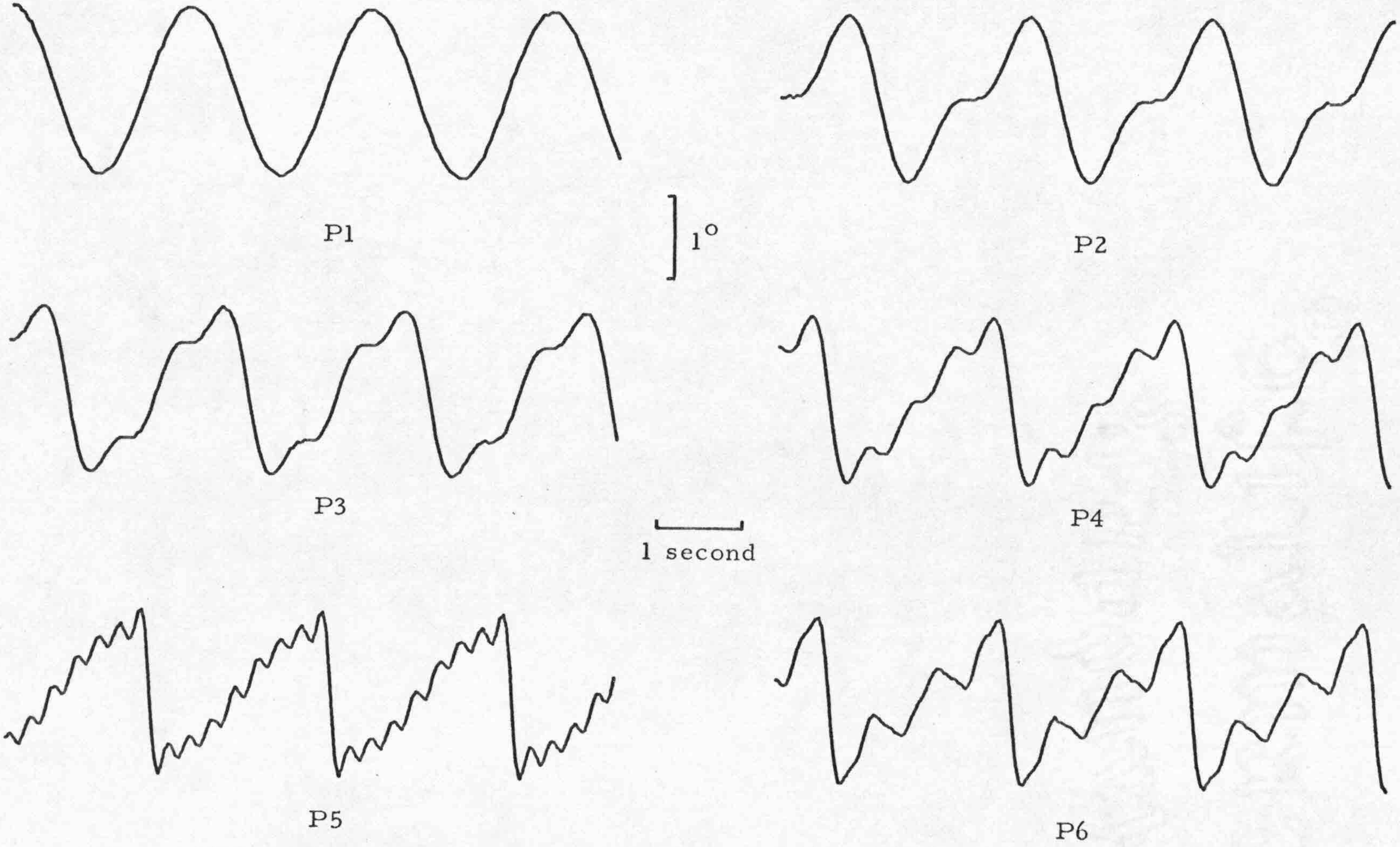

Fig. 6.1 The periodic target motions P1-P6. See Chapter 3 for their harmonic content

In the frequency domain a sinusoid of frequency f_o may be thought of either as a narrow band or a periodic signal. It is the limit, as the bandwidth tends to zero, of a narrow band signal with center frequency f_o. It is also a special case of the general periodic signal, whose spectrum consists of impulses at the harmonic frequencies nf_o (n=1, 2.....). Are the sinusoids distinguished by their narrow band property, their periodic property or both? In an attempt to answer this, time delays and correlation coefficients were computed for target motions consisting of band-pass filtered Gaussian random noise and periodic motions (B1-B6 and P1-P6 respectively) as described in chapter 3.

The change in complexity of the periodic waveforms P1-P6 can be seen in Fig. 6.1, which shows a section of the time trace for each waveform. Eye movement power spectra in response to P2, P4 and P6 are shown in Figs. 6.2a, 6.2b and 6.2c respectively. The spectra show that for P2(component magnitudes of 100 (f_o), 50 ($2f_o$); see chapter 3), the response consists almost entirely of the two harmonics* with little spread in the spectra. Despite the relatively complicated waveform of P4 (component magnitudes 100(f_o), 35($2f_o$), 25($3f_o$), 25($4f_o$)) the spectra show that again eye movements are confined to the harmonics of the target motion. P6 (component magnitudes 100(f_o), 50($2f_o$), 70($3f_o$), 20($4f_o$), 10($5f_o$), 10($6f_o$), 10($7f_o$), 10($8f_o$)) contains eight harmonics with the last four harmonics contributing only a small portion to the waveform. Nevertheless, it is apparent from the spectra that the eye is responding at all of these

---

* The component at frequency nf_o is referred to as the nth harmonic.

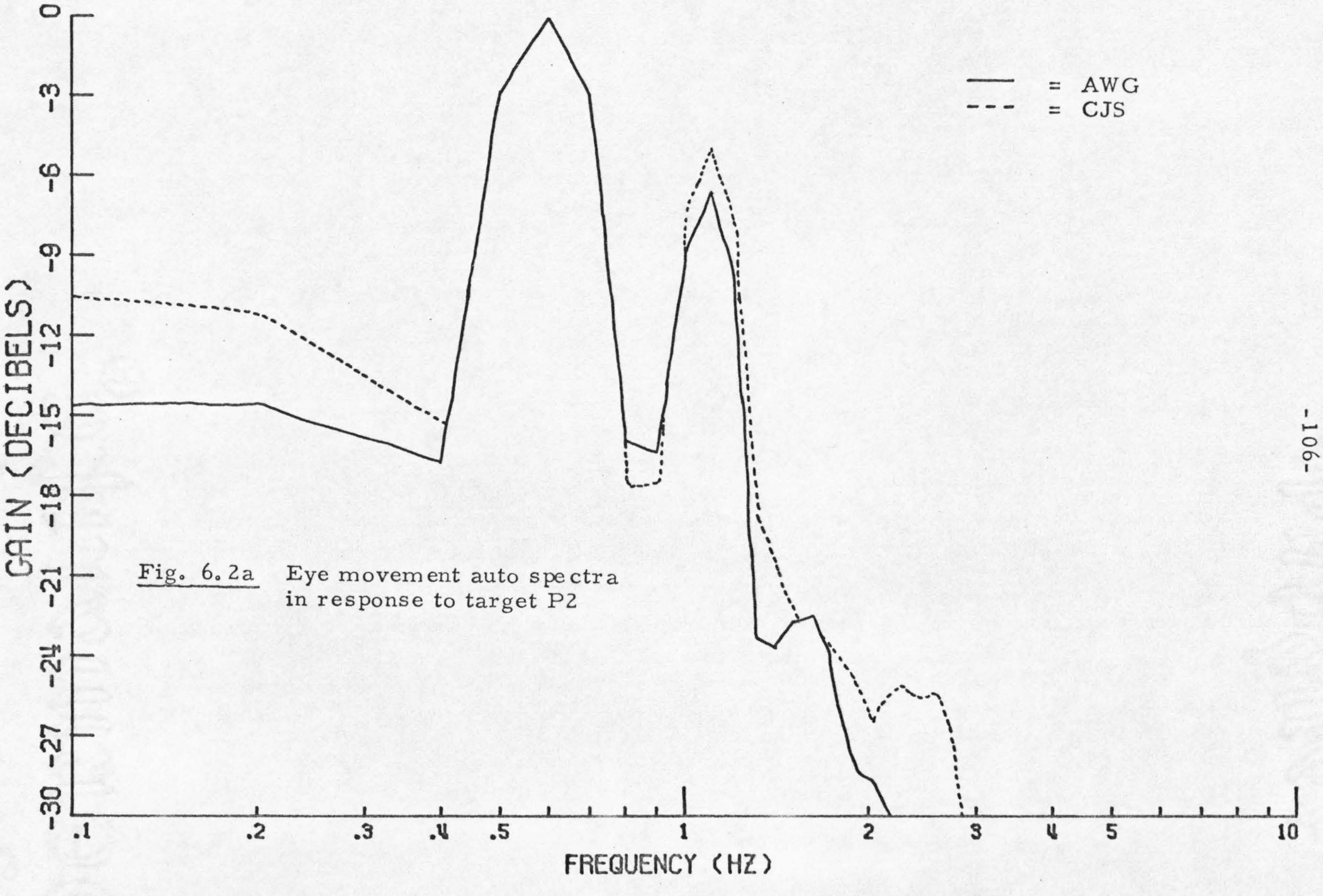

Fig. 6.2a Eye movement auto spectra in response to target P2

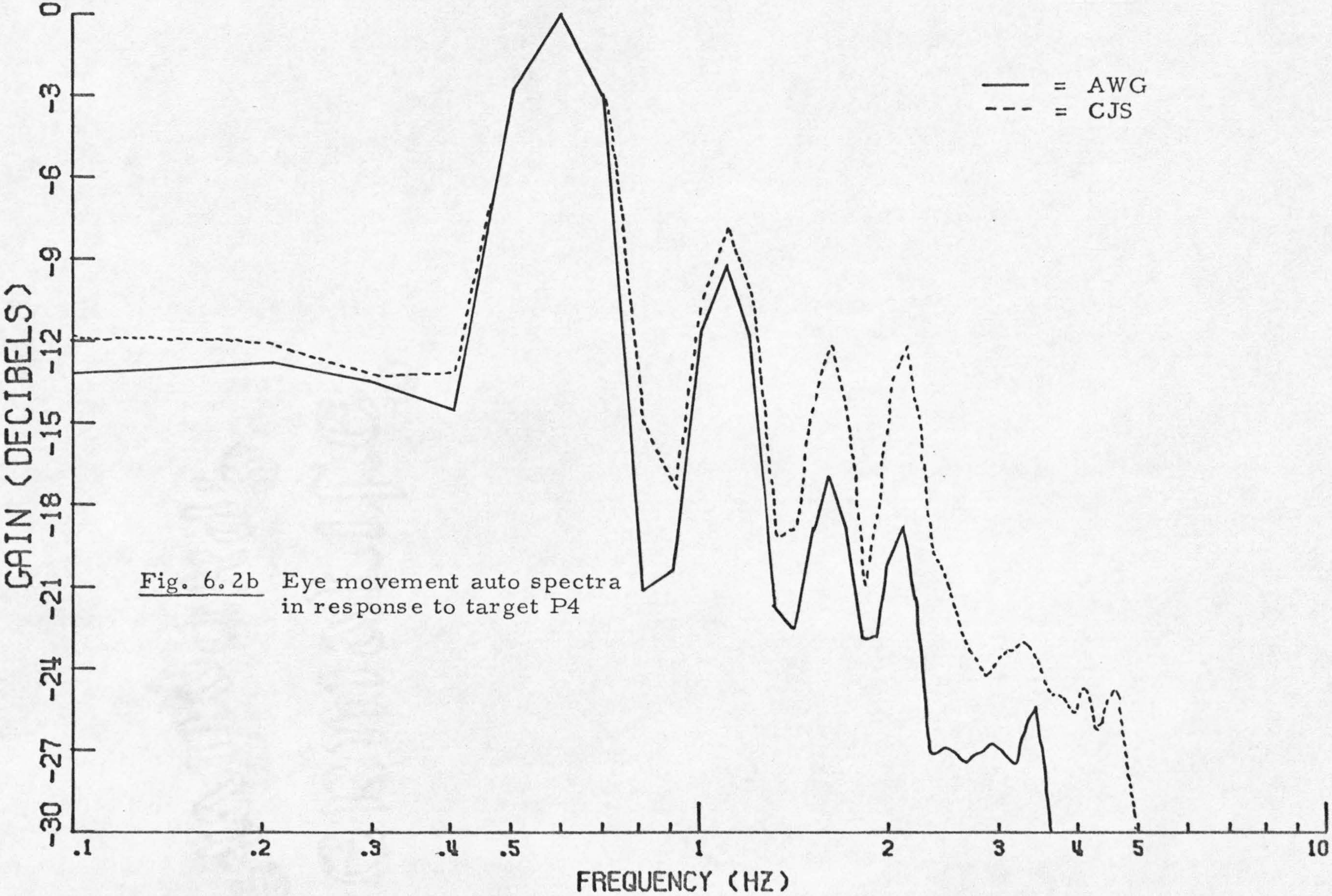

Fig. 6.2b Eye movement auto spectra in response to target P4

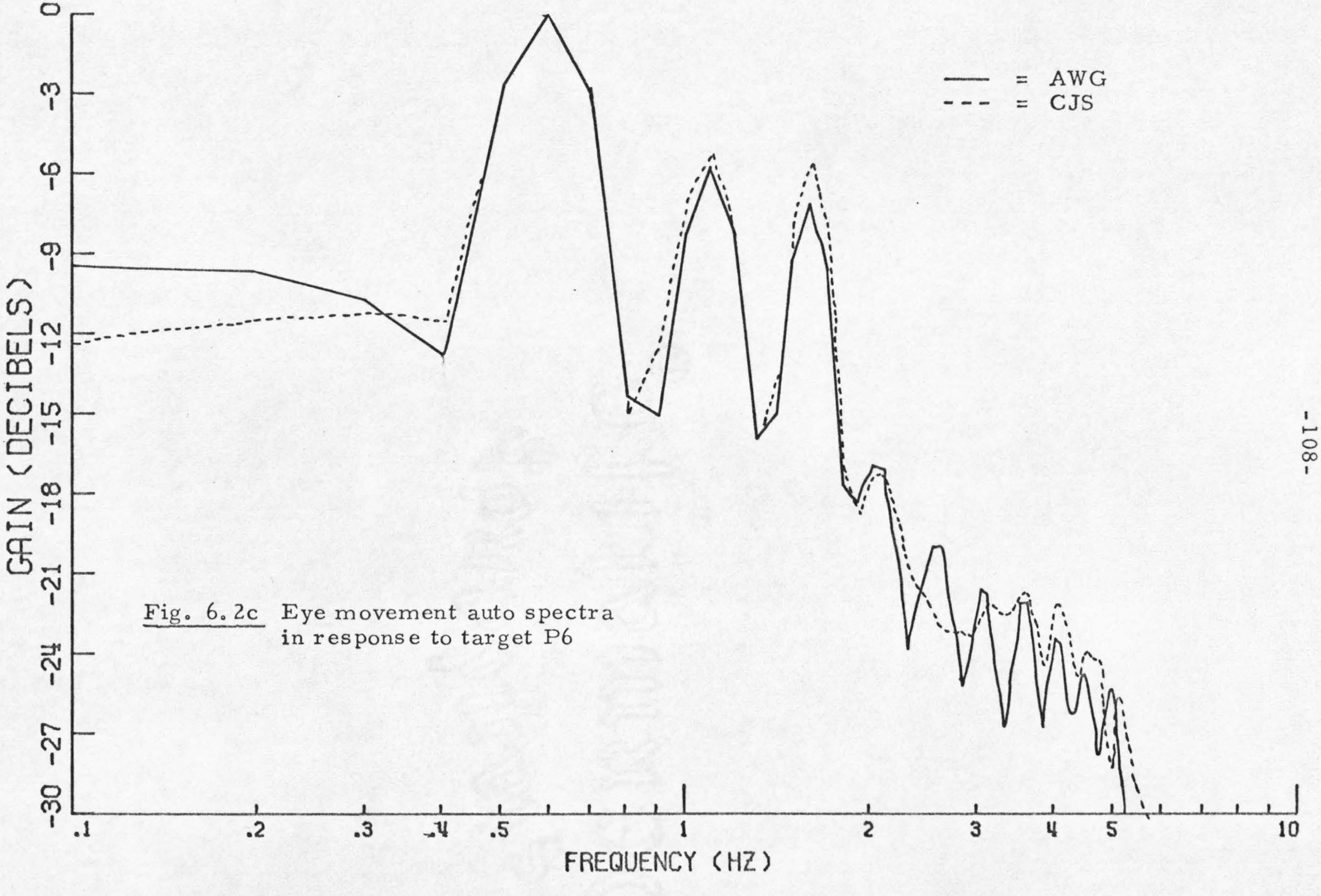

Fig. 6.2c Eye movement auto spectra in response to target P6

harmonics (except the 5th for CJS), although in this case the eye movements appear to contain low amplitude 9th and 10th harmonics not present in the input.

Tables 6.1a and 6.1b show representative peak correlation coefficients and time delays in response to P1-P6. It is interesting to note that although the tracking of P4 involves considerable inaccuracies (average peak coefficient of .866 for CJS), the spectra show that these are not caused by responding at frequencies not present in the input. Evidently the oculomotor system is very proficient at detecting the harmonic content of periodic signals. The tables show that, in general, increasing the number of harmonics in the target motion (increasing from P1 through to P5) increases the time delay and reduces the tracking proficiency as reflected in the correlation coefficients. P5 and P6 both have eight harmonics, but while the first three harmonics make up 95.6% of P6,[*] they make up only 89.8% of P5. Comparison shows that the delays for P6 are smaller than for P5. Thus for periodic target motions containing the same frequencies, the tracking improves as the lower harmonics are emphasized more.

These conclusions do not apply to square wave tracking, which is a far more complex process than is generally accredited. Beeler (1965) has shown that the time lag involved in tracking a square wave is a function of its frequency, and that prediction is shown only when

---

[*] This figure is calculated as the ratio of power contained in the first three harmonics to the power contained in all the harmonics. The power contained in any harmonic is proportional to its amplitude squared.

Run No.	Vertical Target	Left Vertical Delay MS	Left Vertical Coef.	Right Vertical Delay MS	Right Vertical Coef.
253	P1	0	.979	0	.975
254	P2	0	.951	0	.914
255	P3	58	.917	38	.925
256	P4	67	.909	48	.914
257	P5	125	.892	115	.870
258	P6	67	.854	58	.829

Table 6.1a Peak correlation coefficients and time delays in response to targets P1-P6 (AWG)

Run No.	Vertical Target	Left Vertical Delay MS	Left Vertical Coef.	Right Vertical Delay MS	Right Vertical Coef.
247	P1	0	.923	0	.958
248	P2	19	.917	19	.882
249	P3	67	.932	58	.915
250	P4	86	.876	86	.883
251	P5	125	.854	125	.779
252	P6	77	.881	77	.814

Table 6.1b Peak correlation coefficients and time delays in response to targets P1-P6 (CJS)

the frequency lies in the range of about .5 hz to 1 hz. Thus a square wave as a class of target motion cannot be classified as predictable or unpredictable. The square wave is also distinct from other periodic target motions in that the response is made up almost entirely of saccades. In fact, it seems as if the prediction mechanism for square waves may well be different from that for smooth, continuous target motions. I shall not consider the square wave problem in this thesis.

Increasing the harmonic content of a waveform increases the RMS (root mean square) speed (velocity magnitude) of the target motion. The results of tables 6.1a and 6.1b are therefore suggestive of a system whose performance depends on input velocity, a point that will be pursued later in this chapter. It is apparent, then, that the time delays of the oculomotor system are not the same, or even similar, for all classes of periodic target motions, despite the correspondence of target motion and eye movement frequency components.

How narrow must the target motion spectrum be for the delays to be like those in response to a pure sine wave? The spectra of the band-pass filtered noise waveforms B1-B6 were shown in Fig. 3.2, and Figs. 6.3a and 6.3b show typical responses for AWG and CJS. For frequencies above the center frequency, .5 hz, the bandwidth of the eye movements increases with increasing bandwidth of the target motion as was the case for low-pass filtered noise. For frequencies below the center frequency, the eye movement bandwidth tends to follow that of the target motion, but with less

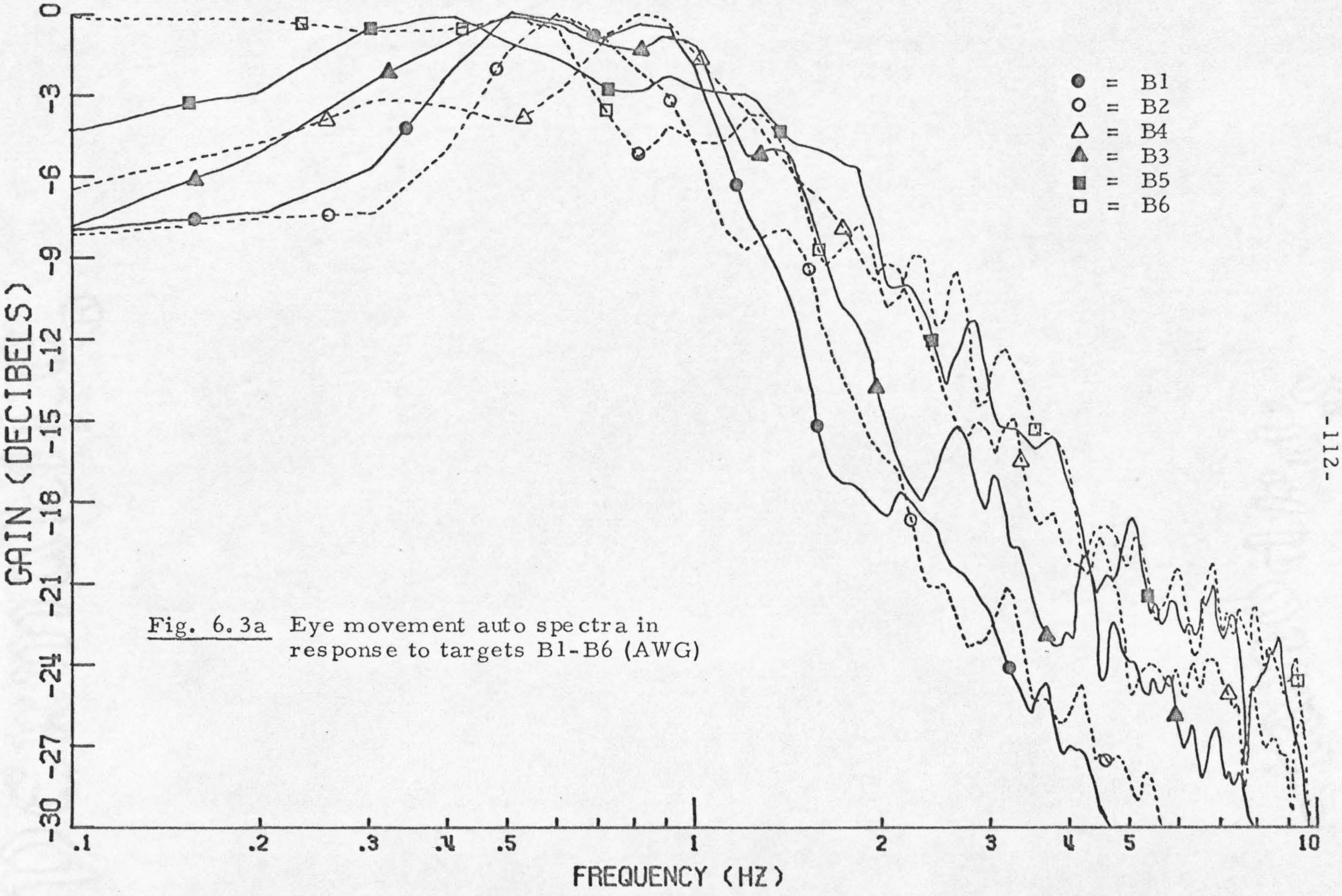

Fig. 6.3a Eye movement auto spectra in response to targets B1-B6 (AWG)

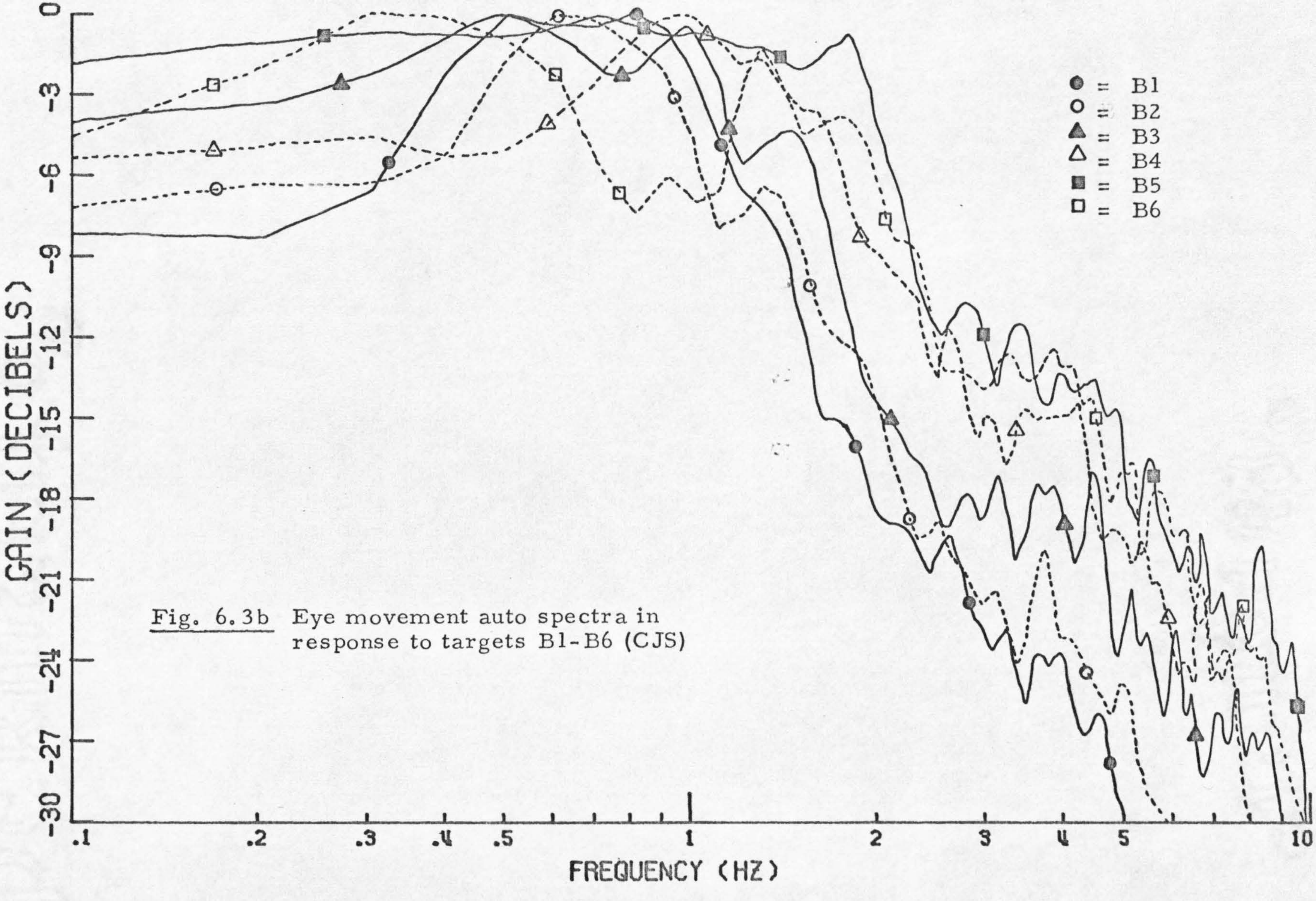

Fig. 6.3b Eye movement auto spectra in response to targets B1-B6 (CJS)

success than on the high frequency side. In particular, there is a tendency for the spectra to become flat below the center frequency.

It must be stressed that although the noise is narrow band, the target motions are definitely not periodic. Although highly unlikely, it could be conceivable that the oculomotor system may attempt to handle these targets by producing eye movements consisting of the sum of a sinusoid at the center frequency plus a noise component. If this were the case, the eye movement power spectra would show a distinct spike at the center frequency. Figs. 6.3a and 6.3b show that this is not the case and that the eye movements are devoid of any periodic components.

Tables 6.2a and 6.2b show representative peak correlation coefficients and time delays for both subjects. It is readily seen that the time delays are not those of a pure sine wave. In contrast to the low-pass filtered noise time delays, these time delays are strongly dependent on target bandwidth. A reason for this will be suggested later. Again, it is noticed that the data of these tables is suggestive of a velocity dependence.

It has been demonstrated that the distinguishing features of a sinusoidal target are twofold. In order to elicit the characteristic low time delays, the target motion must be periodic. Furthermore, the harmonics (other than the fundamental) must be restricted in their contribution to the total motion, resulting in an effectively narrow spectrum. In the data presented here, the signal P2 apparently satisfies these conditions in addition to the sinusoid P1. I further suspect that the harmonics should not exceed a certain

Run	Vertical	Left Vertical		Right Vertical	
No.	Target	Delay MS	Coef.	Delay MS	Coef.
217	B1	58	.911	58	.921
218	B2	77	.905	77	.913
219	B3	96	.881	96	.891
220	B4	125	.862	125	.850
221	B5	144	.803	144	.803
222	B6	173	.624	173	.622

Table 6.2a Peak correlation coefficients and time delays in response to targets B1-B6 (AWG)

Run	Vertical	Left Vertical		Right Vertical	
No.	Target	Delay MS	Coef.	Delay MS	Coef.
223	B1	58	.899	48	.896
224	B2	86	.890	77	.821
225	B3	115	.852	115	.817
226	B4	115	.769	115	.673
227	B5	125	.761	125	.764
228	B6	144	.734	144	.677

Table 6.2b Peak correlation coefficients and time delays in response to targets B1-B6 (CJS)

frequency limit. For example, if f_o were shifted to 1 hz, it is probable that P2 would show a considerable increase in time delay. However, this is merely conjecture.

2.2 What is the Source of the Time Delays? Is there a Predictor?

Does the oculomotor system contain a predictor, or can the time delays be explained by a mechanism similar to that of St-Cyr and Fender (1969b)? Recall that in the latter case, the time delays are comprised of the time required for neural signals to propagate from the retina through the relevant portions of the brain to the extraocular muscles, plus a delay time dependent on the target motion. The minimum possible time delay then is the propagation time, which is not easy to estimate. Related neurophysiological measurements in animals suggest a very rough estimate of 30-40 milliseconds (Bizzi, 1968; Cohen and Feldman, 1968; Cohen et al., 1965; Hyde and Eason, 1959; Pasik and Pasik, 1964; Robinson and Fuchs, 1969). However, such an estimate is very crude, and no reliance can be placed on it. Tables 4.3a and 4.3b show average sine wave delays of 8.6 milliseconds for AWG and 10.0 milliseconds for CJS. Tables 6.1a and 6.1b show sine wave delays of zero for both subjects, and delays for P2 of zero for AWG and 19.0 milliseconds for CJS. Many of these delays are obviously less than the propagation time (no matter how it is estimated, it is undoubtedly greater than 10 milliseconds and certainly not zero), strongly supporting the notion of a predictor.

What is the nature of the predictor? From the results of the experiments using periodic target motion and band-pass filtered Gaussian random motion, a few properties of the predictor are apparent. It can act only on periodic signals, and only effectively if the harmonic content is such that the bandwidth of the signal is sufficiently narrow. An interesting question is how much prediction is occurring in the signals P3-P6. It may be, for instance, that for these more complex periodic waveforms the system predicts the fundamental sinusoid and treats the remainder of the waveform as unpredictable. Or it may be that these waveforms are treated simply as unpredictable. This aspect is further investigated in section 2.4.

Further evidence of prediction in the oculomotor system is provided by square wave tracking data. Fuchs (1967b) plotted the time lag as a function of the cycle number for .5 and .8 hz square wave target motions. He found that in the first six or so cycles, the lag decreased monotonically from a high initial value to a much lower steady state value. In contrast he found that monkeys did not show this effect although in all other respects their eye movements appear to be qualitatively similar to those of humans (Fuchs, 1967a). Sugie (1971) modeled some aspects of the predictor for sine and square waves by estimating the target periodicity subject to some stochastic variation.

The problem is now reduced to explaining the delays for unpredictable target motions or the unpredictable components of the target motion. Phrased another way, the question might read: given a set of target waveforms and corresponding time delays, what can be concluded about the tracking mechanism? I have shown that the band-pass filtered noise targets B1-B6 are unpredictable, and I shall use these as the basis in my derivations.

The time delay model of St-Cyr and Fender is still appealing, and may be incorporated in the above framework by considering it as the mechanism for unpredictable targets. However, I feel that the basis of the model, that is the curve of ΔS (the average distance, in the scalar sense, the retinal image moves in a time interval Δt) versus Δt (Fig. 8 in their paper) should be linear. Consider the retinal image displacement waveform broken into n equidistant samples, as is of course true in the digital representation. Let ΔS_i be the scalar distance moved by the retinal image between the ith sample and the (i+1)th sample. Then ΔS^r, the average distance (arc length) moved in r sample intervals is given by:

$$\Delta S^r = \frac{1}{m} \sum_{i=1}^{m} [\Delta S_i + \Delta S_{i+1} + \ldots + \Delta S_{i+r-1}] \qquad \text{where } m=n-r$$

$$= \frac{1}{m} \sum_{i=1}^{m} \Delta S_i + \frac{1}{m} \sum_{i=1}^{m} \Delta S_{i+1} + \ldots + \frac{1}{m} \sum_{i=1}^{m} \Delta S_{i+r-1}$$

$$= \Delta S^1 + \Delta S^1 + \ldots + \Delta S^1$$

$$= r \, \Delta S^1$$

In other words, if the sample interval is τ, then in an interval $\Delta t = r\tau$, the retinal image moves an average distance of $r\Delta S^1$. This is not a non-linear curve as shown by St-Cyr and Fender, but a straight line whose slope is the average speed (scalar) $\overline{V}$ of the retinal image. In retrospect it is obvious that the average distance

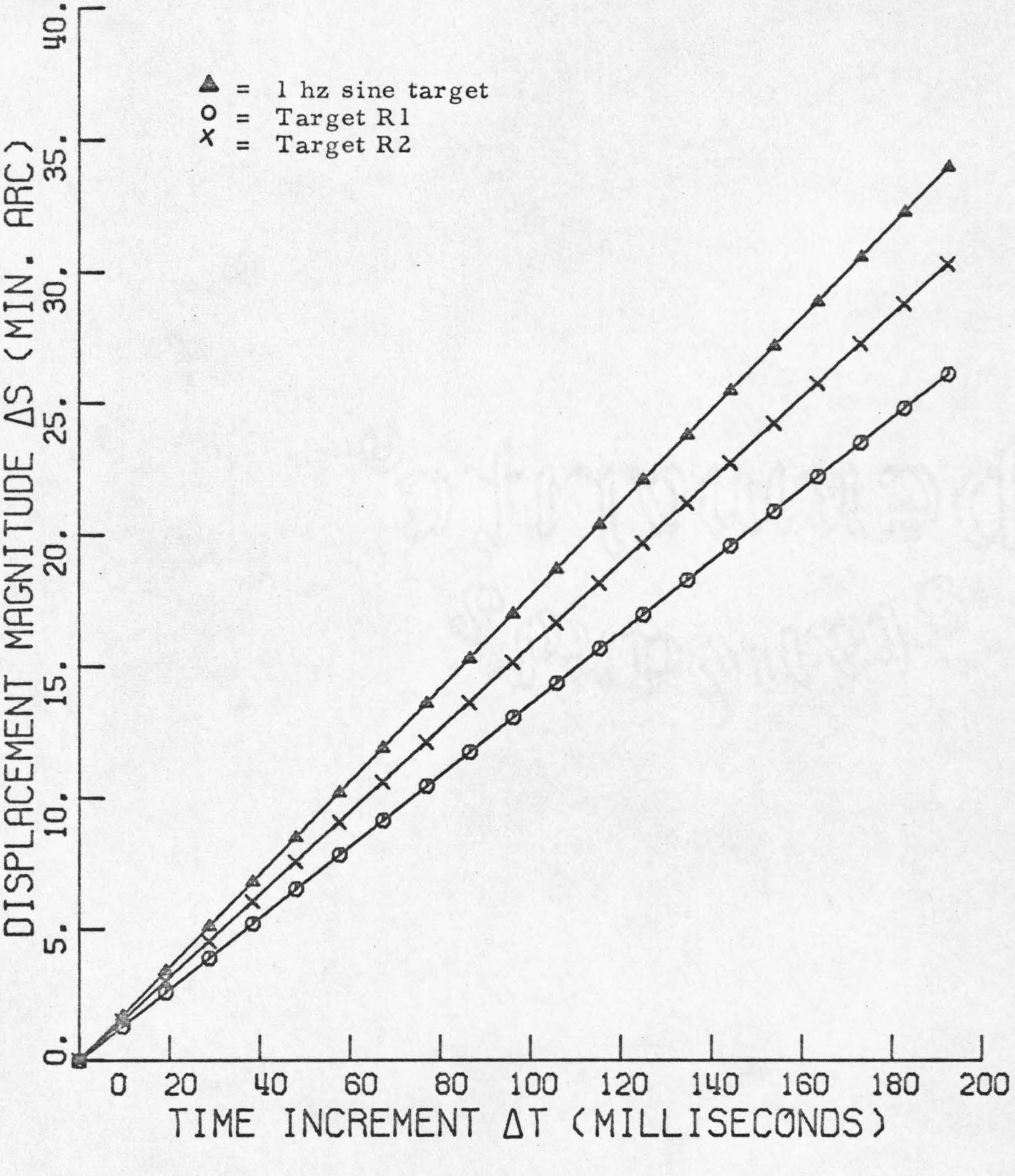

Fig. 6.4 The average scalar distance Δs moved by the retinal image in a time interval Δt plotted as a function of Δt. Subject AWG

travelled in a time Δt must be $\bar{V}\Delta t$, a linear relationship. This is verified in Fig. 6.4 which shows the plots for targets R1 and R2 as well as a 1 hz sinusoid for AWG. I must conclude that the shape of St-Cyr and Fender's curves are due to a difference in interpretation of the averaging process.

The model (see page 96) may now be simplified as follows. If the average retinal speed is $\bar{V}$, and the width of a receptor is W; then for a compute time T_c:

$$\delta S = \bar{V}T_c \quad \text{and} \quad \bar{\delta t} = W/\bar{V}$$

Thus $\quad (\delta S-\delta S_o)(\bar{\delta t} - \delta t_o) = C \quad$ becomes

$$(\bar{V}T_c-\delta S_o)(W/\bar{V}-\delta t_o) = C$$ which may be written as

$$WT_c = \rho+(\bar{V}T_c)\delta t_o+(W/\bar{V})\delta S_o$$ where $\rho = C-\delta S_o\,\delta t_o$, a constant.

This equation is linear in the unknown constants δS_o, δt_o, and ρ. The time T_c is given by $T_c = T_d-T_p$ where T_d is the measured time delay and T_p is the propagation delay. For any target waveform, $\bar{V}$ and T_c are easily determined (assuming some value for T_p), and since W is known, the unknown constants are trivially determined from the data by a linear regression analysis.

To test the feasibility of the above model, the regression analysis was performed on the data for targets B1-B6. The problem of T_p was circumvented by trying successively 10, 20, 30, 40 and 50 milliseconds. The data did not fit the model at all satisfactorily. This statement is made on the basis that for all values of T_p, the regression coefficients δS_o, δt_o, and ρ had standard deviations that were in excess of their mean values. The standard deviations of δS_o and δt_o were also in excess of the mean values of δS and δt respectively. The reason for the poor fit in this case is apparent. The constants δS_o and δt_o turn out to be much less than values for δS and $\overline{\delta t}$ respectively. As such, this is desirable, since the model is only appealing in this case. As a result, the model is approximately $(\delta S)(\overline{\delta t}) = C$ or $(\overline{V}T_c)(W/\overline{V}) = C$, that is T_c = constant which is not the case for B1-B6.

In both the experiments where the target motions were band-pass filtered Gaussian noise, and those with periodic target motions, the qualitative correspondence between target speed and time delay was mentioned. To quantify this relationship, the time delay is plotted as a function of $\overline{V}$, the average speed of the retinal image. Figures 6.5a and 6.5b show these plots for target motions B1-B6 for both subjects. It appears as if the data could be adequately described by a linear relationship, suggesting the following simple model. Let $\overline{V}$ be the average speed of the retinal image for a target motion with overall time delay T_d, and let V_o and K be constants. Then I propose that T_c, the time delay associated with the waveform is given by:

$$T_c = K(\overline{V} - V_o)$$

or

$$(T_d - T_p) = K(\overline{V} - V_o)$$

that is

$$T_d = K\overline{V} + (T_p - KV_o)$$

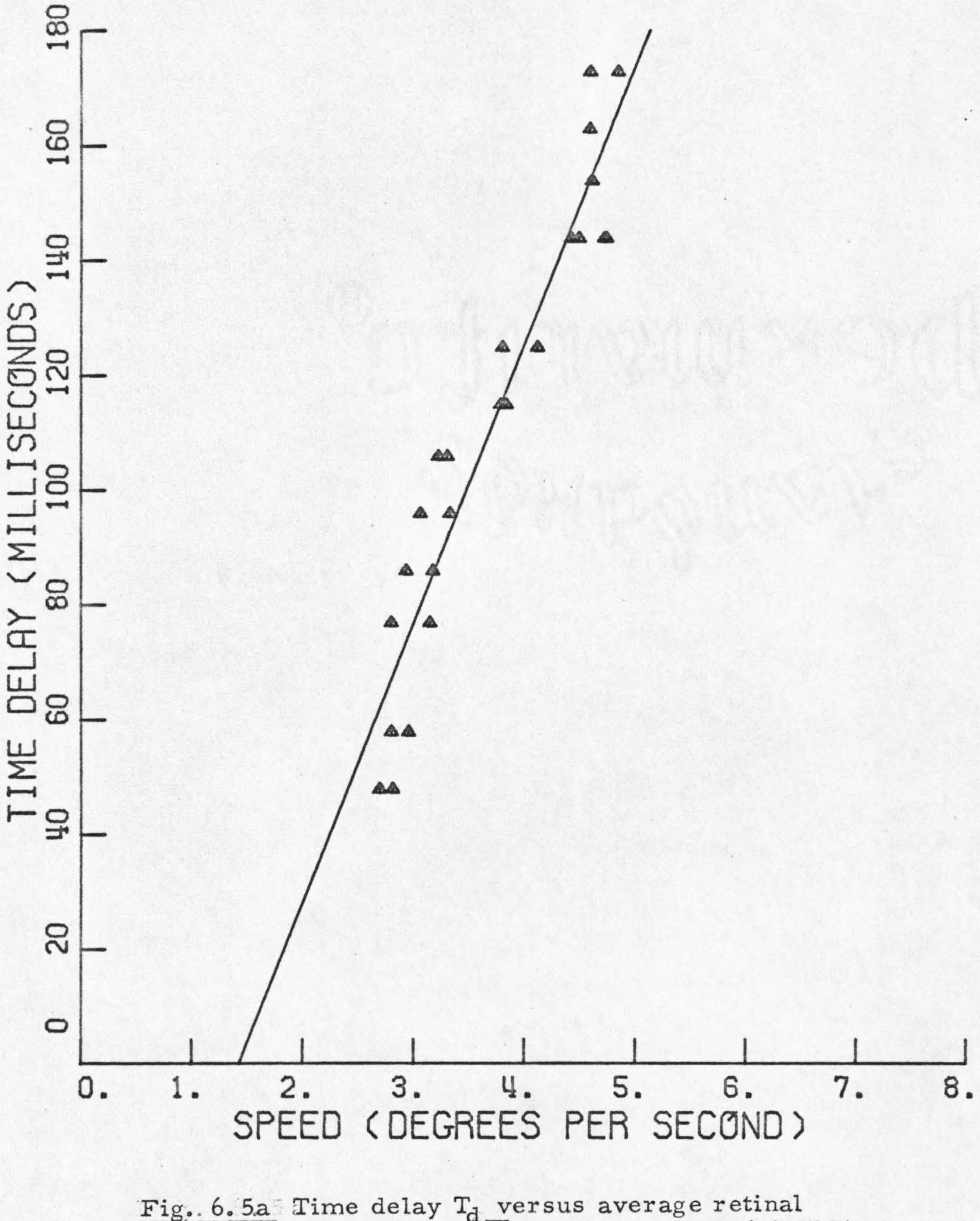

Fig. 6.5a Time delay T_d versus average retinal image speed $\overline{V}$ for targets B1-B6 (AWG)

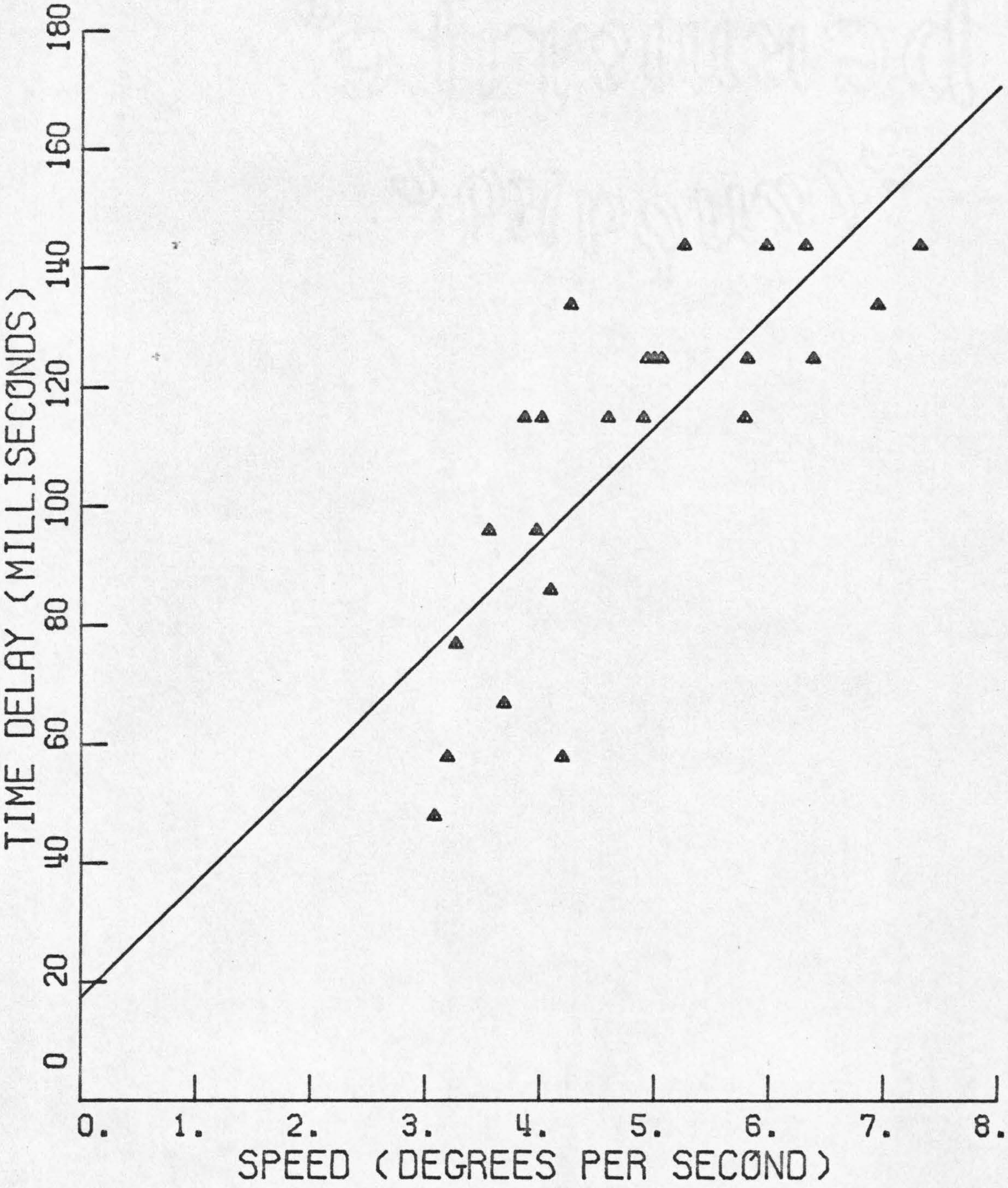

Fig. 6.5b Time delay T_d versus average retinal image speed $\overline{V}$ for targets B1-B6 (CJS)

Since the propagation time T_p is incorporated in the intercept, it need not be independently determined to test the model.

Figs. 6.5a and 6.5b show the plots of $\overline{V}$ versus T_d together with the least squares fitted straight lines for AWG and CJS respectively. For AWG, the fit is excellent. The slope is 48.7 (standard deviation 3.4) and the intercept -69.8 (standard deviation 12.7). That is K = 48.7 milliseconds/degree per second and $T_p - KV_o = -69.8$ milliseconds. As an illustration, if T_p is 35 milliseconds, then V_o is 2.15 degrees per second. For CJS the fit is not as good. The slope is 19.2 (standard deviation 3.3) and the intercept 17.3 (standard deviation 16.3). In this case a T_p of 35 milliseconds would give a V_o of .92 degrees per second. It is interesting to note that if the 6 points with velocities above 5.5 degrees per second were omitted from Fig. 6.5b, then the straight line would be almost the same as that for AWG, and would be a much better fit.

2.3. The Model Applied to Periodic Waveforms

It has already been established that the periodic targets P1 and P2 are tracked in a predictive mode. The question was raised as to whether the targets P3-P6 were tracked in a purely non-predictive manner, or whether there was a predictive component present. Figs. 6.6a and 6.6b show the plots of T_d versus $\overline{V}$ for the waveforms P3-P6. For AWG the fitted straight line has slope 35.3 (standard deviation 7.8) and intercept -74.2 (standard deviation 33.3). The straight line fitted for CJS has slope 29.6 (standard deviation 4.2) and intercept -74.6 (standard deviation 22.3). For a

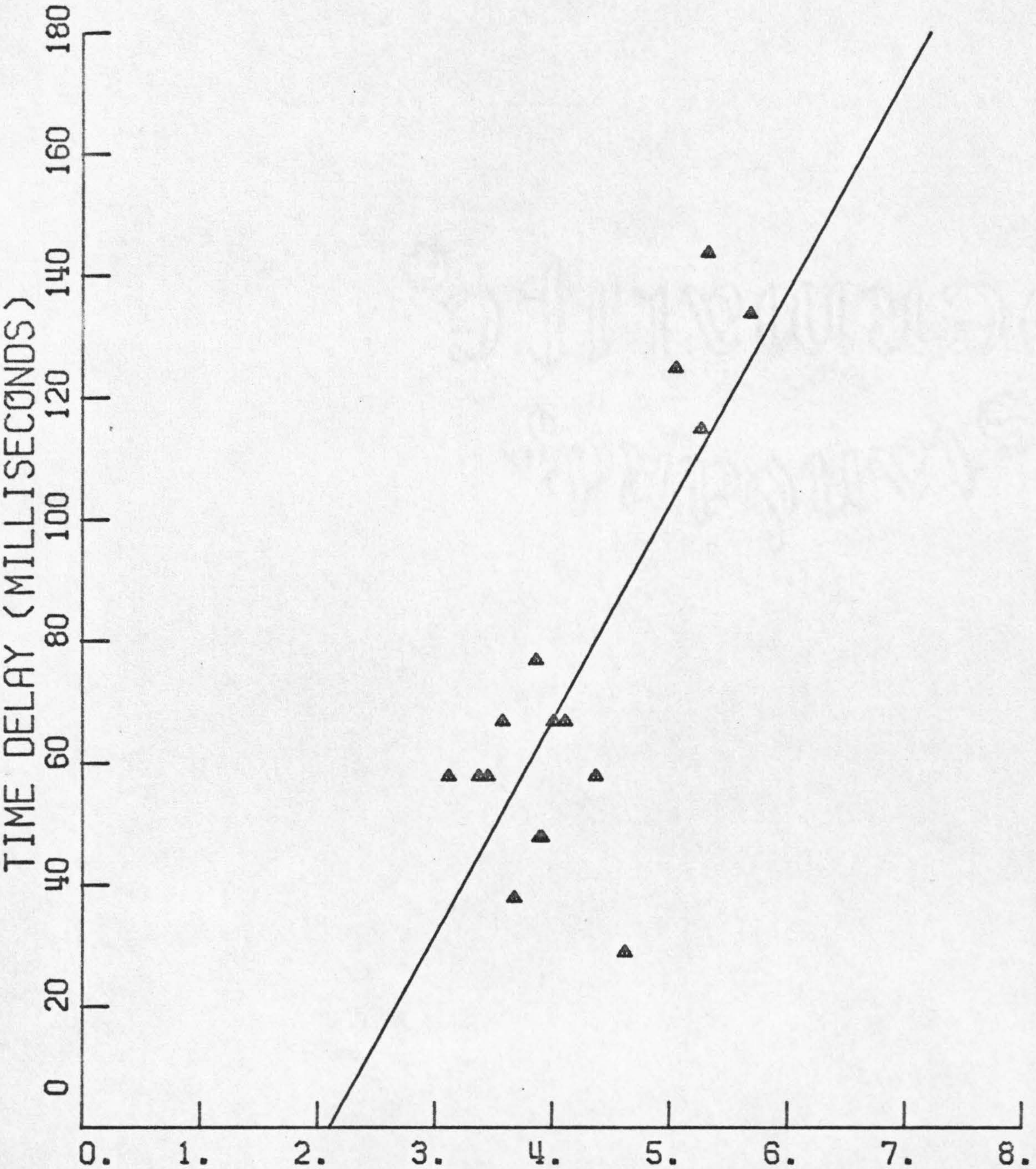

Fig. 6.6a Time delay T_d versus average retinal image speed $\overline{V}$ for targets P3-P6 (AWG)

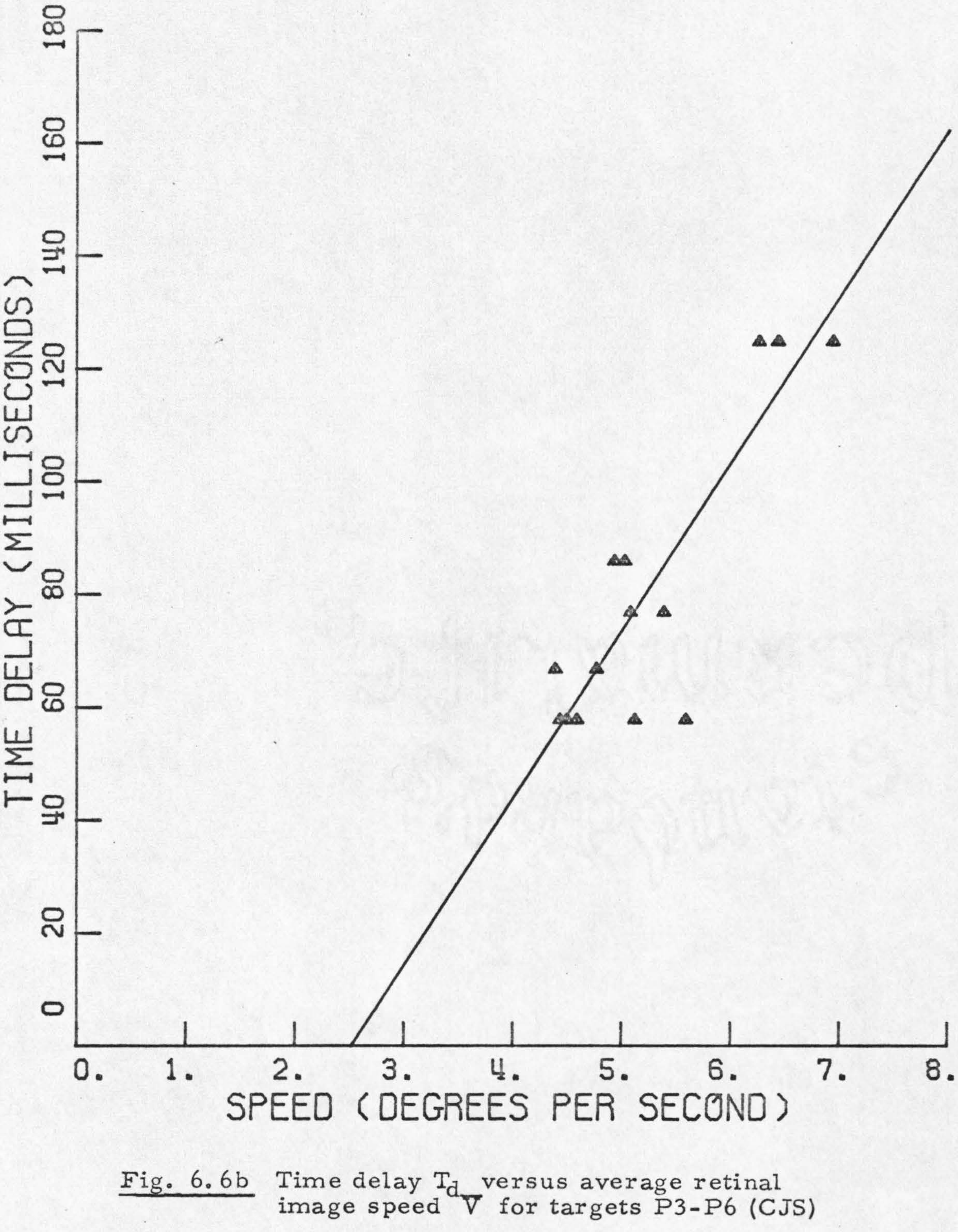

Fig. 6.6b Time delay T_d versus average retinal image speed $\overline{V}$ for targets P3-P6 (CJS)

T_p of 35 milliseconds, the threshold V_o would be 3.15 degrees per second for AWG and 3.7 degrees per second for CJS. Figs. 6.6a and 6.6b show that the data do fit the model quite well. It is very significant that the model is applicable to periodic target motions as well as to filtered random motions. The parameter V_o is higher for both subjects than for the band-pass filtered noise data. Alternately, direct comparison of Figs. 6.6a and 6.6b with Figs. 6.5a and 6.5b shows that at corresponding velocities, the time delays are smaller for P3-P6 than for B1-B6. This leads me to speculate that a predictive component is present in tracking P3-P6. Subtracting this predictive component from the total waveform would leave the non-predictive tracking mechanism with a lower speed waveform to track, hence the reduced time delay.

If the eye movements and target motion could be split into predictive components and non-predictive components, then the above hypothesis would be proved. Figures 6.2a, 6.2b, and 6.2c show that the responses to P3-P6 do contain components at frequency f_o (.5 hz). If there is a predictive component, it may be taken, as a first approximation, as the first harmonic component at frequency f_o. Subtracting this from the total waveform leaves an approximation to the non-predictive component. This procedure was applied to the target motion and eye movements for P3-P6 for both subjects. The peak correlation coefficients and time delays for the non-predictive components should then be respectively lower and higher than the corresponding values for the total waveform. Tables 6.3a and 6.3b show typical 'non-predictive' values corresponding to the total

Run No.	Vertical Target	Left Vertical Delay MS	Left Vertical Coef.	Right Vertical Delay MS	Right Vertical Coef.
255	P3	58	.657	48	.716
256	P4	67	.615	58	.643
257	P5	134	.616	134	.585
258	P6	77	.695	67	.686

Table 6.3a Peak correlation coefficients and time delays in response to the non-predictive components of targets P3-P6 (AWG)

Run No.	Vertical Target	Left Vertical Delay MS	Left Vertical Coef.	Right Vertical Delay MS	Right Vertical Coef.
249	P3	67	.744	67	.695
250	P4	106	.674	106	.670
251	P5	144	.517	134	.408
252	P6	86	.756	77	.639

Table 6.3b Peak correlation coefficients and time delays in response to the non-predictive components of targets P3-P6 (CJS)

waveform values of tables 6.1a and 6.1b. The correlation coefficients are much lower, and the time delays are higher. Although the time delay changes are not as large as expected, they are always increases and never decreases. This tends to confirm the postulate of the presence of a predictive component. However, for several reasons this extraction process is rather arbitrary and error prone, discouraging vindictive conclusions. In the first place, the predictive component (assuming it exists) is not necessarily simply the first harmonic. A greater source of potential error is the assumption that the .5 hz sinusoidal target component elicits a .5 hz sinusoidal eye movement. From eye movement records it is clear that the response to a sinusoid is not perfectly sinusoidal, and may be thought of as having components at higher harmonics. Thus the non-predictive eye movements isolated here have potential errors greater than those due to experimental measurement and computation alone. What effect these may have, especially on the time delays, is difficult to say. Despite these ominous warnings, I feel that the agreement between these calculations and the reasoning in the previous paragraph does lend support to the hypothesis of a predictive component in tracking P3-P6.

2.4 Time Delays for Low-Pass Filtered Gaussian Random Motion.

In section 2, I pointed out that time delays obtained for targets R0-R5 were nearly constant and of the order of 150 milliseconds. In contrast, St-Cyr and Fender obtained time delays varying between about 120 and 300 milliseconds for similar target motions. This discrepancy can be explained by the differences in the methods of calculating time delays.

Consider the method of St-Cyr and Fender, which ascribes equal weight to the phase lags of all frequency components whose magnitude is greater than -30 db relative to the maximum component magnitude. Fig. 3.1 shows that the power spectra for R0-R5 differ little below .5 hz and that they differ only over a relatively narrow frequency range. For the following argument, consider a comparison of R1 and R2, whose major differences occur between 1 hz and 3 hz. Thus the phase lags of the eye movement responses to R1 and R2 are not expected to differ much below 1 hz, but are expected to differ above that. With a frequency resolution of .1 hz, the phase curves would have 9 data points below 1 hz and 21 between 1 hz and 3 hz. Least squares fitting a pure time delay therefore tends to emphasize the differences, and different time delays would be expected.

On the other hand, R1 and R2 are already respectively 9 and 6 db down at 1 hz, and 24 and 18 db down at 2 hz. Since the cross-correlation function effectively weights components proportional to their amplitude, my method tends to emphasize the common aspects of R1 and R2. Large differences in time delays are therefore not expected. These arguments, of course, apply to all target motions R0-R5.

For waveforms B1-B6, Fig. 3.2 shows that the spectra are similar over only a small region, so that delays are expected to differ, as is the case.

3. Interpretation and Implications of the Model

Does the model make sense physiologically? The following heuristic discussion illustrates my interpretation of a possible way in which the model could be implemented by the oculomotor system. In the discussion the quantities velocity and speed are used in the strict sense as a vector and as a scalar respectively. Suppose that at some point in time the speed of the retinal image V is sampled, and its value above threshold (assume for the moment it is above threshold) $V-V_o$ is calculated. The compute time T_c is proportional to this value with proportionality constant K, and dictates a holding time T_h of $2T_c$. For a time interval T_h, the system averages the instantaneous retinal image velocity as $\overrightarrow{V_a}$. At the end of this interval, an error velocity of $\overrightarrow{V_a}$ is passed on to the rest of the system. Once again the instantaneous speed of the retinal image is sampled to give a new T_h. During this time the velocities are again averaged, while the error velocity is maintained at the average $\overrightarrow{V_a}$ computed during the previous interval. This process is repeated for the duration of the tracking task.

Several properties of such a model are immediately apparent. The system is sample data with a sample interval dependent on the nature of the target motion. Moreover, these variations result in an entirely natural way without the need to postulate any contrived stochastic distributions. Is a sample interval proportional to the retinal image speed logical? High retinal image speeds indicate rapid and non-smoothly moving targets. Especially in view of the propagation delay T_p, it is easy to see that if the system responded immediately to such retinal errors, the eye movements could become rather erratic, approximating the target motion rather poorly. A better approach might be for the eye to replace the retinal image motion by a smoothed motion, avoiding the vain responses caused by the second order wiggles of the target which are not really relevant to the overall trend of the target motion. On the other hand, if the retinal image speed is small, the target motion must be relatively smooth and slow, so that immediate action on the tracking error is appropriate. Viewed in this light, a sample interval proportional to the retinal image speed is quite logical. So far I have purposely side-stepped the issue of distinction between the smooth pursuit and saccadic systems. There are two ways in which my model may be viewed. Subscribing to the traditional approach of a velocity sensitive smooth pursuit system divorced from the position sensitive saccadic system at the retinal image level (Rashbass 1961), it might be tempting to relegate my model to the smooth pursuit branch only. In this case, the saccadic branch could still be handled by current models such as that of Young *et al* (1968). This would mean that the data points in Figs. 6.5a and 6.5b would have error components caused by the saccadic loop.

On the other hand, it is quite conceivable that my sampling mechanism may be common to both branches. If the speed were below threshold or above some critical value (such as 100 degrees/second), the sample time T_c would be taken as, say, 200 milliseconds. The output of the model could easily be a position average and a velocity average, fed to two separate branches if necessary.

When viewed in this light, I think it is clear that the model is capable, with modification if necessary, of reproducing many of the results of step, pulse and step-ramp target experiments as well as those in response to periodic and random motions. To achieve this the speed V may have to be sampled by a finite pulse width, and may even have to be modified by position error. In fact, I feel that the sampling would almost certainly be of finite width. The concept of simultaneous velocity and position sampling, with a sample interval determined by the mechanism outlined above, is not at all distressing, but rather appealing.

From tables 6.2a and 6.2b it is clear that this model is quite capable of sample intervals less than Robinson's 75 milliseconds. In this context, an objection that might be raised against the model is that figures 6.5a and 6.5b imply that ramps with velocities above about 4 or 5 degrees per second would elicit large sample intervals contradicting experimental observation. However, it is quite possible that there may be a second limiting mechanism so that, for example, velocities between 5 and 100 degrees per second would be treated as near threshold velocities resulting in small sample intervals.

At this point I stress that I do not regard my model as the final answer to the oculomotor system. In fact I know that it is an over-simplification and is bound to be contradicted by future experiments. What then is its value? It is my conviction that, at the present time, the field of eye movements is dominated by dogmas often based on slender evidence. These dogmas seem to be accepted without alternate explanations being sought, a situation that can only slow down progress.

In contrast, my model shows that, for example, there are ways in which the system responses can behave in an apparently continuous manner at some times and in a sampled manner at others. It also shows that smooth pursuit and saccadic systems can have more in common than is commonly conceded. There are undoubtedly a whole host of results that could be reinterpreted profitably, especially in the light of some of the latest evidence. The main virtue of my model is in demonstrating some of these alternate approaches.

VII. ASYMPTOTIC BEHAVIOR OF THE POWER SPECTRA

Different types of eye movements are mediated by different portions of the brain and involve different neural pathways. As yet, these brain centers and neural paths have not been unequivocally resolved, and the literature contains a multitude of conflicting evidence and opinions (for example Bizzi, 1968; Cohen et al., 1965; Cohen and Feldman, 1968; Hyde and Eason, 1959; Pasik and Pasik, 1964; Robinson and Fuchs, 1969). However, it is certain that all signals reach the extraocular muscles via the cranial nerves extending from the oculomotor nuclei, leading to the concept of the final common path. These components, from the oculomotor nuclei to the eyeball itself, are common to all types of eye movements. The muscle-eyeball mechanics are particularly important, and it is impossible to explain the dynamics of any eye movements without reference to them. In the work that follows, this will frequently be referred to simply as the mechanical system.

1. The Mechanics of Eye Movements - A Brief Review

Westheimer (1954) studied saccades in response to a target step ranging in magnitude from 2 to 30 degrees, and on the basis of his analysis proposed what is probably the original model of the mechanical system. He concluded that saccades were produced by a step change in muscle tension, and the eyeball muscle mechanics behaved like a second order system with a damping constant of .7 and a natural frequency of 19 hz (later modified by Westheimer (1958) to 38 hz).

Robinson (1964) measured eye movements in the range of 5 to 40 degrees in response to externally applied torque steps. He expressed the transfer function in terms of a fourth order differential equation, and since the gain was down 3 db at 1 hz, he described the system as heavily overdamped. The rapid response of saccades was explained by postulating that the muscle torque consists of a step plus a pre-emphasis pulse. In 1965, Robinson performed similar experiments on smooth pursuit movements, measuring muscle forces during the execution of ramp type movements, with velocities ranging from 2 to 10 degrees per second. He found a transfer function very similar to that found in his saccadic experiments, and again explained rapid responses of smooth pursuit movements by pre-emphasis. Childress and Jones (1966) performed experiments similar to those of Robinson and arrived at basically the same model.

By attaching a small piece of magnetic material to a contact lens, Thomas (1966) was able to apply forces to the eyeball by a coupling magnetic field. To derive the system transfer function, he measured eye movements by means of an accelerometer attached to the lens. Working in a frequency range from 10 hz to 100 hz, Thomas concluded that the system was underdamped, with a natural frequency in the vicinity of 40 hz. Bengi and Thomas (1968) used the same accelerometer measurement technique on fixational movements. They found a 40 hz resonance peak in the velocity spectrum, and found that this peak shifted down in frequency as the inertia of the eyeball was increased by adding weights. This was taken as confirmation of Thomas' finding of an underdamped system as opposed to Robinson's and Childress and Jones' claim of an overdamped system. Extending his experiments, Thomas (1969) refined his model, and although he retained the notion of an underdamped system, decided that the saccade producing torque is pre-emphasized in a manner somewhat similar to Robinson's pre-emphasis.

At first sight it seems as if Thomas' findings cannot be reconciled with those of Robinson and Childress and Jones. However, in a review paper, Robinson (1968) compared the two transfer functions in detail and showed that they agreed closely for frequencies above 10 hz. Both confirmed the underdamped nature of the system in this range. Thomas did not consider frequencies below 10 hz, and in this range the models of Robinson and Childress and Jones are overdamped in nature.

Findlay (1970) recorded eye movements during fixation and isolated the tremor component. From the power spectra of this component, he deduced a second order underdamped model for the muscle eyeball dynamics, with time constants .002 seconds and .02 seconds. The frequency range was essentially 10-200 hz, and the model is based on the assumption that the tremor producing forces have a flat spectrum in this range. Findlay claims that his findings are in agreement with Robinson's overdamped system, although the time constants are different. However, in the frequency range he used, he should have observed the underdamped properties common to both Robinson's and Thomas' model.

2. Eye Movement Power Spectra

The eye movement power spectra provide a powerful tool for studying the eyeball-muscle dynamics and the nature of the extraocular muscle active state tensions producing the eye movements. If one of the above linear models is accepted, then the power spectra uniquely determine the active state tensions. The question is whether any of the above models are suitable for use with the type of eye movements recorded here? The eye movements used by Robinson and by Childress and Jones were saccades much larger than those occurring in this work, and also in the case of Robinson, constant velocity targets giving rise to movements larger than those here. Thus, it may well be that these models are not suitable for my analysis. While Thomas' model was derived for frequencies above 10 hz, the relevant range here is below 10 hz, and often below 5 hz. Once again, it would be unwise to apply Thomas' model, as it stands, to my results. The eyeball-muscle system is a relatively simple mechanical system designed to operate over a range of the order of 100 degrees. For the relatively very small range of movements in my experiments (2 degrees), the muscle-eyeball dynamics can almost certainly be adequately represented by a linear system. This notion is supported by the reasonable success and agreement of the above linear models for larger movements.

Auto power spectra of eye movements in response to the low-pass filtered Gaussian random target motions R0-R5 showed consistent asymptotic behavior. The linear trend commenced in the vicinity of -12 db, and the slope of the line was approximately

-30 db per decade. This is illustrated in figures 4.2a and 4.2b. Eye movement power spectra in response to the band-pass filtered Gaussian random motions B1-B6 show similar asymptotic behavior, with the same -30 db per decade slope. Figs. 6.3a and 6.3b illustrate this.

Figures 4.2a, 4.2b, 6.3a and 6.3b show that as the target motion bandwidth increases, the bandwidth of the eye movements increases. Since this is accomplished without change in the asymptotic behavior between about 1 hz and 3 hz, it can be concluded that the mechanical system has no effective poles or zeros between 1 hz and 3 hz. In other words, the tentative conclusion is reached that all the poles and zeros are either below 1 hz or above 3 hz. Since the spectra of target waveforms R0-R5 and B1-B6 all have the same linear trend between about -12 db and -30 db, the constancy of the eye movement spectra asymptotes is not surprising in itself. The linear portions of the target motion spectra have slopes of about -50 db per decade, which makes the smaller 30 db per decade seem surprisingly low. It might be tempting to naively conclude that the oculomotor system has "one more zero than pole" below 1 hz. However, the situation demands close investigation. Moreover, St-Cyr (1969) used low-pass filtered Gaussian random motions with a slope of about -32 db per decade below -12 db, yet he, too, obtained eye movement power spectra with asymptotes of about -30 db per decade.

2.1. Power Spectra of Eye Movements During Fixation. Stabilized Retinal Image Viewing, and Open Loop Tracking.

The main problem in explaining the shape of the power spectra is deciding which factors are due to the mechanical system, and which are due to processing in the central nervous system. Changing the nature of the processing without changing the mechanical system could help. To this end, power spectra were obtained for eye movements during fixation and during stabilized retinal image viewing. For these experiments the quantization error was reduced giving an estimated overall resolution of 15-25 seconds of arc. The problem of drift in the stabilized retinal image condition was overcome by destabilizing the image for about $1\frac{1}{2}$ seconds between stabilized intervals of 9.9 seconds (1024 samples).

Typical eye movement power spectra for both viewing conditions are shown in figures 7.1a and 7.1b. These figures show that for both subjects the nature of the spectra is the same for fixation as for stabilized retinal image viewing. This indicates that the spectra are produced almost entirely by a source independent of the retinal image. For stabilized retinal images, the spectra would be determined entirely by this stochastic generator. During normal fixation the retinal errors are very small, so that their contribution to the spectra, via the oculomotor control paths, might be expected to be small compared to that of the stochastic generator.

The slopes of the spectra are approximately -20 db per decade, and, in fact, for experimental results the spectra are excellent representations of a linear first order filter with a cutoff frequency of about .2 hz to .3 hz. All that can be rigorously concluded is that the generator and the mechanical system together have the first order filter type properties. However, in view of the undoubted stochastic

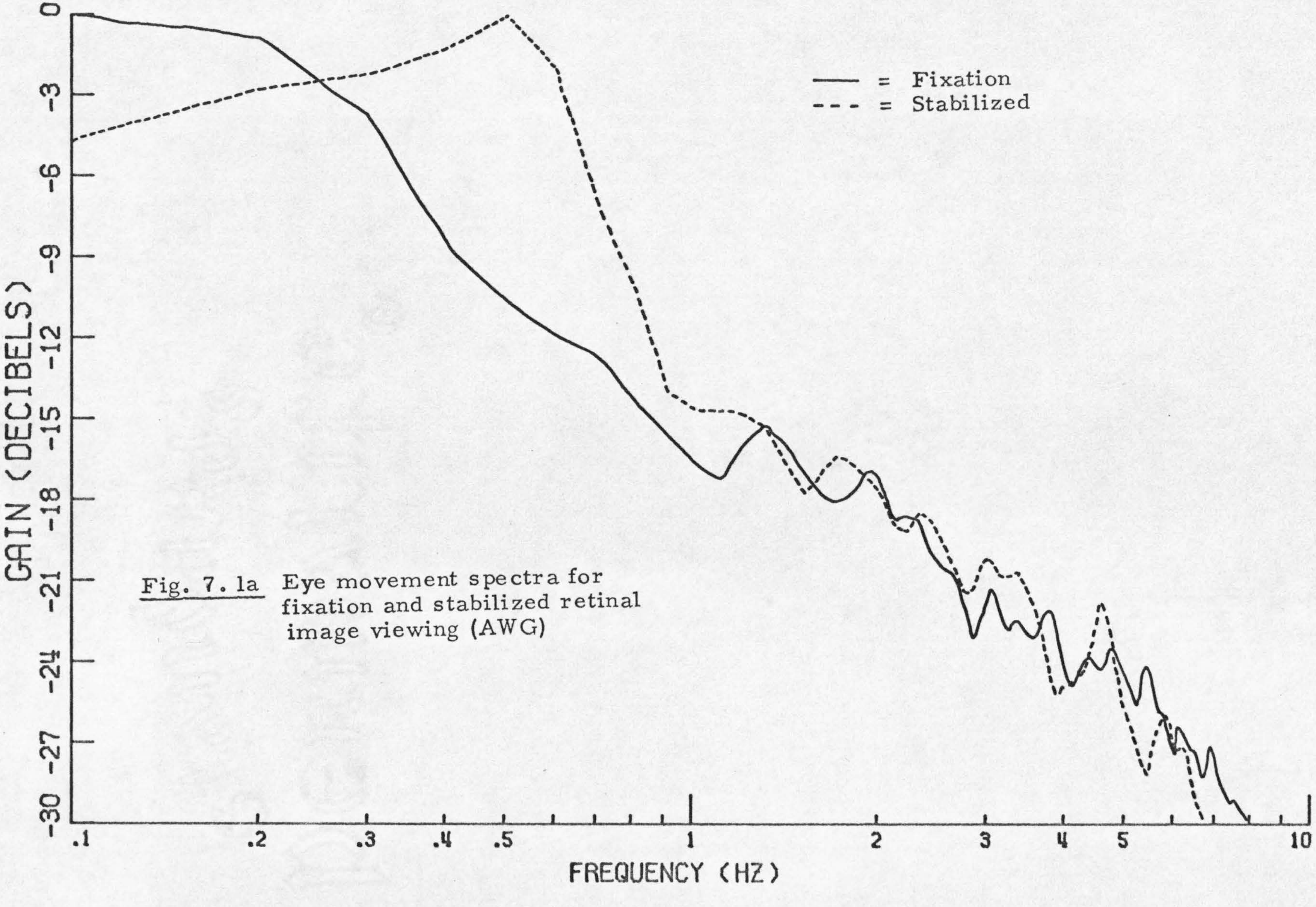

Fig. 7.1a Eye movement spectra for fixation and stabilized retinal image viewing (AWG)

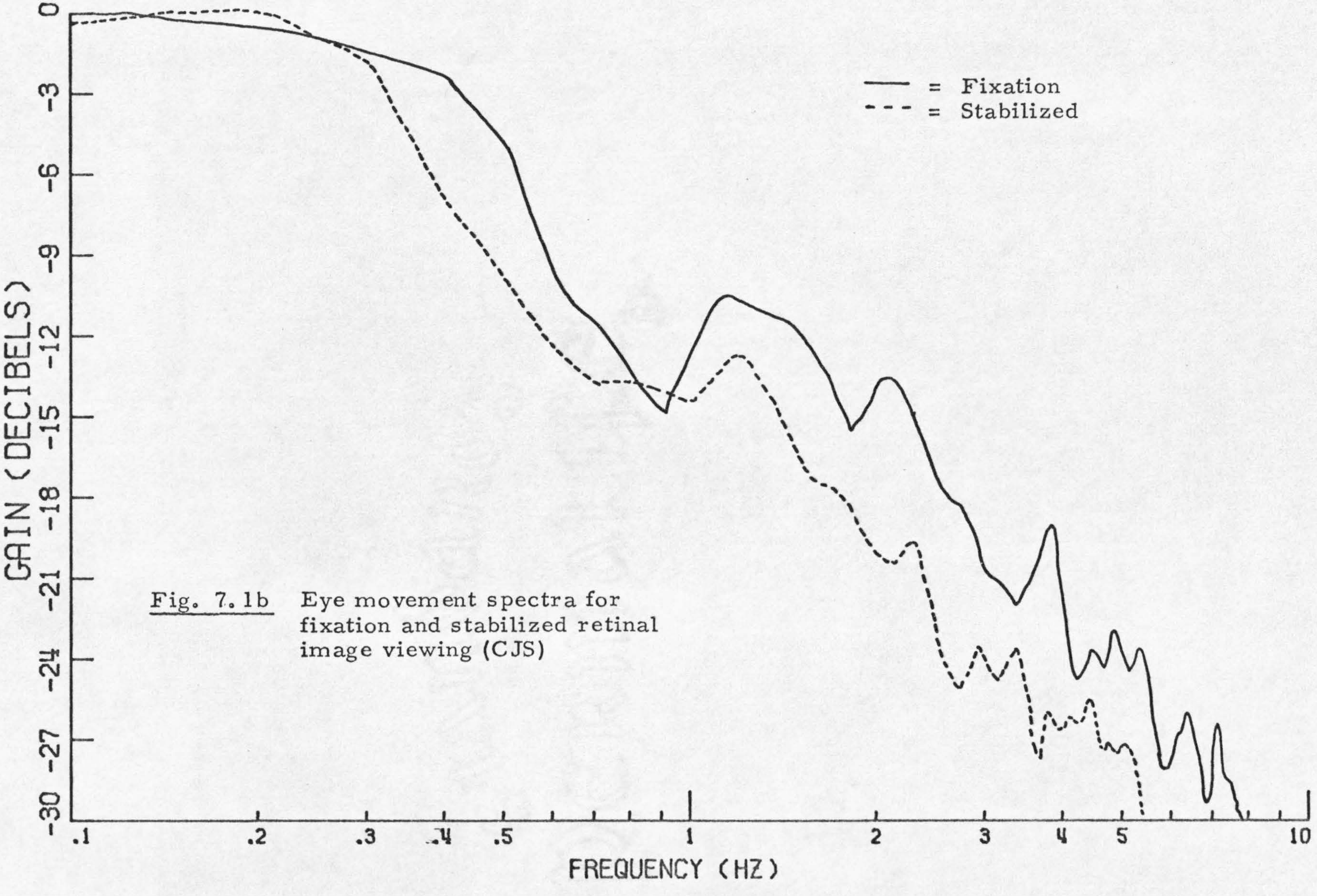

Fig. 7.1b Eye movement spectra for fixation and stabilized retinal image viewing (CJS)

nature of the generator and the linear properties of the mechanical system for such small movements, it is reasonable to attempt a separation. It is quite likely that the generator frequency spectrum is white in the range .1 hz to 10 hz, in which case the system behaves precisely as a first order filter with cutoff frequency between about .2 hz and .3 hz. This conclusion is valid only for small movements in the range .1 hz to 10 hz.

In terms of the above theory, it is now possible to separate the spectral contributions of the random noise tracking experiments. Since the mechanical system is behaving as a first order filter, the -30 db per decade slope indicates that the active state tension has a spectrum with a linear rolloff of 10 db per decade in the region of about -12 db to -30 db. It can be concluded that the oculomotor control system is producing an active state tension with an asymptotic roll-off of 10 db per decade, apparently independent of the spectral characteristics of the target motion. As the bandwidth of the target motion increases, the bandwidth of the active state tension increases.

The non-linearity of the oculomotor control system has been repeatedly demonstrated. In view of this, the closed loop nature of the system makes it difficult to pinpoint the cause of this 10 db per decade roll-off. Since the target motion spectrum does not affect this 30 db per decade roll-off, it is probable that this figure is independent of the slope of the retinal image motion spectrum. The open loop power spectra should then also fall off at 30 db per decade. Figure 7.2 shows representative spectra for both subjects tracking

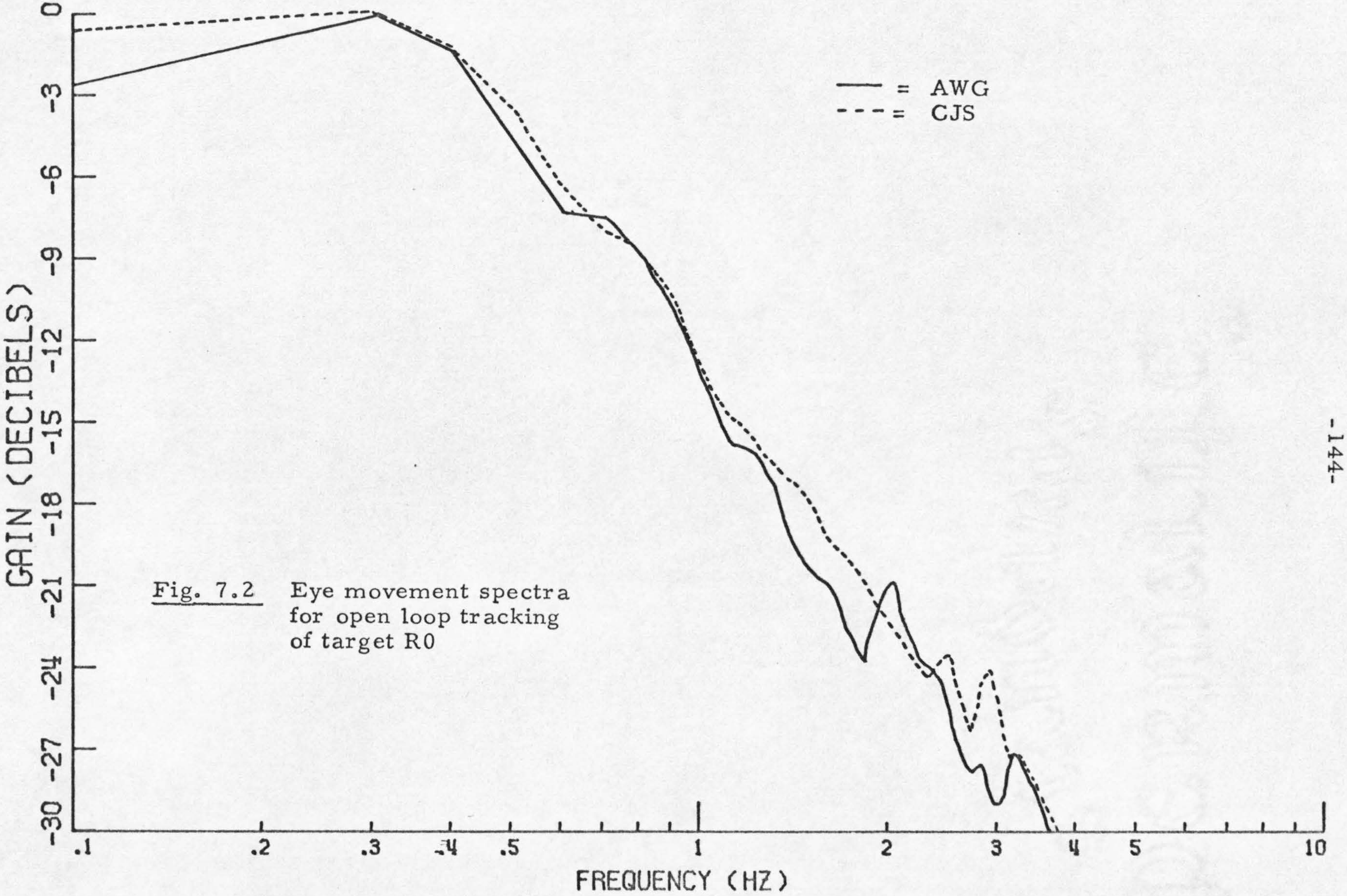

Fig. 7.2 Eye movement spectra for open loop tracking of target R0

R0 in an open loop mode.[*] These spectra do indeed exhibit the same 30 db per decade roll-off. What mechanism in the oculomotor control system is responsible for this strange property? At present I have no answer, nor can I find a convincing reason why the system should strive for such a characteristic.

---

[*] For these experiments the range of the projector was extended to three degrees from the primary position. This was sufficient to accommodate the larger eye movements and drift encountered in open loop tracking.

VIII. CONCLUSION

Since detailed conclusions are presented at the end of each section in this thesis, only the major points are summarized here.

1. Two-Dimensional Properties.

It appears to be generally accepted that the eye movement mechanism consists of independent vertical and horizontal channels, although little work has been done confirming or contradicting this.

The vertical - horizontal interaction was investigated by using a two dimensional target motion consisting of a sinusoid in one of the directions vertical or horizontal, and low-pass filtered Gaussian random noise in the orthogonal direction. The sinusoid was always the same, but six different bandwidth random motions were used. Increasing the bandwidth increased the "randomness" and information content of the noise. It was found that the random motion component reduced the proficiency of tracking the sinusoid in the orthogonal direction. However, while the efficiency of tracking the random motion was highly dependent on the bandwidth, tracking of the sinusoid was only slightly dependent on the noise (orthogonal motion) bandwidth. The system should therefore be thought of as consisting of two independent channels with a small amount of mutual cross-talk. These facts are in agreement with an observation of St-Cyr and Fender (1969c) and the work of Feinstein (1970).

It is tempting to assume that the two channels are always the vertical and horizontal components, especially as small vertical and horizontal movements are mediated by essentially distinct muscle pairs. However there is no evidence to suggest this. To find out whether the system is capable of recognizing the two-component nature of the target motion, the above target motions were rotated. That is, the sinusoidal component was presented along some arbitrary direction, which was neither horizontal nor vertical, with the random motion component orthogonal to it. Normal tracking was compared to tracking which was constrained to be implemented by a vertical and a horizontal channel. It was found that the two tracking channels are not always vertical and horizontal. The system did recognize the two-component structure of the target motion and rotated its frame of reference so that the two tracking channels coincided with the directions of the two components of target motion. This recognition occurred not only when the two target motion components were a sinusoid and low-pass filtered Gaussian random motion, but even when the components were both random motions, but with different bandwidths.

2. Time Delays, Prediction and Power Spectra.

Prediction of sinusoids in the oculomotor control system has been demonstrated on several occasions by researchers such as Dallos and Jones (1963), Michael and Jones (1966) and Stark, Vossius and Young (1962). However, their analyses were not exhaustive and St-Cyr and Fender (1969b) rejected the idea of a predictor and postulated a mechanism to explain the time delays for low-pass filtered Gaussian random motions as well as for sinusoids. In this thesis I approached the problem by examining the time delays in response to various periodic signals and various bandwidths of narrow-band Gaussian random motions as well as sinusoids. I showed that there is indeed prediction, and that this prediction only occurs when the target motion is periodic. Moreover, the harmonic content has to be sufficiently small so that the signal is in effect narrow-band as well. For periodic motions where the harmonic content is not sufficiently small, it appears as if the signal is split into a predictive component and a non-predictive component.

It was found that for unpredictable target motions, the time delay and average speed of the retinal image were related in a linear fashion. Based on this, I proposed a model to explain the time delays, both for the random motions and the periodic motions. My experiments did not prove that the system is sampled data or that it is continuous. However, the model can be interpreted as representing a sampled data system, whose sample interval is a function of the target motion. The variable sample interval makes this model capable of behaving similarly to Young's (1962) sampled data model for step targets as well as behaving in an apparently continuous manner for suitable ramp target motions. I believe that the system operates in a closed loop manner for both saccadic and smooth pursuit movements. With the sampling mechanism proposed above instabilities for closed loop smooth pursuit movements need not occur.

The power spectra of eye movements in response to the low-pass filtered Gaussian random motions showed that the eye movement bandwidth increases as the target motion bandwidth is increased. The assymptotic behavior of the power spectra showed a 30 db per decade fall-off, even though the target motion spectra fall-off was of the order of 50 db per decade in this region. In the open loop mode the power spectra still displayed a 30 db per decade fall-off. Power spectra for movements during both fixation and stabilized retinal image viewing displayed asymptotic roll-off of 20db per decade. It was suggested that, for the types of movements in this thesis, the eye-ball muscle dynamics behaved as a first order filter with a cutoff frequency of about .25 hz. The "active state tension" during tracking seems to decrease at the rate of 10 db per decade irrespective of the fall-off rate of the random target motions.

APPENDIX 1.

1. Mutual Information Between Two Gaussian Random Variables

The derivations of this section are taken from Gel'fand and Yaglom (1957).

Consider discreet random variables x and y ranging over finite sets. Let x take on n values $x_1, x_2, \dots x_n$ with probabilities $P_x(1), P_x(2), \dots P_x(n)$, and let y take on m values $y_1, y_2, \dots y_m$ with probabilities $P_y(1), P_y(2), \dots P_y(m)$. Let the joint probability of x and y taking on values of x_i and y_j respectively be $P_{xy}(i, j)$. Then "the amount of information about the variable x contained in the variable y (or, more precisely, the average amount of information about the variable x conveyed by specifying the value of the variable y)" is given by:

$$J(x, y) = \sum_{i=1}^{n} \sum_{j=1}^{m} P_{xy}(i, j) \log \frac{P_{xy}(i, j)}{P_x(i) P_y(j)} \quad .$$

If $P_{xy}(i, j) = 0$, the corresponding term in the summation is taken as zero. Since the above expression is symmetric in x and y, it may be considered as the mutual information between x and y.

In the simple case where x and y are one dimensional Gaussian random variables, it can be shown that:

$$J(x, y) = -\tfrac{1}{2} \log [1 - r^2(x, y)]$$

where $r(x, y)$ is the correlation coefficient of x and y. This unique relationship between information and the correlation coefficient is not unexpected. The finer points of this relationship are discussed by Bell (1962). Note that if $r(x, y) = 0$, then $J(x, y) = 0$, and if

$r(x, y) = \pm 1$, then $J(x, y) = \infty$.

2. The Relationship Between Bandwidth and Information

Consider a linear filter with a transfer function $Y(f)$. Let the input be an ensemble with entropy H_n per degree of freedom in the band W, and let the entropy per degree of freedom of the output be H_n'. Then it can be shown (for example Goldman, 1953) that

$$H_n' = H_n + \frac{1}{2W} \int_0^W \log|Y(f)|^2\, df$$

Thus the entropy loss per degree of freedom of the linear filter is

$$H = -\frac{1}{2W} \int_0^W \log|Y(f)|^2\, df$$

Consider the low-pass filter $Y(s) = \frac{1}{1+s/\omega_c}$, therefore

$$|Y(f)|^2 = \frac{1}{1+(f/f_c)^2}$$

The entropy loss per degree of freedom over the band W is:

$$\begin{aligned} H &= \frac{1}{2W} \int_0^W \log\,[1+(f/f_c)^2]\, df \\ &= \frac{1}{2W} \Big[f\log[1+(f/f_c)^2]-2f+2f_c \tan^{-1}\frac{f}{f_c}\Big]_0^W \\ &= \tfrac{1}{2}\log[1+(W/f_c)^2]-1+\frac{f_c}{W}\tan^{-1}\frac{W}{f_c} \end{aligned}$$

Over the 50 hz band, the entropy loss, in bits per degree of freedom, of the filters generating the waveforms R0-R6 are respectively:

R0:15.04 R1:13.69 R2:11.53 R3:10.36 R4:8.98 R5:7.63 .

If the information content of the waveform R0 is taken as the reference level, then the information content above this level of the waveforms R1-R5 are respectively (in bits per degree of freedom):

R1:1.35 R2:3.51 R3:4.68 R4:6.06 R5:7.41 .

It is clear that increasing the bandwidth of the Gaussian noise increases its information content.

BIBLIOGRAPHY

1. Barlow, H. B., "Eye movements during fixation," J. Physiol., Lond. 116 (1952), pp. 290-306.

2. Barlow, H. B., "The slippage of contact lenses and other artifacts in relation to fading and regeneration of supposedly stable retinal images," Quart. J. Exp. Psychol. 15 (1963), pp. 36-51.

3. Beeler, G. W., Fender, D. H., and Nobel, P. S. "Perception of pattern and color in the stabilized retinal image," Nature, Lond. 203 (1964), p. 1200.

4. Beeler, G. W., "Stochastic processes in the human eye movement control system," Doctoral Dissertation, California Institute of Technology (1965).

5. Bell, C. B., "Mutual information and maximal correlation as measures of dependence," Ann. Math. Stat. 33 (1962), pp. 587-595.

6. Bengi, H., and Thomas, J. G., "Fixation tremor in relation to eye-ball muscle mechanics," Nature, Lond. 217 (1968), pp. 773-774.

7. Bizzi, E., "Discharge of frontal eye field neurons during saccadic and following eye movements in unanesthetized monkeys," Exp. Brain Res. 6 (1968), pp. 69-80.

8. Bizzi, E. and Schiller, P. H., "Single unit activity in the frontal eye fields of unanesthetized monkeys during eye and head movement," Exp. Brain Res. 10 (1970), pp. 151-158.

9. Blackman, R. B., Data Smoothing and Prediction, Addison-Reading, Massachusetts (1965).

10. Blackman, R. B. and Tukey, J. W., The Measurement of Power Spectra, Dover Publications, New York (1958).

11. Box, G. E. P. and Muller, M. E., "A note on the generation of random normal deviates," Ann. Math. Stat. 29 (1958) pp. 610-611.

12. Byford, G. H., "Eye movement recording," Nature, Lond. 184 (1959), pp. 1493-1494.

13. Byford, G. H. "The fidelity of contact lens eye movement recording," Optica Acta 9 (1962), pp. 223-236.

14. Byford, G. H. and Stuart, H. F., "An Apparatus for the measurement of small eye movements," J. Physiol. 159 (1961), pp. 2P-3P.

15. Carpenter, M. B., "Central oculomotor pathways," in The Control of Eye Movements, Edited by C. C. Collins, Academic Press, New York (1971).

16. Childress, D. S. and Jones, R. W., "Mechanics of horizontal movement of the human eye," J. Physiol. 188 (1967), pp. 273-284.

17. Cogan, D. G., Neurology of the Ocular Muscles, Charles C. Thomas, Springfield, Ill. (1956).

18. Cohen, B. C., Goto, K., Shanzer, S. and Weiss, A., "Eye movements induced by electric stimulation of the cerebellum in the alert cat," Exptl. Neurol. 13 (1965), pp. 145-161.

19. Cohen, B. and Feldman, M., "Relationship of electrical activity in pontine reticular formation and lateral geniculate body to rapid eye movements," J. Neurophysiol. 31 (1968). pp. 806-817.

20. Cooley, J. W. and Tukey, J. W., "An algorithm for the machine calculation of complex Fourier series," Math. of Computation 19 (April 1965), pp. 297-301.

21. Cornsweet, T. N., "Determination of the stimuli for involuntary drifts and saccadic eye movements," J. Opt. Soc. Am. 46 (1956), pp. 987-993.

22. Cornsweet, T. N., "New technique for the measurement of small eye movements," J. Opt. Soc. Am. 48 (1958), pp. 808-811.

23. Dallos, P. J., "A small signal analysis of the human eye fixation mechanism," Doctoral Dissertation, Northwestern University (1962).

24. Dallos, P. J. and Jones, R. W., "Learning behavior of the eye fixation control system," IEEE Trans. Automatic Control AC-8 (1963), pp. 218-227.

25. Davenport, W. B. and Root, W. L., Random Signals and Noise, McGraw-Hill, New York (1958).

26. Davson, M., The Eye, Academic Press, New York (1962).

27. Deckert, G. H., "Pursuit eye movements in the absence of a moving visual stimulus," Science 143 (1964), pp. 1192-1193.

28. Ditchburn, R. W., "Eye movements in relation to retinal action," Optica Acta 1 (1955), p. 71.

29. Ditchburn, R. W. and Foley-Fisher, J. A., "Assembled data in eye movements," Optica Acta 14 (1967), pp. 113-118.

30. Ditchburn, R. W. and Ginsborg, B. L., "Involuntary eye movements during fixation," J. Physiol., Lond. 119 (1953), pp. 1-17.

31. Duke-Elder, S., System of Opthalmology, C. V. Mosby Company, St. Louis (1961).

32. Feinstein, R., "Interaction of the horizontal and vertical eye movement systems," Doctoral Dissertation, The University of Michigan, (1970).

33. Fender, D. H., "Torsional motions of the eye-ball," Brit. J. Opthalmol. 39 (1955), pp. 65-72.

34. Fender, D. H., "The eye-movement control system: evolution of a model," in Neural Theory and Modeling (Proc. Ojai Symp.), edited by R. F. Reiss, Stanford University Press, Stanford, California (1962).

35. Fender, D. H., "Techniques of systems-analysis applied to feedback pathways in the control of eye movements," Symp. Soc. Exptl. Biol. 18 (1964), pp. 401-419.

36. Fender, D. H., "Contact lens stability," in Biomedical Sciences Instrumentation, Vol. 2, edited by W. E. Murray and P. F. Salisbury, Plenum Press, New York (1964).

37. Fender, D. H. and Nye, P. W., "An investigation of the mechanisms of eye movement control," Kybernetik 1 (1961), pp. 81-88.

38. Findlay, J. M., "Frequency analysis of human involuntary eye movements," Kybernetik 8 (1971), pp. 207-214.

39. Franklin, J. N., "Numerical simulation of stationary and non-stationary Gaussian random processes," Siam Review 7 (1965), pp. 68-80.

40. Fuchs, A. F., "Saccadic and smooth pursuit eye movements in the monkey," J. Physiol., Lond. 191 (1967a), pp. 609-631.

41. Fuchs, A. F., "Periodic eye tracking in the monkey," J. Physiol., Lond. 193 (1967b), pp. 161-171.

42. Fuchs, A. F., "The saccadic system," in The Control of Eye Movements, Edited by C. C. Collins, Academic Press, New York (1971).

43. Fuchs, A. F. and Kornhuber, H. H., "Extra-ocular muscle afferents to the cerebellum of the cat," J. Physiol., Lond. 200 (1969), pp. 713-722.

44. Gel'fand, I. M. and Yaglom, A. M., "Calculation of the amount of information about a random function contained in another such function," Am. Math. Soc. Transl., ser 2 12 (1957), pp. 199-246.

45. Hyde, J. E. and Eason, R. G., "Characteristics of ocular movements evoked by stimulation of brain stem of cat," J. Neurophysiol. 22 (1959), pp. 666-678.

46. Ishihara, S., Tests for Color-Blindness, Kanehara Shuppan, Tokyo (1960).

47. Kertesz, A. E. and Jones, R. W., "The effect of angular velocity of stimulus on human torsional eye movements," Vision Research 9 (1969), pp. 995-998.

48. Krauskopf, J., Cornsweet, T. N., and Riggs, L. A., "Analysis of eye movements during monocular and binocular fixation," J. Opt. Soc. Am. 50 (1960), pp. 572-578.

49. Mackensen, G., "Die Geschwindigkeit horizontaler Blickbewegungen," Graefes Arch. für Opthal. 160 (1958), pp. 47-64.

50. Matin, L., "Measurement of eye movements by contact lens techniques: analysis of measuring systems and some new methodology for three dimensional recording," J. Opt. Soc. Am. 54 (1964), pp. 1008-1018.

51. Matin, L., Matin, E. and Pearce, D. G., "Eye movements in the dark during the attempt to maintain a prior fixation position," Vision Research 10 (1970), pp. 837-857.

52. Michael, J. A. and Jones, G. M., "Dependence of visual tracking capability upon stimulus predictability," Vision Research 6 (1966), pp. 707-716.

53. Nachmias, J., "Two-dimensional motion of the retinal image during monocular fixation," J. Opt. Soc. Am. 49 (1959), pp. 901-908.

54. Nachmias, J., "Determiners of the drift of the eye during monocular fixation," J. Opt. Soc. Am. 51 (1961), pp. 761-766.

55. Pasik, P. and Pasik, T., "Oculomotor functions in monkeys with lesions of the cerebrum and the superior culliculus," The Oculomotor System edited by M. B. Bender, Harper and Row, New York, (1964).

56. Pavlidis, T., "A neural net simulating the saccadic eye movement," Technical Report No. 13 (May 1966), Department of Electrical Engineering, Princeton University, Princeton, New Jersey.

57. Rashbass, C., "Relationship between saccadic and smooth tracking eye movements," J. Physiol., Lond. 159 (1961), pp. 326-338.

58. Rashbass, C. and Westheimer, G., "Disjunctive eye movements," J. Physiol., Lond. 159 (1961), pp. 339-360.

59. Rashbass, C. and Westheimer, G., "Independence of conjugate and disjunctive eye movements," J. Physiol., Lond. 159 (1961), pp. 361-364.

60. Richards, P. I., "Computing reliable power spectra," IEEE Spectrum 4 (1967), pp. 83-90.

61. Riggs, L. A., Ratliff, F., Cornsweet, J. C. and Cornsweet, T. N., "The disappearance of steadily fixated visual test objects," J. Opt. Soc. Am. 43 (1953), pp. 495-501.

62. Riggs, L. A., Armington, J. C. and Ratliff, F., "Motions of the retinal image during fixation," J. Opt. Soc. Am. 44 (1954), pp. 315-321.

63. Riggs, L. A. and Niehl, E. W., "Eye movements recorded during convergence and divergence," J. Opt. Soc. Am. 50 (1960), pp. 913-920.

64. Riggs, L. A. and Schick, A. M. L., "Accuracy of retinal image stabilization achieved with a plane mirror on a tightly fitting contact lens," Vision Research 8 (1968), pp. 159-169.

65. Robinson, D. A., "The mechanics of human saccadic eye movement," J. Physiol., Lond. 174 (1964), pp. 245-264.

66. Robinson, D. A., "Mechanics of human smooth pursuit eye movements," J. Physiol., Lond. 180 (1965), pp. 569-591.

67. Robinson, D. A., "The oculomotor control system: a review," Proc. IEEE 56 (1968), pp. 1032-1049.

68. Robinson, D. A., "Oculomotor unit behavior in the monkey," J. Neurophysiol. 33 (1970), pp. 393-404.

69. Robinson, D. A. and Fuchs, A. F., "Eye movements evoked by stimulation of frontal eye fields," J. Neurophysiol. 32 (1969), pp. 637-649.

70. Schiller, P. H., "The discharge characteristics of single units in the oculomotor and abducens nuclei of the unanesthetized monkey," Exp. Brain Res. 10 (1970), pp. 347-362.

71. Skavenski, A. A. and Steinman, R. M., "Control of eye position in the dark," Vision Research 10 (1970), pp. 193-203.

72. Smith, W. M., "Control of eye fixation by auditory feedback," Psychon. Science 1 (1964), pp. 233-234.

73. Stark, L., Vossius, G. and Young, L. R., "Predictive control of eye tracking movements," IRE Trans. Human Factors in Electronics HFE-3 (1962), pp. 52-57.

74. Starr, A., "A disorder of rapid eye movements in Huntington's Chorea," Brain 90 (1967), pp. 545-563.

75. St-Cyr, G. J., "Control mechanisms in the human binocular oculomotor system," Doctoral Dissertation, California Institute of Technology (1969).

76. St-Cyr, G. J. and Fender, D. H., "The interplay of drifts and flicks in binocular fixation," Vision Research 9 (1969a), pp. 245-265.

77. St-Cyr, G. J. and Fender, D. H., "Nonlinearities of the human oculomotor system: time delays," Vision Research 9 (1969b), pp. 1491-1503.

78. St-Cyr, G. J. and Fender, D. H., "Nonlinearities of the human oculomotor system: gain," Vision Research 9 (1969c), pp. 1235-1246.

79. Sugie, N., "A model of predictive control in visual target tracking," IEEE Trans. on Systems, Man and Cybernetics SMC-1 (1971), pp. 1-7.

80. Thomas, J. G., "The torque-angle transfer function of the human eye," Kybernetik 3 (1967), pp. 254-263.

81. Thomas, J. G., "The dynamics of small saccadic eye movements," J. Physiol., Lond. 200 (1969), pp. 109-127.

82. Westheimer, G., "Mechanisms of saccadic eye movements," A.M.A. Arch. Opthalmol. 52 (1954), pp. 710-724.

83. Westheimer, G., "Eye movement responses to a horizontally moving visual stimulus," A.M.A. Arch. Opthalmol. 52 (1954), pp. 932-941.

84. Westheimer, G., "A note on the response characteristics of the extraocular muscle system," Bull. Math. Biophys. 20 (1958), pp. 149-153.

85. Westheimer, G., "Saccadic eye movements," contribution to the International Colloquium "Eye Movement and Brain Function," Bratislava, Oct. 1970, published by Slovak Academy of Sciences, Bratislava, 1971.

86. Wheeless, L. L., "The effect of intensity on the eye movement control system," Doctoral Dissertation, University of Rochester (1965).

87. Wheeless, L. L., Boynton, R. M. and Cohen, G. H., "Eye-movement responses to step and pulse-step stimuli," J. Opt. Soc. Am. 56 (1966), pp. 956-960.

88. Whitteridge, D., "Central control of eye movements," in Handbook of Neurophysiology, vol. 2, The Am. Physiol. Soc. Baltimore, Md.: Williams and Wilkins (1960).

89. Yarbus, A. L., "Motion of the eye on interchanging fixation points at rest in space," Biofizika 2 (1957), pp. 698-702, (English transl., Biophysics 2, pp. 679-683).

90. Young, L. R., "A sampled data model for eye tracking movements," Doctoral Dissertation, Massachusetts Institute of Technology (1962).

91. Young, L. R., "Measuring eye movements," Am. J. Med. Electronics 2 (1963), pp. 300-307.

92. Young, L. R. and Stark, L., "Variable feedback experiments testing a sample data model for eye tracking movements," IEEE Trans. Human Factors in Electronics HFE-4 (1963), pp. 38-51.

93. Young, L. R., Forster, J. D. and Van Houtte, N., "A revised stochastic sample data model for eye tracking movements," Fourth NASA - University Conf. on Manual Control, Ann Arbor, Michigan (March 1968).

94. Zuber, B. L. and Stark, L., "Microsaccades and the velocity-amplitude relationship for saccadic eye movements," Science 150 (1965), pp. 1459-1460.